Office of Graduate Studies
Dissertation/Thesis Approval Form

This form is for use by all doctoral and master's students with a dissertation/thesis requirement. Please print clearly as the library will bind a copy of this form with each copy of the dissertation/thesis. All doctoral dissertations must conform to university format requirements, which is the responsibility of the student and supervising professor. Students should obtain a copy of the Thesis Manual located on the library website.

Dissertation/Thesis Title: Micro Coaxial Helicopter Controller Design

Author: Želimir Husnić

This dissertation/thesis is hereby accepted and approved.

Signatures:

Examining Committee

Chair

Members

Academic Advisor

Department Head

Office of Graduate Studies • 3141 Chestnut Street • Randell Hall 240 • Philadelphia, PA 19104
Tel: 215-895-0366 • Fax: 215-895-0495 • Email: graduate@drexel.edu • Web: www.drexel.edu/provost/graduatestudies

Micro Coaxial Helicopter Controller Design

A Thesis

Submitted to the Faculty

of

Drexel University

by

Zelimir Husnic

in partial fulfillment of the

requirements for the degree

of

Doctor of Philosophy

December 2014

Dedications

To my parents and family.

Acknowledgments

There are many people who need to be acknowledged for their involvement in this research and their support for many years.

I would like to dedicate my thankfulness to Dr. Bor-Chin Chang, without whom this work would not have started. As an excellent academic advisor, he has always been a helpful and inspiring mentor. Dr. B. C. Chang provided me with guidance and direction.

Special thanks goes to Dr. Mishah Salman and Dr. Humayun Kabir for their mentorship and help.

I would like to convey thanks to my entire thesis committee: Dr. Chang, Dr. Kwatny, Dr. Yousuff, Dr. Zhou and Dr. Kabir.

Above all, I express my sincere thanks to my family for their unconditional love and support.

Table of Contents

List of Tables

List of Figures

Abstract

Micro Coaxial Helicopter Controller Design
Zelimir Husnic
Advisor: Professor Bor-Chin Chang, Ph.D.

One of the advantages of the micro coaxial helicopter is in its maneuverability. It can perform some flight maneuvers that a fixed-wing aircraft cannot do - like hovering, perching, vertical take-off and landing, flying backwards, or moving sideways to the left or to the right. It is also more agile than the conventional helicopter with a counter-gyro effect rotor at the tail of the fuselage. However, due to its small size and sensitivity to disturbances, the micro coaxial helicopter is more challenging to control than a full-scale helicopter.

In this work, the flight dynamics of the micro coaxial helicopter were investigated and a simplified model for the autonomous flight control system design was constructed. System identification techniques as used in full-scale helicopters have been successfully applied to the micro coaxial unmanned helicopter. The essential parts of system identification include model theory, experimental data acquisition, parameter estimation, and model validations. The multivariable tracking and H2 control theory were employed to design a flight control system that would provide desired stability and performance for autonomous flight of a variety of maneuvers mentioned above. With a well-designed autonomous flight control system, the micro coaxial helicopter can be deployed for battle field awareness in battle fields, surveillance for search and rescue, border patrol, counter-terrorism operations, etc.

Chapter 1: Introduction

Unmanned Aerial Vehicles (UAVs) are of great interest to many scientists. Miniature and micro rotorcrafts are particularly interesting. The miniature/micro coaxial configuration helicopter is chosen over the single-rotor configuration in this work due to its maneuverability, versatility, stability and easiness to control. Micro helicopters are more agile than their full-scale equivalents. Their compact size and ability to hover, turn, and move in various directions, make the small-scale rotorcraft well-suited for operations in dynamic environments. Micro rotorcrafts have remarkable advantages over fixed-wing aircraft for specific types of missions particularly when the aircraft is required to remain stationary (hover) or maneuver in tightly constrained environments.

1.1 Vehicles to be Discussed

Unlike fixed-wing aircraft, the helicopter's main airfoil is the rotor mounted atop its fuselage on a hinged shaft (mast) connected with the vehicle's engine and flight controls. Because a helicopter can perform more actions than a fixed-wing aircraft, it is more difficult to fly. The helicopter must compensate for a variety of forces. The helicopter is a type of aircraft in which lift is obtained by means of one or more power-driven rotors. When the rotor of a helicopter turns, it produces reaction torque which tends to make the aircraft to spin. The helicopter's speed is limited by the fact that if the blades rotate too fast they will produce compressibility effects on the blade moving forward and stall effects on the rearward moving blade, at the same time. The main reason that makes a coaxial helicopter so special is because it uses two contra-rotating rotors to compensate each other's gyro-effect torque. The coaxial helicopter has its rotors reactive moments compensating each other directly in their axis of rotation.

The dynamic modeling of full-scale helicopters is described in the literature. Basically, the micro size of this rotorcraft causes certain details to be somewhat different. The modeling starts with the classical rigid-body equations. We assume that the speeds in any direction shall be so small that no

aerodynamic forces act on the body of the helicopter. Therefore, only gravitation and the different forces and moments from the main rotors are acting on the helicopter. First of all, a micro helicopter has a much faster time domain response due to its small size. Therefore, without employing an extra stability augmentation device, it would be difficult to control it. The fly-bar is used to improve the stability characteristic around the pitch and roll axes and to minimize the actuator force required. In any kind of flight (hovering, vertical, forward, side-ward, or backward), the total lift and thrust forces of a rotor are perpendicular to the tip-path plane or plane of rotation of the rotor. The tip-path plane is the imaginary circular plane outlined by the rotor blade tips in making a cycle of rotation. The rotor force components could be expressed in terms of a set of axes fixed in the helicopter. Such a formulation is necessary to study the forces and moments on the whole helicopter. However, it is more typical, when considering the rotor as a lifting device, to regard it as making a thrust, defined along some convenient direction, together with small components of force in the other two perpendicular directions. During a horizontal or vertical flight, there are four forces acting on the helicopter: lift, thrust, weight, and drag.

Lift is the force required to support the weight of the helicopter. Thrust is the force required to overcome the drag on the fuselage and other helicopter components. In straight-and-level unaccelerated forward flight, lift equals weight and thrust equals drag (straight-and-level flight is flight with a constant heading and at a constant altitude). If lift exceeds weight, the helicopter climbs; if lift is less than helicopter weight, the helicopter descends. If thrust exceeds drag, the helicopter speeds up; if thrust is less than drag, it slows down.

1.2 Coaxial Benefits

The main reason that makes a coaxial helicopter so special is because it uses two contra-rotating rotors to compensate each other's torque that they apply to the helicopter fuselage when they rotate. Without a tail rotor, a coaxial helicopter can devote all the power in developing lift, which increases the power efficiency of a coaxial helicopter. As far as power is concerned, the coaxial helicopter has a considerable edge over its single-rotor counterpart, since almost all power is used for developing the lift, while the single-rotor helicopter's tail rotor power consumption accounts for 10-12% of total

power. Also, the coaxial configuration has a more compact structure than a single-rotor because it does not need to mount a rear shaft longer than the main rotor's blade-swept radius in the airframe. The result of this is a reducing of coaxial-rotor helicopter size by 35-40% as compared with the single-rotor one. The moment of inertia of coaxial helicopter decreases, which increases the controllability and maneuverability of the helicopter.

1.3 Motivation

Just like other UAV (unmanned aerial vehicles), micro coaxial helicopters can be deployed for missions that involve dangerous, dull, and dirty tasks. A micro coaxial helicopter is especially suitable to indoor applications like inside the caves, tunnels, or collapsed buildings, where perching, hovering, and the ability to maneuver around obstacles in a narrow space is vital. The micro aircraft is one solution. Tasks for an indoor flight could include surveillance, urban search and inspection. A rotorcraft has significant advantages over fixed wing when it is required to hover or maneuver in tightly constrained environments. The micro rotorcraft's compact size and ability to hover, turn, and move in numerous directions make the small-scale rotorcraft well-suited for operations in challenging, dynamic environments. Rescue teams can safely enter the disaster site when they acquire sufficient information by site assessment. Site examination provides the information necessary for rescuers to accomplish a mission, such as possible location of survivors and their condition, and dangerous situations that might threaten rescuer's lives. To achieve indoor flight, the aircraft needs to negotiate narrow corridors and all types of obstacles, as well as provide useful information. Therefore, this aircraft needs to be able to fly in six degrees of freedom with minimum twisting and be equipped with sensors to know its own states and detect the environment. As far as power is concerned, the coaxial helicopter has a considerable edge over its single-rotor helicopter. The contra-rotation of coaxial rotors leads to significant reduction in power. In order to perform indoor flight with sensors, the micro coaxial rotorcraft should be highly efficient. The micro coaxial additional development shall provide a design that maximizes efficiency and provides optimum size for the micro rotorcraft. The micro coaxial rotorcraft has been investigated to exploit the advantages of coaxial configurations and is expected to be appropriate to indoor missions where hover performance is desired.

Chapter 2: Helicopter Flight Dynamics

2.1 Introduction

Descriptions of the dynamic modeling for helicopters are available in the literature [1] and [2]. However, due to the size of the micro coaxial helicopter, the details of the dynamic model need to be modified. The modeling starts with the classical rigid-body equations. We assume that the speed of the vehicle in any direction is rather slow, so that the aerodynamic forces on the vehicle are negligible. Therefore, only gravitation and the forces and moments from the main rotors are acting on the helicopter. The micro helicopter shown in Figure 2.1 has a faster time response due to its small size. Consequently, without employing a stabilization mechanism, it would be difficult to control. The fly-bar is used to improve the stability characteristic around the pitch and roll axes and to minimize the actuator force required. Rotors' reactive moments are compensated automatically throughout the flight. The details of the flight dynamics equations for the micro coaxial equations will be discussed in the following subsections.

Figure 2.1: Blade CX2 Helicopter

2.2 Helicopter Nomenclature

To describe the motion of an aircraft, usually we need three reference frames: the Earth-Center Frame, the Local Geographic Frame and the Aircraft Frame [3].

The aircraft frame, also called the body-fixed frame, is described by a set of Cartesian axes attached to the aircraft with the center of mass as the origin, as shown in Figure 2.2. Conventionally, the x-axis points forward along the nose, the y-axis points out along the starboard wing, and the z-axis points down.

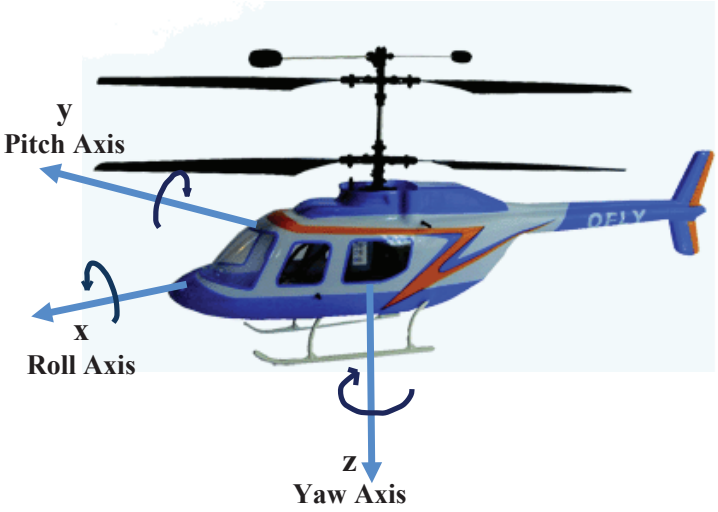

Figure 2.2: Body axis system used in helicopter dynamics analysis

As with any rigid body entity, the dynamic state of an aircraft may be considered to exist in a six degree-of-freedom (6DoF) isometric space described by three translational displacements and three rotational displacements (angles). Together, these six degrees, or parameters, can be used to fully describe the translational position and angular orientation of the rigid vehicle body at any point in time. In most cases, the time rate of change, or velocities, of these six parameters are also of interest for analysis and control. Combining the six positional parameters with their respective velocities yields 12 states.

The origin of the body-fixed coordinate frame is the center of gravity of the body, and the body is assumed to be rigid, an assumption that eliminates the need to consider the forces acting between individual elements of mass. We will model the helicopter as a rigid body moving in space. As shown in Figure 2.3, we use the variables (x, y, z) to represent the position of the helicopter in body coordinates. Euler angles are a means of representing the spatial orientation of any frame of the space as a composition of rotations from a reference frame. Body axis system is fixed in the vehicle, with the origin, usually the center of mass, consisting of the following axes:
longitudinal (x - axis), lateral (y - axis) and normal or vertical (z - axis).

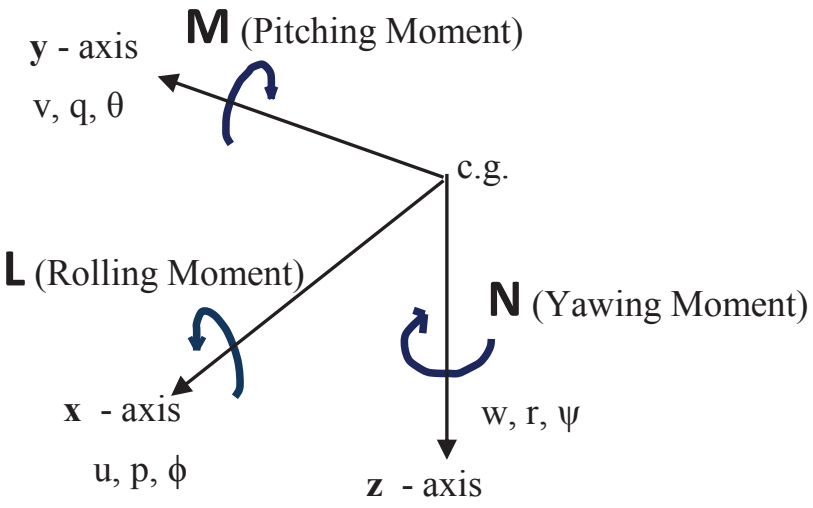

Figure 2.3: Definition of the helicopter body axes system

2.3 Rigid Body Dynamics

The standard rigid body dynamical equation will be used to model the motion of the helicopter in its environment. Quaternion Rotations and Euler Rotations (Euler angle rates and Angular velocity of the body frame) can be found in the literature [1], [2], [3] and [4]. The forces and moments refer to a system of body-fixed axes centered at the aircrafts center of gravity/mass. In general, the axes will be oriented at an angle relative to the principal axes of inertia, with the x direction pointing forward along approximately convenient fuselage reference line as described in literature [3]. The equations of motion for the six DoFs are assembled by applying Newton's laws of motion relating

the applied forces and moments to the resulting translational and rotational accelerations.

2.3.1 Reference Frames/Coordinates

To describe the position and behavior of an aircraft, we need to introduce two more reference frames in addition to the body frame. These two reference frames are ECEF (earth-centered earth-fixed) and NED (north-east-down) reference frames as described in the following [1], [2], [3] and [4].

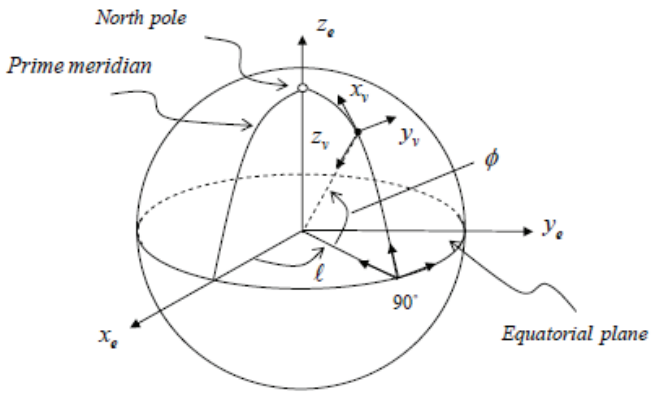

Figure 2.4: ECEF and NED reference frames

F_e : Earth-centered earth-fixed (ECEF) frame, origin at earth's cm, axes in the equatorial plane and along the spin axis with x_e - axis passing through the prime meridian.

F_v : Geographic (Local navigation) system frame, origin at vehicle's cm, axes in north, east, and down directions (NED reference frame).

The NED frame can be obtained through the following ECEF to NED transformation:

Perform a right-handed longitude rotation through the angle "l" (the longitude of the aircraft position) about the z_e - axis. Then perform a left-handed rotation about the y_e - axis for 90 degree, and finally have another left-handed lateral rotation with the angle "ϕ" (the lateral position of the aircraft) about the y_e - axis.

Recall that the body frame has its origin the vehicle's cm, with the positive x-axis is pointing to the aircraft nose, positive y-axis towards the right wing, and the positive z-axis downward. Consider Figure 2.5, in which the upper left graph is the NED frame with axes (x_v, y_v, z_v) and upper right

one is the body frame with axes (x_b, y_b, z_b). The attitude (or orientation) of the helicopter is defined by the Euler angles (ϕ, θ, ψ), which is explained as follows. Assume initially that the body frame coincides with the NED frame. Then rotate the body frame about the z axis following the right-hand rule by "ψ" angle and now the body axes are (x', y', z') as shown in the lower left graph. Next, rotate the new body axes about the y' axis following the right-hand rule by "θ" angle, and the axes of the body frame become (x", y", z") as shown in the lower center graph. Finally, rotate the axes (x", y", z") about the x" axis following the right-hand rule by "ϕ" angle, and the axes of the body frame become (x_b, y_b, z_b). The three rotation angles (ϕ, θ, ψ) are called Euler angles that define the attitude of the vehicle.

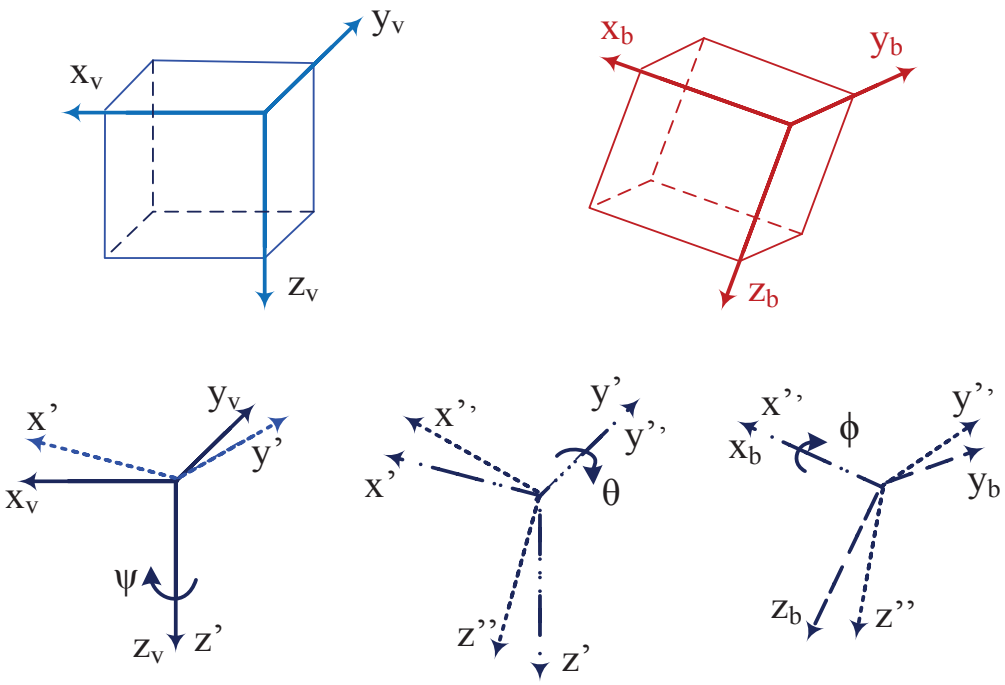

Figure 2.5: Body frame transformation

Assume a vector representation initially is $[x_v \ y_v \ z_v]$'. After the first rotation about the z-axis through the angle ψ , the vector representation will become $[x' \ y' \ z']$ as shown in the following.

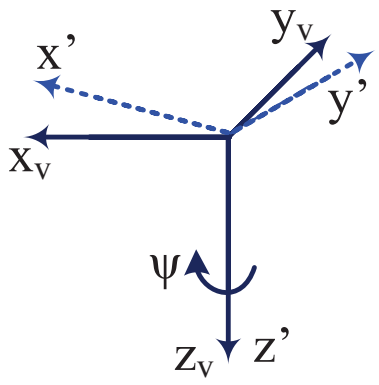

Figure 2.6: Rotation about z-axis

$$\begin{bmatrix} x' \\ y' \\ z' \end{bmatrix} = \begin{bmatrix} \cos\psi & \sin\psi & 0 \\ -\sin\psi & \cos\psi & 0 \\ 0 & 0 & 1 \end{bmatrix} \begin{bmatrix} x_v \\ y_v \\ z_v \end{bmatrix} = R_1 \begin{bmatrix} x_v \\ y_v \\ z_v \end{bmatrix} \qquad 2.3.1a$$

After the rotation about the y-axis through the (pitch) angle θ, the vector representation will become $[x" \ y" \ z"]$ as shown in the following.

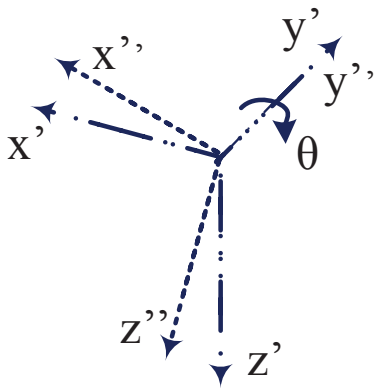

Figure 2.7: Rotation about y-axis

$$\begin{bmatrix} x'' \\ y'' \\ z'' \end{bmatrix} = \begin{bmatrix} \cos\theta & 0 & -\sin\theta \\ 0 & 1 & 0 \\ \sin\theta & 0 & \cos\theta \end{bmatrix} \begin{bmatrix} x' \\ y' \\ z' \end{bmatrix} = R_2 \begin{bmatrix} x' \\ y' \\ z' \end{bmatrix} \qquad 2.3.1b$$

Subsequently the rotation about x-axis (roll), through the angle ϕ, the vector representation will become $[x_b\ y_b\ z_b]$' as shown in the following. Note that the vector representation in the body frame is $[x_b\ y_b\ z_b]' = R_3{*}R_2{*}R_1{*}[x_v\ y_v\ z_v]'$.

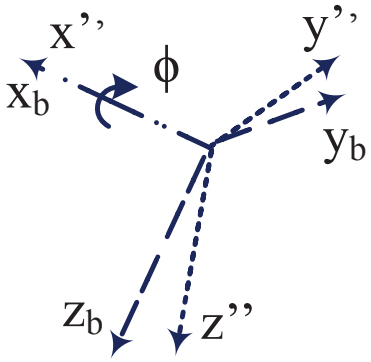

Figure 2.8: Rotation about x-axis

$$\begin{bmatrix} x_b \\ y_b \\ z_b \end{bmatrix} = \begin{bmatrix} 1 & 0 & 0 \\ 0 & \cos\phi & \sin\phi \\ 0 & -\sin\phi & \cos\phi \end{bmatrix} \begin{bmatrix} x'' \\ y'' \\ z'' \end{bmatrix} = R_3 \begin{bmatrix} x'' \\ y'' \\ z'' \end{bmatrix} \qquad 2.3.1c$$

Since the gravitational force is always pointing to the center of the earth, the gravitational acceleration components along the body frame x, y and z axes can therefore be written in terms of the Euler roll and pitch angles as described in literature [1]

$$a_{x_g} = -g \sin\theta$$
$$a_{y_g} = g \cos\theta \sin\phi \qquad 2.3.1d$$
$$a_{z_g} = g \cos\theta \cos\phi$$

The equations of motion can be derived by connecting the rates of change of the linear and angular momentum to the applied forces and moments. The equations are created with assumption of constant mass. Also, the equations are constructed with respect to selection of a subjective material point inside the fuselage and expression derivation for the absolute acceleration of this point.

The acceleration can then be integrated over the fuselage volume to derive the effective change in angular momentum and therefore the total inertia force. A similar process leads to the angular acceleration and corresponding inertial moment. The center of the moving axes is located at the helicopter's center of mass. As the helicopter translates and rotates, the axes therefore remain fixed to seleceted point in the fuselage.

The linear velocity vector of the fuselage CG is denoted by $\vec{v}$.

The coordinate vector of the linear velocity with respect to the body-fixed frame is

$$v^B = [u \;\; \mathrm{v} \;\; \mathrm{w}]^T \qquad 2.3.1e$$

Similarly, the angular velocity $\vec{\omega}$ of the fuselage, is represented in the body-fixed frame by

$$\omega^B = [\mathrm{p} \;\; \mathrm{q} \;\; \mathrm{r}]^T \qquad 2.3.1f$$

The vector sum of the external forces and moments (torques) that act on the fuselage.

$$f^B = [\mathrm{X} \;\; \mathrm{Y} \;\; \mathrm{Z}]^T \qquad 2.3.1\mathrm{g}$$

The f^B represents the components of the force vector with respect to the body-fixed frame.

The sum of all external moments are denoted by τ^B

$$\tau^B = [\mathrm{L} \;\; \mathrm{M} \;\; \mathrm{N}]^T \qquad 2.3.1h$$

Positive direction of the angular velocity and moment components refers to the right-hand rule about the respective axis. The equation of Newton's second law is valid only in an inertial reference frame.

Therefore, Newton's second law for the translational motion of the helicopter is given by:

$$\vec{f} = m \left.\frac{d\vec{v}}{dt}\right|_I \qquad 2.3.1k$$

Where "m" denotes the total mass of the helicopter.

The operand $\frac{d(o)}{d(t)}\,|_I$ shown above, denotes the time derivative of a vector in space as viewed by an observer in the inertial reference frame.

The time derivative with respect to the inertial reference frame is

$$\left.\frac{d\vec{v}}{dt}\right|_I = \left.\frac{d\vec{v}}{dt}\right|_B + \vec{\omega} \times \vec{v} \qquad 2.3.2a$$

The operator "$\times$" is the vector cross product.

The operand $\frac{d\vec{v}}{dt}\,|_B$ denotes the time derivative of a velocity vector with respect to the body-fixed reference frame.

In general, these terms denote the derivative of a vector from the viewpoint of an observer in the body-fixed frame. The change of the vector's direction due to the angular velocity of the body-fixed frame is not conceivable by the observer on the body-fixed frame. This change is detected by the observer on the inertial frame.

Newton's second law for the translational motion is

$$\begin{aligned} X/m &= -v\,r + w\,q + \dot{u} \\ Y/m &= -w\,p + u\,r + \dot{v} \\ Z/m &= -u\,q + v\,p + \dot{w} \end{aligned} \qquad 2.3.2b$$

To conclude the derivation of the equations of motion, Newton's second law is applied to all moments that act on the CG. The reference point for calculating the angular momentum and the external moments is rigidly attached to the CG of the helicopter. Furthermore, using the body-fixed reference frame for the analysis is advantageous since the moments and the products of inertia do not vary with time given that the mass distribution of the helicopter does not change.

The angular momentum components of the body-fixed reference frame are given by

$$H^B = I\omega^B \qquad 2.3.2c$$

where I denotes the inertia matrix

$$I = \begin{bmatrix} I_{xx} & -I_{xy} & -I_{xz} \\ -I_{yx} & I_{yy} & -I_{yz} \\ -I_{zx} & -I_{zy} & I_{zz} \end{bmatrix} \qquad 2.3.2d$$

The respective moments of inertia are 2.3.2e

$$I_{xx} = \sum \left({y^2}_m + {z^2}_m\right) dm$$

$$I_{yy} = \sum \left({x^2}_m + {z^2}_m\right) dm$$

$$I_{zz} = \sum \left({x^2}_m + {y^2}_m\right) dm$$

The products of inertia are 2.3.2f

$$I_{xy} = I_{yx} = \sum x_m \, y_m \, dm$$

$$I_{xz} = I_{zx} = \sum x_m \, z_m \, dm$$

$$I_{yz} = I_{zy} = \sum y_m \, z_m \, dm$$

The above sums apply to all elementary masses dm of the helicopter, and x_m, y_m and z_m are the distances of each elementary mass from the CG. It is assumed that the principal axes coincide with the axes of the body-fixed frame; therefore, it follows that

$$I_{xy} = I_{yx} = 0 \qquad I_{yz} = I_{zy} = 0 \qquad I_{xz} = I_{zx} = 0 \qquad 2.3.2g$$

Newton's second law for the rotational motion dictates that the external moments acting on the helicopter are equal to the time rate of change of the angular momentum with respect to the inertial reference frame. Substituting differentiation of free vectors and the time derivative components of the angular momentum is the analytic expression of Newton's second law for the rotational motion of the helicopter.

Force equilibrium along the body axis

$$L = I_{xx}\,\dot{p} + (I_{zz} - I_{yy})\,q\,r$$
$$M = I_{xx}\,\dot{q} + (I_{xx} - I_{zz})\,p\,r \qquad 2.3.2h$$
$$N = I_{zz}\,\dot{r} + (I_{yy} - I_{xx})\,p\,q$$

The above equations are called Newton Euler equations in the body-fixed frame's coordinates.

Integration of the position and orientation dynamics equations provides all required information for determining the helicopter motion in the configuration space.

As mentioned earlier, the orientation of the helicopter is parameterized by the Z-Y-X Euler angles. In this case, each intermediate rotation takes place about an axis of a frame that is produced by a preceding rotation.

In aeronautics applications, it is desirable that each rotation takes place about the axis of a fixed frame. In this convention, the Euler angles are called pitch, roll and yaw angles.

The helicopter rigid body dynamics are completed by defining the external body frame force and torque.

As explained in this work, I_{xz} is much smaller than the other terms and, due to the symmetry of the helicopter with respect to the x-z plane, I_{xy} and I_{yz} are zero.

The offset between the rotor axis and the helicopter's center of gravity is expected to be zero. It is assumed that the helicopter's center of gravity is in-line with the rotor axis.

Definition of the helicopter body axes system is shown in Figure 2.3

Body axis system is fixed in the vehicle, with the origin, usually the center of mass, consisting of the following axes: longitudinal (x - axis), lateral (y - axis) and normal (z - axis).

The coaxial configuration helicopter is special due to the fact that it embodies a principle of the reactive moment compensation fundamentally different from that of the single-rotor configuration, described in the literature [1], [2] and [4].

The forces and torque are balanced when the helicopter is in stable condition. Unbalance of force will result in linear acceleration, while unbalance of torque will result in angular acceleration. In hovering, force balance is achieved when the sum of the thrust from two main rotors equals the

gravitational force. All forces and torques in all directions sum to zero. At hover, force directions are concentric with the rotor shaft. The helicopter's position and orientation in body coordinates will always be zero. The velocity and acceleration terms are greatly simplified by using these coordinates. The aerodynamic interaction between the rotor and the fuselage is ignored.

2.4 Rotor Aerodynamics in Axial Flight

The coaxial helicopter rotors' reactive moments are compensated automatically throughout the flight, thus requiring no interference on the part of the pilot. Aerodynamic symmetry is the most important feature of the coaxial helicopter. It enhances significantly its controllability and stability.

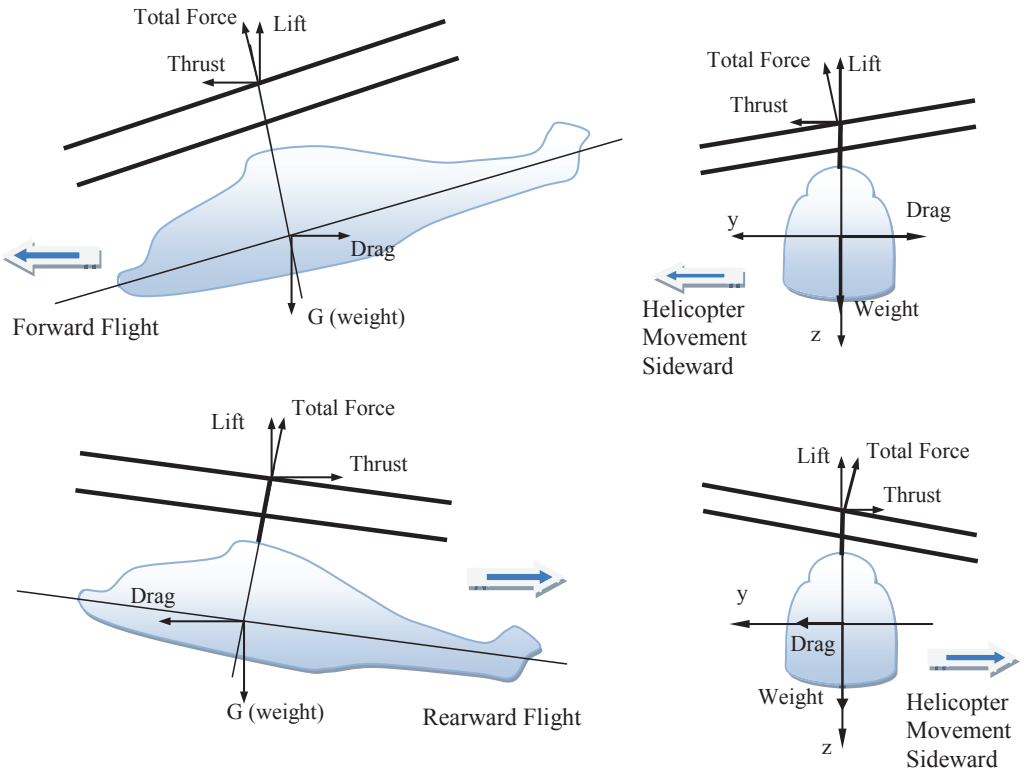

Figure 2.9: Helicopter forces and moments during flight

The coaxial design ensures a smooth combination of efficient control and aerodynamic damping, which provides good controllability. The standard rigid body dynamical equation will be used to model the motion of the helicopter.

The forces and torque are balanced when the helicopter is in stable equilibrium condition. In hovering, force balance is achieved when the sum of the thrust from two main rotors equals the gravitational force. All forces and torques in all directions sum to zero. At hover, force directions are concentric with the rotor shaft. The helicopter's position and orientation in body coordinates will always be zero. The velocity and acceleration terms are greatly simplified by using these coordinates. The aerodynamic interaction between the rotor and the fuselage is ignored. The offset between the rotor axis and the helicopter's center of gravity is expected to be zero. It is assumed that the helicopter's center of gravity is in line with the rotor axis.

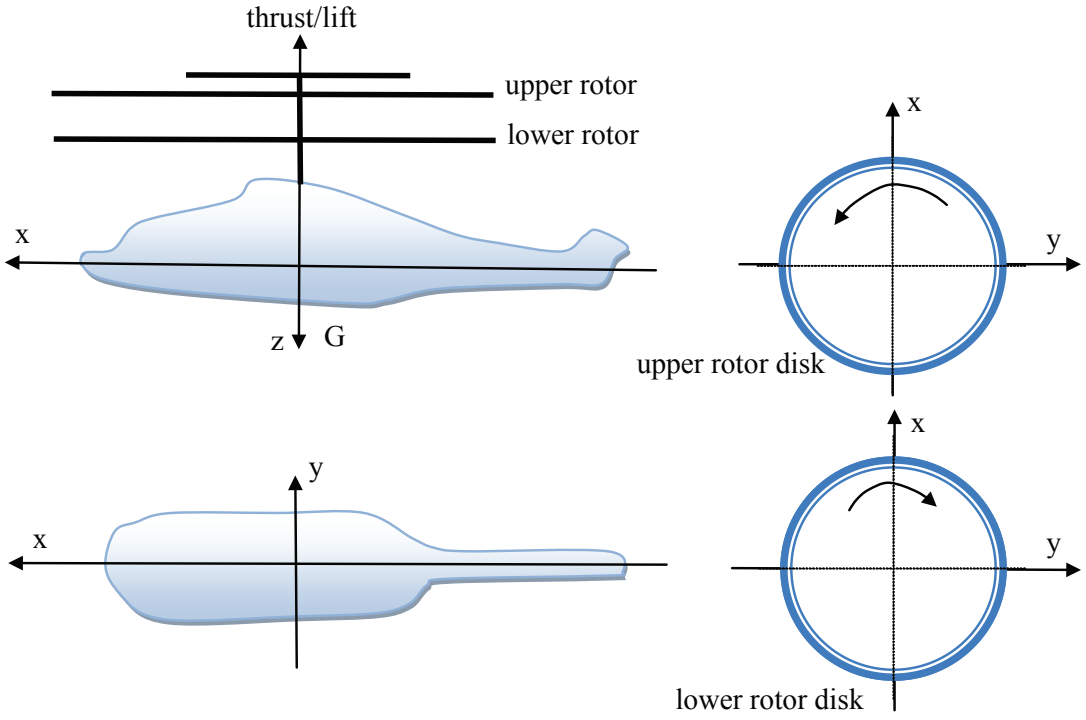

Figure 2.10: Coaxial Helicopter forces and moments

The external (aerodynamics and body) forces, external (aerodynamics) moments and moments of inertia, are the sum of the fuselage, upper and lower rotor, described in the literature [4].

$$
\begin{aligned}
X &= -X_u - X_l - X_{pl} - mvr + mwq - Gsin\theta \\
Y &= Y_u + Y_l + Y_{pl} - mwp + mur - Gcos\theta sin\phi \\
Z &= -Z_u - Z_l - Z_{pl} - muq + mvp + Gcos\theta cos\phi \\
L &= L_u + L_l - L_{pl} - (I_y - I_z)\, qr \\
M &= M_u + M_l - M_{pl} - (I_z - I_x)\, pr \\
N &= N_u + N_l - N_{pl} - (I_x - I_y)\, pq
\end{aligned}
\qquad 2.4.1
$$

2.5 Thrust

The helicopter rotor produces an upward thrust by driving a column of air downwards through the rotor plane. A relationship between the thrust produced and the velocity communicated to the air can be obtained by the application of Newtonian mechanics - the laws of conservation of mass, momentum and energy - to the overall process. The rotor is considered as an 'actuator disc', across which there is a sudden increase of pressure, uniformly spread. In hover, the column of air passing through the disc is a defined stream tube above and below the disc: outside this stream tube the air is undisturbed. No rotation is imparted to the flow. The total force in the axial direction acting on the control surface consists of the rotor thrust plus the pressure forces on the ends of the cylinder described in literature [4].

In hovering flight axial velocity is zero. In estimating the efficiency in hovering flight, it is important to consider losses that affect hover performance including profile drag, no uniform inflow, slip stream rotation, and tip losses. The thrust force of the rotor is proportional to the thrust coefficient, the area swept out by the rotor, air density, and the square of the circular velocity of the blade tip. For a given rotor at a constant air density, the thrust depends on the number of revolutions and the thrust coefficient. The induced velocity may be calculated when the thrust is known.

For a given rotor at a constant air density, the thrust depends on the number of revolutions and the thrust coefficient. The induced velocity may be calculated when the thrust is known.

Following simple momentum theory, the thrust generated from a rotor in hover can be written as

$$\mathbf{T} = T_u + T_{li} + T_{lo} \tag{2.5.1}$$

where T is thrust, T_u is upper rotor disk thrust, T_{li} is inner area of lower rotor disk thrust, T_{lo} is outer area of lower rotor disk thrust.

The thrust force equation described in this work and literature [4] recognize and distinguish influence of the upper rotor disk, inner and outer area of lower rotor disk for thrust and flow velocity.

Far upstream of the rotor, the air velocity relative to the rotor is the rate of climb and the pressure. As air is sucked into the disc from above, the pressure falls. An increase of pressure occurs at the disc, after which the pressure falls again in the outflow, eventually arriving back at the initial or atmospheric level. As the air approaches the rotor, the airspeed increases at the rotor itself. Because the airflow is continuous, there is no sudden change of velocity at the rotor, but there is a jump of pressure. The slipstream velocity continues to increase downstream of the rotor.

2.6 Torque

As mentioned in Sec. 2.4, when the helicopter is hovering, the force directions are concentric with the rotor shaft. To calculate the power, we must consider the rate at which kinetic energy is being imparted to the air. The primary task is to determine the lift and drag coefficients of the rotor blades since these two quantities determine the thrust and power required for given speed in forward flight or hover. Thus the lift and drag coefficients are the two quantities from which performance may be assessed. The total drag is composed of pressure or form drag and viscous drag. The power loss due to drag is very hard to predict because it is a much smaller force and is thus sensitive to small changes in pressure.

The main rotor torque described in literature [4] can be approximated as a sum of induced torque due to generated thrust, and torque due to profile drag on the blade:

$$\mathbf{Q} = Q_u - Q_l \qquad 2.6.1a$$

$$\mathbf{Q_l} = Q_{li} + Q_{lo} \qquad 2.6.1b$$

where Q is rotor torque, Q_u is upper rotor disk torque, Q_l is lower rotor disk torque, Q_{lo} is outer area of lower rotor disk torque, Q_{li} is inner area of lower rotor disk torque.

The torque equation is described in this work and literature identify influence of the upper rotor disk and the lower rotor disk.

2.6.1 Rotor Aerodynamics

While simple momentum theory can be used to estimate the efficiency of rotors, a more accurate aerodynamic theory is needed to incorporate blade geometry, sectional orientation and twist condition. Blade element theory evolved to incorporate the effects of drag and twist on rotor performance. This theory permits the derivation of the equations for the thrust and torque coefficients as described in the literature [1], [2] and [4]. In hover, the column of air passing through the disc is a clearly defined stream tube above and below the disc: outside this stream tube the air is undisturbed. No rotation is imparted to the flow. The column of air passing through the disc is shown in Figure 2.11.

As air is sucked into the disc from above, the pressure falls. An increase of pressure Δp occurs at the disc, after which the pressure falls again in the outflow, eventually arriving back at the initial or atmospheric level p_∞. Velocity in the stream tube increases from zero at 'upstream infinity' to a value "vi" at the disc and continues to increase as pressure falls in the outflow, reaching a value V_∞ at 'downstream infinity'. Continuity of mass flow in the stream tube requires that the velocity is continuous through the disc. Energy conservation, in the form of Bernoulli's equation, can be applied separately to the flows before and after the disc.

Using the incompressible flow assumption, we have in the inflow as shown in this work.

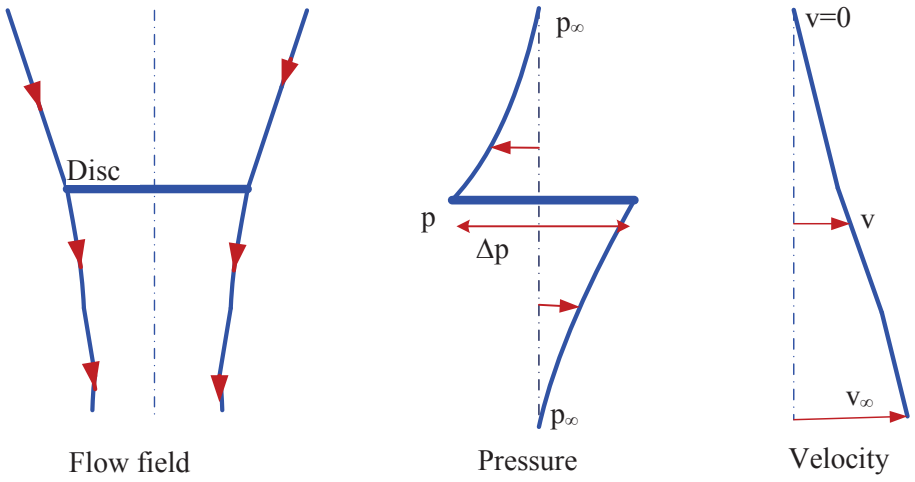

Figure 2.11: Actuator disc concept for rotor in hover

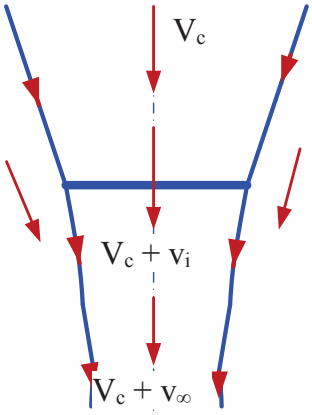

Figure 2.12: Flow field in vertical climb

Now, by momentum conservation, the thrust "T" on the disc is equal to the overall rate of increase of axial momentum of the air

$$T = \rho \ A \ v_i \ v_\infty \qquad 2.6.11a$$

Thus half the velocity communicated to the air occurs above the disc and half below it, and the relationship between thrust and the velocity v_i is shown in Figure 2.13

$$v_i = 2 \ v_\infty$$
$$T = 2 \ \rho \ A \ {v_\infty}^2 \qquad 2.6.1b$$

Far upstream of the rotor, the air velocity relative to the rotor is the rate of climb V_c and the pressure is p_∞. As air is sucked into the disc from above, the pressure falls. An increase of delta pressure occurs at the disc, after which the pressure falls again in the outflow, eventually arriving back at the initial or atmospheric level. As the air approaches the rotor, the airspeed increases to $V_c + v_i$ at the rotor itself. Because the airflow is continuous there is no sudden change of velocity at the rotor, but there is a jump of delta pressure. The slipstream velocity continues to increase downstream of the rotor, reaching a value in the ultimate wake of V_c+v_2.

The total force in the axial direction acting on the control surface consists of the rotor thrust plus the pressure forces on the ends of the cylinder. To calculate the power being supplied by the rotor, we must consider the rate at which kinetic energy is being imparted to the air. The helicopter with single main rotor thrust is,

$$T = \rho A \left(V_c + v_2\right) v_2 \qquad 2.6.11c$$

Control volume for the helicopter with single main rotor in axial flight is shown in Figure 2.13. Control volume for a coaxial helicopter in axial flight is shown in Figure 2.14.

Coaxial rotor air flow is shown in Figure 2.14. Air flow is separated on two parts: inner area defined by upper rotor flow and outer area between flow of upper and lower rotor. The disk theory defines the rotor's flow for the ideal case. Following simple momentum theory, the thrust generated from a rotor in hover can be written as

$$\begin{aligned}
&\mathbf{T} = T_u + T_{li} + T_{lo} \\
&\mathbf{T_u} + \mathbf{T_{li}} = \rho A V_u * V_2 \\
&\mathbf{T_{lo}} = \rho \left(A - {r_1}^2 * \pi\right) (V_c + V_{lo}) V_{uo} \\
&\mathbf{T} = \rho A V_u V_2 + \rho \left(A - {r_1}^2 * \pi\right) (V_c + V_{lo}) V_{uo}
\end{aligned} \qquad 2.6.11d$$

The torque and thrust equation described in this work and literature [4] recognize and distinguish the influence of the upper rotor disk and lower rotor disk.

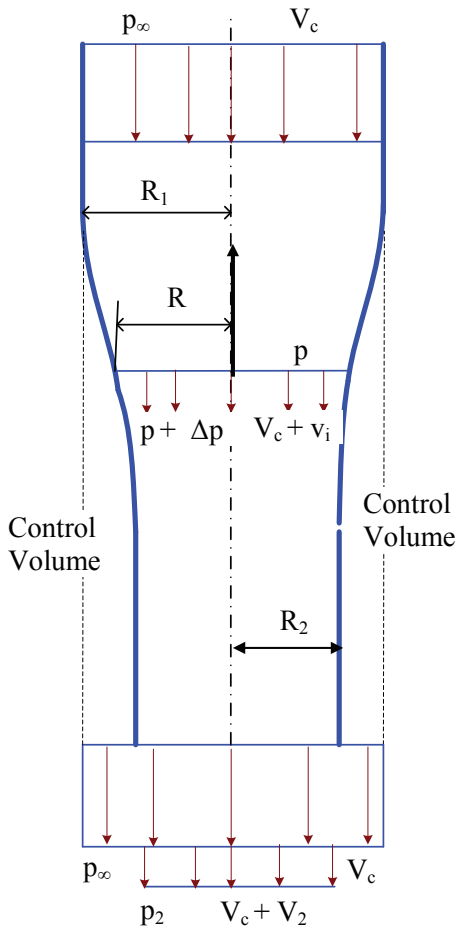

Figure 2.13: Helicopter's control volume with single main rotor

The rotor torque can be approximated as a sum of induced torque due to generated thrust, and torque due to profile drag on the blade:

$Q=Q_u$ - $(Q_{li} + Q_{lo})$ 2.6.11e

$Q_l=Q_{li}+Q_{lo}$

where V_u is upper rotor disk velocity, V_{li} is inner area of lower rotor disk velocity, V_{lo} is outer area of lower rotor disk velocity, V_{uo} is outer area of undisturbed flow velocity, V_c is axial velocity of the rotor, V_2 is inner area of undisturbed flow velocity, V_{l22} is undisturbed flow velocity in outer area of lower rotor, Ω is angular velocity.

The rotor torque can be approximated as a sum of induced torque due to generated thrust, and torque due to profile drag on the blade (see Figure 2.15):

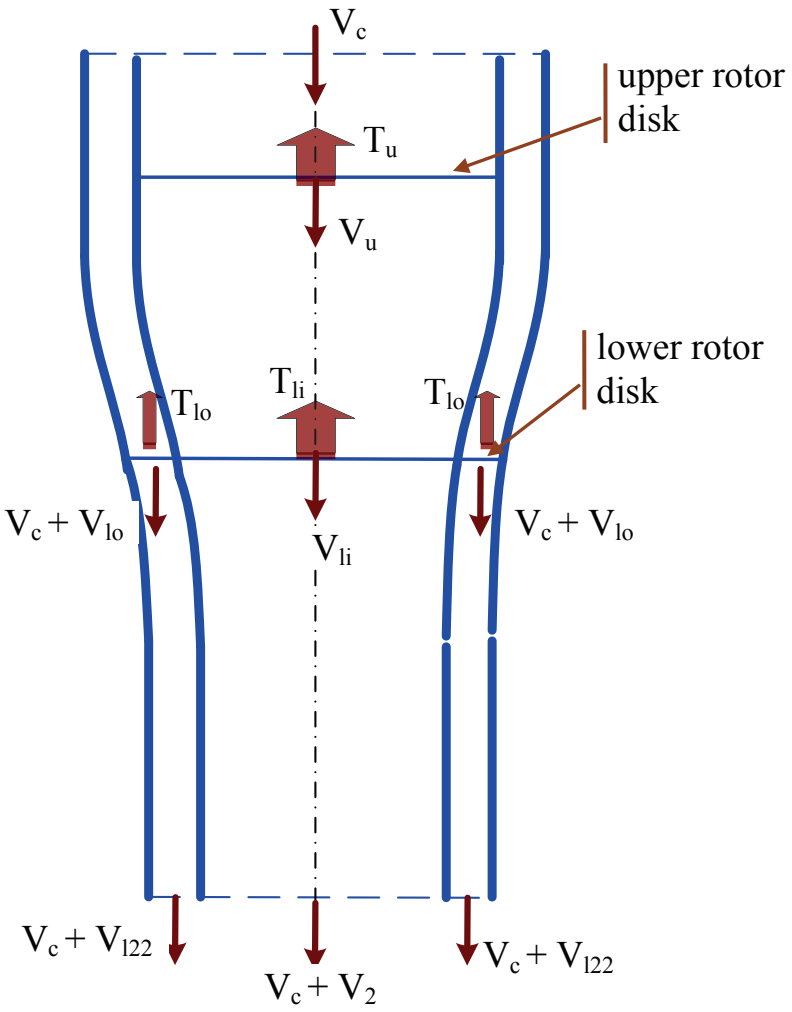

Figure 2.14: Control volume for coaxial helicopter

$$\mathbf{Q} = Q_u - Q_l$$

$$\mathbf{Q_l} = Q_{li} + Q_{lo}$$

$$\mathbf{Q_{li}} = (T_{li}V_{li})/\Omega \qquad 2.6.11f$$

$$\mathbf{Q_{lo}} = (T_{lo}(V_c + V_{lo}))/\Omega$$

$$\mathbf{Q} = (T_uV_u - T_lV_{li} - T_{lo}(Vc + V_{lo}))/\Omega$$

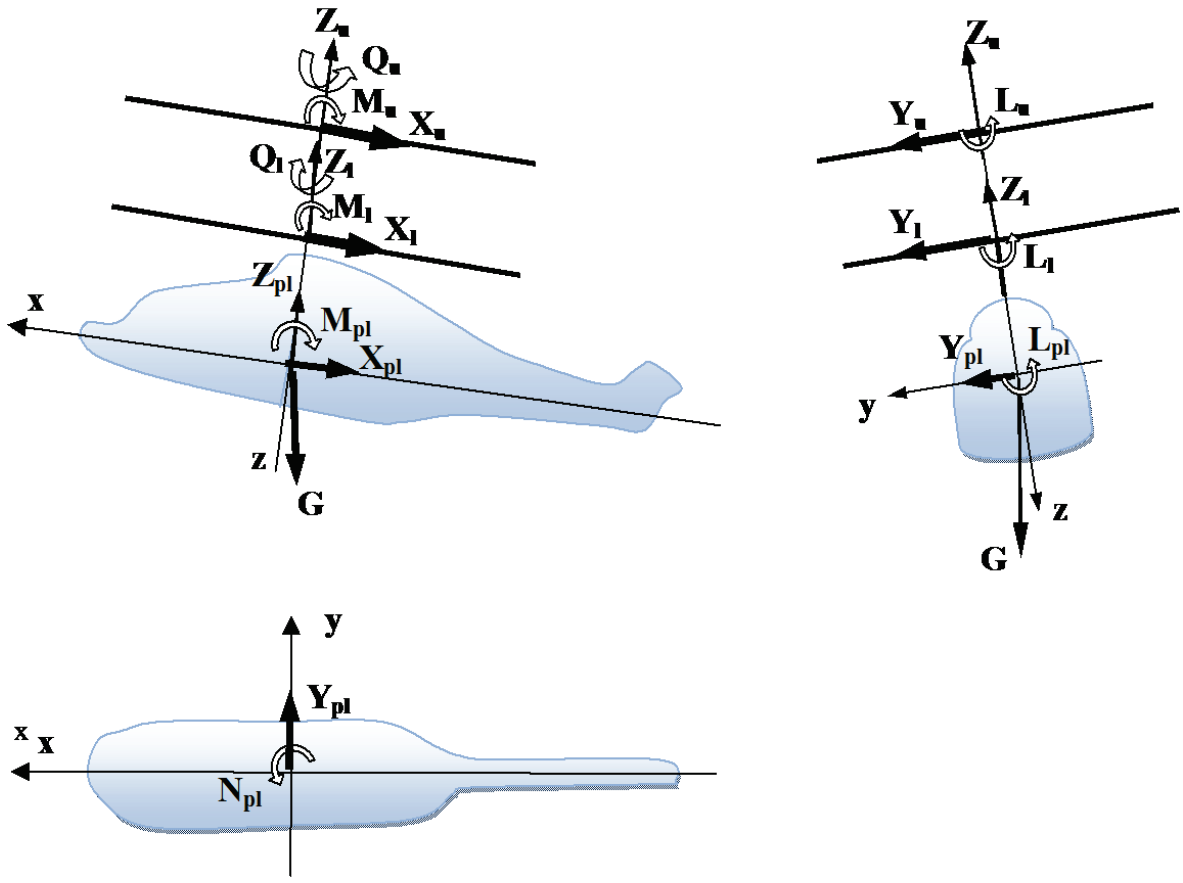

Figure 2.15: Coaxial Helicopter Forces (a)

Force equilibrium along the body axis

$$
\begin{aligned}
X &= -mvr + mwq - Gsin\theta + m\dot{u} \\
Y &= -mwp + mur - Gcos\theta sin\Phi + m\dot{v} \\
Z &= -muq + mvp - Gcos\theta cos\Phi + m\dot{w} \\
L &= I_x\dot{p} - (I_y - I_z)\, qr \\
M &= I_y\dot{q} - (I_z - I_x)\, pr \\
N &= I_z\dot{r} - (I_x - I_y)\, pq
\end{aligned}
\qquad 2.6.11g
$$

The external (aerodynamics and body) forces, external (aerodynamics) moments and moments of inertia, are the sum of the fuselage, upper and lower rotor, described in the literature [4].

$$
\begin{aligned}
X &= -X_u - X_l - X_{pl} - mvr + mwq - Gsin\theta \\
Y &= Y_u + Y_l + Y_{pl} - mwp + mur - Gcos\theta sin\Phi \\
Z &= -Z_u - Z_l - Z_{pl} - muq + mvp + Gcos\theta cos\Phi \\
L &= L_u + L_l - L_{pl} - (I_y - I_z)\, qr \\
M &= M_u + M_l - M_{pl} - (I_z - I_x)\, pr \\
N &= N_u + N_l - N_{pl} - (I_x - I_y)\, pq
\end{aligned}
\qquad 2.6.11h
$$

The upper and lower rotor forces for case of a horizontal straightforward flight along y-axis are:

$$
\begin{aligned}
L_u &= T_u\, y_T + Y_u\, z_{up} + L_{up} \\
L_l &= T_l\, y_T + Y_l\, z_{lr} + L_{lr}
\end{aligned}
\qquad 2.6.11i
$$

Terms such as y_T are zero due to the offset between the rotor axis and the center of gravity. The offset between the rotor axis and the helicopter's center of gravity is expected to be zero. It is assumed that the helicopter's center of gravity is in line with the rotor axis.

$$
\begin{aligned}
Y_u &= \tfrac{L_u - L_{up}}{z_{up}} \\
Y_l &= \tfrac{L_l - L_{lr}}{z_{lr}}
\end{aligned}
\qquad 2.6.11j
$$

The upper and lower rotor forces for case of a horizontal straightforward flight along x-axis are:

$$
\begin{aligned}
M_u &= -T_u\, x_T + X_u\, z_{up} + M_{up} \\
M_l &= -T_l\, x_T + X_l\, z_{lr} + M_{lr}
\end{aligned}
\qquad 2.6.11k
$$

Terms such as x_T are zero due to the offset between the rotor axis and the center of gravity. The offset between the rotor axis and the helicopter's center of gravity is expected to be zero. It is assumed that the helicopter's center of gravity is in-line with the rotor axis.

$$
\begin{aligned}
X_u &= \tfrac{M_u - M_{up}}{z_{up}} \\
X_l &= \tfrac{M_l - M_{lr}}{z_{lr}}
\end{aligned}
\qquad 2.6.11l
$$

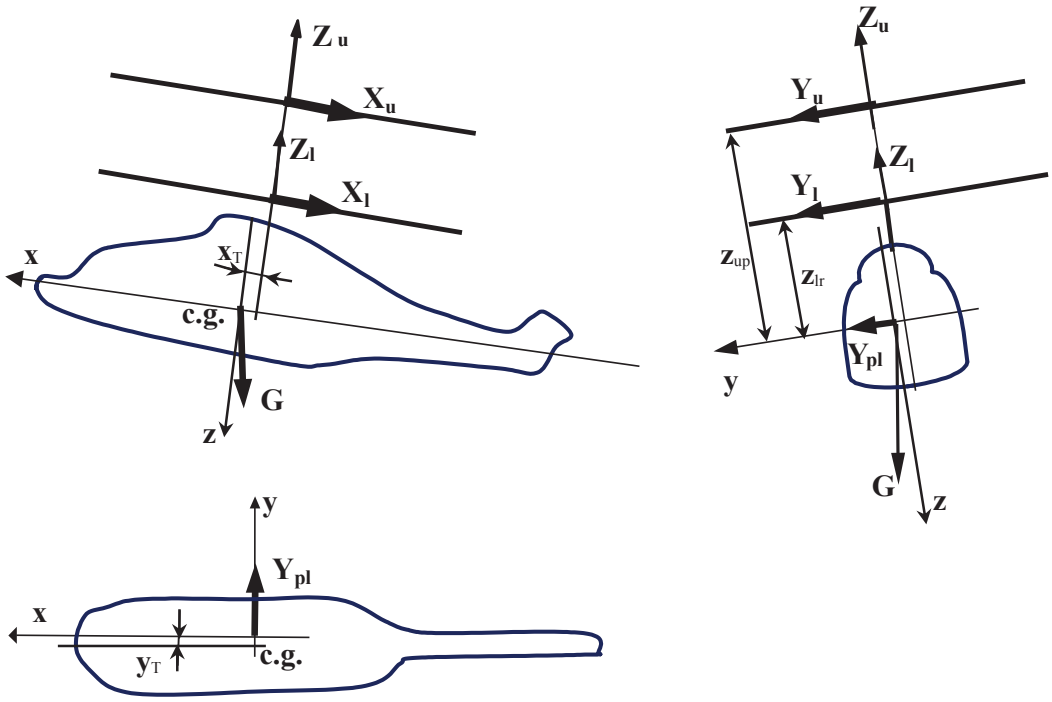

Figure 2.16: Coaxial Helicopter Forces (b)

The upper and lower rotor forces for case of a horizontal straightforward flight along z-axis are:

$$N_u = X_u\, y_T + Y_u\, x_T + N_{up}$$
$$N_l = X_l\, y_T + Y_l\, x_T - N_{lr} \qquad 2.6.11m$$

Terms such as x_T and y_T, are zero due to the offset between the rotor axis and the center of gravity. The offset between the rotor axis and the helicopter's center of gravity is expected to be zero. It is assumed that the helicopter's center of gravity is in line with the rotor axis.

$$N_u = N_{up}$$
$$N_l = -N_{lr}$$
$$N_{up} = m_{up}(1/2)\rho A\Omega_u^2 R^3 \qquad 2.6.11n$$
$$N_{lr} = m_{lr}(1/2)\rho A\Omega_l^2 R^3$$

where N_u is Aerodynamics moment along the z - axis acting at upper rotor, N_{up} is Rotational mo-

ment along the z - axis acting at upper rotor, N_l is Aerodynamics moment along the z - axis acting at lower rotor, N_{lr} is Rotational moment along the z - axis acting at lower rotor, m_{up} is Rotational moment coefficient for upper rotor, m_{lr} is Rotational moment coefficient for lower rotor.

2.7 Thrust and Torque Coefficients

One of the major design parameters for the helicopter are the thrust and torque dimensionless coefficients. In order to achieve the thrust and torque components dimensionless relationships, in this work we use as representative velocity the rotor tip speed as its described in this work and the literature [4]. The thrust force of the rotor is proportional to the thrust coefficient, the area swept out by the rotor, air density, and the square of the circular velocity of the blade tip as described in literature [1], [2] and [4]. The thrust depends on the number of revolutions and the thrust coefficient, at a constant air density. The induced velocity may be calculated when the thrust is known.
Thrust and Torque coefficients C_T and C_Q are given by:

$$\begin{aligned} C_T &= C_{Tu} + C_{Tl} \\ C_Q &= C_{Qu} + C_{Ql} \end{aligned} \qquad 2.7.1$$

The upper and lower thrust coefficients are given by:

$$\begin{aligned} C_{Tu} &= \frac{T_u}{(1/2)\rho A(\Omega_u R)^2} \\ C_{Tl} &= \frac{T_l}{(1/2)\rho A(\Omega_l R)^2} \end{aligned} \qquad 2.7.2a$$

The upper and lower torque coefficient is given by:

$$\begin{aligned} C_{Qu} &= \frac{Q_u}{(1/2)\rho A\Omega^2 R^3} \\ C_{Ql} &= \frac{Q_l}{(1/2)\rho A\Omega^2 R^3} \end{aligned} \qquad 2.7.2b$$

where T_u is upper rotor disk thrust, T_l is lower rotor disk thrust, Q_u is upper rotor disk torque, Q_l

is lower rotor disk torque, R is blade radius, Ω_u is upper rotor angular velocity, Ω_l is lower rotor angular velocity, ρ is density of air at 15 ^0C and sea level, A is the rotor disc area ($A = R^2\ \pi$)

2.8 Figure of Merit

A criterion of efficiency to judge the effectiveness of the rotor in producing thrust is the Figure of Merit. In the hovering flight condition, power is expended in producing thrust T, while the axial flow velocity seen by the rotor V is zero. The lifting rotor needs some other measure of efficiency to judge lifting capability. This is accomplished by comparing the actual power required to hover with the ideal power required to hover. The Figure of Merit equation specifies the relationship among the thrust and torque coefficient, number of blades, solidity, rotor radius and blade chord. The larger the value of FM, the smaller the power required to produce a given thrust, or the larger the thrust per unit power. An ideal rotor FM should equal 1. However, this is based on the assumption of uniform inflow conditions, zero-profile drag, and no tip losses. The FM can be used as a measure of the efficiency of a rotor generating thrust for a given power. It should only be used as a comparative measure between two rotors at the same thrust coefficient. For the main rotor thrust, we assumed that the inflow is steady and uniform. A momentum theory was adapted to compute the thrust coefficient and inflow ratio as a function of airspeed, rotor speed and collective setting. The momentum theory approach was shown to be adequate for estimating steady state main rotor thrust both at hover and in fast forward flight.

This leads to the rotor Figure of Merit, FM, given by

$$FM = \frac{{C_T}^{3/2}}{C_Q\sqrt{2}} \qquad 2.8.1$$

The coaxial helicopter FM has the same form as the single-rotor helicopter FM. The Figure of Merit equation identifies relationships among the thrust and torque coefficient. The larger the value of FM, the smaller the power required to produce a given thrust. The FM should only be used as a relative measure between two helicopters at the same thrust coefficient.

2.9 Inertia

Inertia opposes linear and angular acceleration to stabilize motion. To calculate the moment of inertia, we assume the rotor can be modeled as thin disk, the rotor shaft as thin cylinder and helicopter fuselage as solid cuboid or rectangular prism. Upper and lower rotors are same and they have similar inertia (opposite directions). Direction of rotation is opposite between upper and lower rotor. Inertia of stabilizer bar is neglected. The moment of inertia of helicopter fuselage modeled as solid rectangular prism is shown in Figure 2.17.

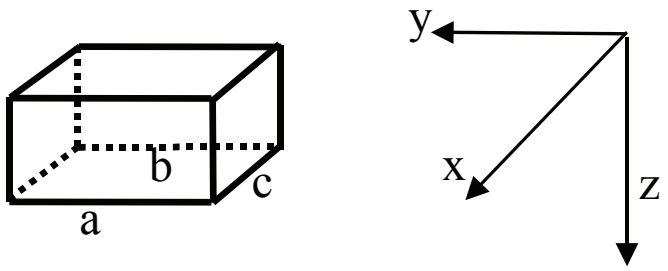

Figure 2.17: Helicopter fuselage moment of inertia

The moment of inertia for axis x, y and z that passes through center of gravity of fuselage.

$$\begin{aligned} I_x &= \tfrac{m(a^2+b^2)}{12} \\ I_y &= \tfrac{m(c^2+b^2)}{12} \\ I_z &= \tfrac{m(a^2+c^2)}{12} \end{aligned} \qquad 2.9.1$$

Mass moment of inertia of blades (bar) about mass center

$$\begin{aligned} I_x &= \tfrac{m(D/2)^2}{6} \\ I_y &= \tfrac{m(D/2)^2}{6} \\ I_z &= \tfrac{mD^2}{12} \end{aligned} \qquad 2.9.2$$

where D is rotor's diameter.

$$I_x = I_y$$
$$I_z = I_x + I_y \qquad 2.9.3$$

The rotor's shaft inertia, modeled as a hollow cylinder

$$I_x = \frac{m({a_s}^2+{b_s}^2)}{4} + \frac{ml^2}{3}$$
$$I_y = \frac{m({a_s}^2+{b_s}^2)}{4} + \frac{ml^2}{3} \qquad 2.9.4$$
$$I_z = \frac{m({a_s}^2+{b_s}^2)}{2}$$

where m is mass (mass of blade or mass of shaft, or mass of fuselage), a_s is outer radius of shaft, b_s is inside radius of shaft, a is length of fuselage (rectangular prism), l is length of shaft, b is height of fuselage (rectangular prism), c is depth of fuselage (rectangular prism).

Chapter 3: Actuator Dynamics

3.1 Introduction

A fully functional flight control is crucial for micro coaxial helicopter. A typical coaxial rotorcraft actuator dynamics system (including the two rotors, swash-plate, pitch links, etc.) is relatively complex. Aerodynamic symmetry is an important coaxial helicopter characteristics. It improves its controllability and stability significantly. Rotors' side forces in different directions balance each other with their lateral moment, which occurs due to their separation being insignificant. As a results of the lack of the tail rotor, the coaxial helicopter is not subject to the constant influence of the alternate side force. The coaxial design confirms a smooth combination of efficient control and aerodynamic damping, which provides good controllability. The micro coaxial helicopter motions are controlled by the two main rotors. We first need to understand the behaviors of the two rotors in flight before analyzing the dynamics of coaxial helicopter. The two rotors are the important mechanisms in this helicopter design because they generate most of the forces and torques applied to the helicopter body.

The upper rotor of the helicopter is not linked to any servo, so a mechanical stabilizer is used to induce cyclic pitch control of the rotor when it senses the inclination of the fuselage. The upper rotor is equipped with an adjustable linkage between the Stabilizer Fly-bar and upper rotor. This linkage allows tuning the tracking of the upper rotor for smoother and more stable performance as described in the literature [4], [14] and [19]. The stabilizer bar with upper rotor forms a Hiller control system. The Hiller control system has the effect of changing in reaction to helicopter tilt to slow and stabilize tilt motion. In the absence of aerodynamic forces and external moments, the fly-bar behaves as a gyroscope, maintaining its orientation relative to inertial space. In a hover, the fly-bar angle is zero.

The lower rotor is connected to two servos, which control the helicopter's pitch and roll. The rotational velocity of rotors is controlled by two different motors. The forward-facing motor changes

Figure 3.1: Upper rotor

Figure 3.2: Lower rotor

the blade speed of the upper rotor while the back motor controls the lower rotor. The parameters relating the angular velocities of the helicopter to the lateral and longitudinal motion, as well as the effects of the velocities on the moments are to be identified. The velocities are also affected by gravitational force acting on the aircraft due to the change in the lateral and longitudinal position.

3.2 Control Inputs

The control system provides external inputs to servo and motor to generate pitch, roll, and rotor speed. These controls cause forces and torques to be applied to the helicopter and result in helicopter movement. There are four inputs available for the model helicopter. The control inputs for the micro

coaxial helicopter are applied in ways different from larger helicopters.

Yaw Control

Yaw control can be performed by varying the difference in rotational speed between the two rotors, creating a torque applied to the fuselage. Helicopter will turn to the left with an increase in speed of the lower rotor while decreasing the speed of the upper rotor. Helicopter will turn to the right with an increase in speed of the upper rotor while decreasing the speed of the lower rotor.

The upper and lower disk direction of the rotor rotation is shown in Figure 2.10.

Thrust Control

Thrust (altitude) control is accomplished by varying the rotational speed (rpm) of the both rotors simultaneously and the same value (Figure 2.9). The rotational velocity of rotors is controlled by two different motors. The front motor changes speed of the upper rotor, while the back motor controls the lower rotor. When the speed of both rotors increases, the helicopter climbs, and when the speed of both rotors decreases, the helicopter descends.

Pitch Control

Pitch (longitudinal pitch) is controlled by varying the angle of the rotors as they go around (tilting the rotor back and forth). When the pitch input is applied to the system, the rear servomotor will push the swash-plate upward/downward, tilting the rotor disk back and forth. The control input for the forward flight is when the rear servo motor, on the left hand side looking from tail, pushes the swash-plate upward. When the control input pitches the nose of the helicopter downward, the helicopter moves forward (forward flight shown in Figure 2.9). The control input for the rearward flight is when the rear servo motor, on the left hand side looking from tail, pushes the swash-plate downward (rearward flight shown in Figure 2.9). When the control input pitches the nose of the helicopter upward, the helicopter moves backward (rearward flight).

Roll Control

When moved left or right the rotor tilts in that direction and the helicopter banks and rolls. Roll is controlled by varying the angle of the rotors left or right. When the control input applied to the system, the forward servomotor will push the swash-plate upward/downward. The control input for

the roll helicopter to the left is when the forward servo motor pushes the swash-plate upward. When the control input left pushes the swash-plate upward, the helicopter rolls to the left. The control input for the roll helicopter to the right is when the forward servo motor push the swash-plate downward. When the control input right pushes the swash-plate downward, the helicopter rolls to the right.

3.3 Linearization

Understanding the flight behavior of helicopters and rising rational descriptions for the many dynamic characteristics, cannot be achieved simply through developing the equations, or even by building a simulation model, only. These are needed but insufficient activities. The development of a deep understanding of flight behavior comes from the intellectual interaction between theory and practice, with an accent on hands-on practice and analytical theory. Most of the understanding of stability has come from somewhat simple theoretical approximations. The equations used during model development process are the three forces (X, Y, and Z) equations and the three moments (rolling, pitching, and yawing) equations are nonlinear.

An essential assumption of linearization is that the external forces X, Y and Z and moments L, M and N can be represented as analytic functions of the disturbed motion variables and their derivatives. Taylor's theorem for analytic functions then implies that if the force and moment functions (i.e., the aerodynamic loadings) and all its derivatives are known at any one point (the trim condition), then the behavior of that function anywhere in its analytic range can be estimated from an expansion of the function in a series about the known point. Using small perturbation theory as described in the literature [1], we assume that, during disturbed motion, the helicopter behavior can be described as a perturbation from the trim, written in the form

$$x = x_e + \delta x \tag{3.3.1}$$

The forces can be written in the approximate form

$$X = X_e + \frac{\partial X}{\partial u}\delta u + \frac{\partial X}{\partial w}\delta w + ... + \frac{\partial X}{\partial \theta_0}\delta\theta_0 + ... \tag{3.3.2}$$

All six forces and moments can be expanded in this manner. The linear approximation also contains terms in the rates of change of motion and control variables with time, but we shall neglect these initially. The partial nature of the derivatives indicates that they are obtained with all the other DoFs held fixed; this is simply another manifestation of the linearity assumption. For further analysis we shall drop the perturbation notation, and write the derivatives in the form,

$$\frac{\partial X}{\partial u} = X_u \qquad etc... \tag{3.3.3}$$

The validity of linearization depends on the behavior of the forces at small amplitude, i.e.; as the motion and control disturbances become very small, the dominant effect should be a linear one.

Trim model is based on a perturbed-state assumptions hence the trim values around the point of linearization must be accounted for in the model. We account for the known trim values by modeling them as fixed preferences. Input preferences are implemented to account for the initial conditions of the inputs. The initial conditions of other states are also modeled through variable preferences.

The basic structure of the model can be defined in the well-known linear state space form.

The linearized equations can be used in state-space modeling.

It's appropriate to choose the output variables to be the state variables as follows:

$$\dot{x} = Ax + B_2 u \tag{3.3.4a}$$

$$y = C_2 x + Du \tag{3.3.4b}$$

Where C = I is identity matrix (n x n), D = 0 is zero matrix (n x m),

The linearized equations of motion for the full 6 DoFs, describing perturbed motion about a general trim condition, can then be written as

$$\dot{x} = Ax + B_2 u(t) + f(t) \tag{3.3.5}$$

where the additional function f(t) has been included to represent atmospheric and other disturbances. The coefficients in the A and B matrices represent the gradient of the forces and moments at the trim point reflecting the strict definition of the stability and control derivatives. C is the output

matrix (which is usually an identity matrix), D is the matrix representing coupling between input and output (which for aircraft applications usually consists of zeros), "u" is the input vector , and "y" is the output vector.

The linearized model's state vector "x" is defined as the change in each state from the nominal linearized condition. For the helicopter control, we define observable states to correspond with the standard 12 states of 6 DoF rigid body model.

$$x = \begin{bmatrix} x & y & z & u & v & w & \phi & \theta & \psi & p & q & r \end{bmatrix}^T \tag{3.3.6}$$

The input vector "u" represents the changes in control inputs, with respect to the linearized condition. It can be separated into components as follows:

$$u = \begin{bmatrix} u_1 & u_2 & u_3 & u_4 \end{bmatrix} = \begin{bmatrix} \delta_{\mathrm{m}} & \delta_{\mathrm{z}} & \delta_{\mathrm{l}} & \delta_{\mathrm{n}} \end{bmatrix} \tag{3.3.7}$$

The state-space equations can be used for the simulation of aircraft motion following a control input using MATLAB and Simulink. The state-space equations have a further advantage in that the equations can be used to simulate not only the single input single output (SISO) motion, but also the multiple input multiple output (MIMO) motion of the aircraft.

The 6-DoF model developed for the micro coaxial helicopter incorporate the state-space representation of the equations of motion. A and B matrices also consist of the derivatives that represent the coupling between the various dynamics. A few of them have a effect on the helicopter dynamics. The others have a negligible effect on the dynamics.

3.4 The Dynamics with Control Inputs

The coaxial design guarantees a smooth combination of efficient control and aerodynamic damping. The controls of micro coaxial helicopter are essentially similar as those for single-rotor helicopters. We will model the helicopter as a rigid body moving in space. In the helicopter model we will use the Rigid Body equations of motion as shown in Equation 2.4.1. The moment of force is a measure of its

tendency to rotate an object about some point. The helicopter components of the resultant moment in the body axis system are L, M and N. The moment of inertia measures the object's ability to resist changes in rotational speed about a specific axis. The larger the moment of inertia the smaller the angular acceleration about that axis for a given torque. Euler angles are means of representing the spatial orientation of any frame of the space as a composition of rotations from a reference frame. Because it is a rigid body, the helicopter's position and orientation in body coordinates will always be zero; however, the velocity and acceleration terms are significantly simplified by using these coordinates. The aerodynamic interface between the rotor and the fuselage is ignored. The standard rigid body dynamical equation will be used to model the motion of the helicopter in its environment. The offset between the rotor axis and the helicopter's center of gravity is expected to be zero. It is assumed that the helicopter's center of gravity is in line with the rotor axis. In order to develop a coupled body/rotor dynamics model, a hybrid model is used in which the rotor and body virtual steady dynamics are combined. The inputs are directly included in the rotor dynamics.
The micro coaxial helicopter forces and moments with direct control inputs could be divided as following:

$$\begin{aligned} Z &= -Z_u - Z_l - Z_{pl} - muq + mvp + Gcos\theta cos\Phi + E_z\delta_z \\ L &= L_u + L_l - L_{pl} - (I_y - I_z)\, qr + E_l\delta_l \\ M &= M_u + M_l - M_{pl} - (I_z - I_x)\, pr + E_m\delta_m \\ N &= N_u + N_l - N_{pl} - (I_x - I_y)\, pq + E_n\delta_n \end{aligned} \tag{3.4}$$

In this work, the following values are used as control inputs:
δ_z is altitude input, δ_l is roll input, δ_m is pitch input, δ_n is yaw input. E_z is the thrust control derivative, E_l is the rolling moment control derivative, E_m is the pitching moment control derivative, E_n is the yawing moment control derivative.
It is assumed that the blade axis, aerodynamics axis, control axis and center of mass axis match. Also, in hovering, the sum of all forces and moments on the helicopter center of mass has to be zero. Identifying stability and control derivatives from flight test data can be used to provide accurate

linear models for control law design or in the estimation of handling qualities parameters. Our principal interest at this time is the application to simulation model validation.

Rotor force and moment derivatives are closely related to individual thrust and flapping derivatives. Many of the derivatives are strongly nonlinear functions of velocity, particularly the velocity derivatives themselves. The derivatives are also nonlinear functions of the changes in down-wash during perturbed motion, and can be written as a linear combination of the individual effects, as in the thrust coefficient change with advance ratio.

There are three approaches to estimating stability and control derivatives: analytic, numerical, backward - forward differencing scheme and system identification techniques.

The system identification approach seeks to find the best overall model fit and, as such, will embody the effects of any nonlinearities and couplings into the equivalent derivative estimates. The states are no longer perturbed independently; instead, the nonlinear model, or test aircraft, is excited by the controls so that the aircraft responds in some 'optimal' manner that leads to the maximum ability to identify the derivatives. The derivatives are varied as a group until the best fit is obtained.

Chapter 4: Experimental Study

4.1 Introduction

In order to correctly predict the micro coaxial helicopter flight dynamics, a comprehensive physical model is essential. This model should be as general as possible, creating the minimum number of assumptions. These data were to be used to estimate some of the parameters of the rotor model. The results from the experimental test were to be used to validate the helicopter model. Also, experimental tests have an impact on learning about the micro coaxial helicopter configuration. Along with gathering data, the fixture is being used for safe testing of the helicopter. The test fixture holds the helicopter, keeping it from coming into contact with objects as well as people. While using the test fixture shown in Figure 4.1, it was found that it would be necessary to isolate roll, pitch and yaw.

4.2 Micro Coaxial Helicopter Modeling Process

The helicopter testing and measurement was performed to better understand technical characteristics of the helicopter and vital parts.

The modeling process includes the following steps:

1. Existing configuration measurement includes the following: blade characteristics (dimensions, weight), DC motor characteristics (electro. characteristics, weight), servo motor characteristics (electro. characteristics, weight), major parts weight.

2. Helicopter testing using the Test bench includes the following: testing in hover, vertical (axial) flight test, the helicopter testing with different load/weights (min. to max. weight).

3. Development includes the following: the helicopter configuration development with a new blade, theoretical explanation and rationale to use a new blade design, investigation and estimate of possibility to use other DC Motor than the existing one, theoretical explanation and rationale to use a new electrical motor.

4.3 Investigation

To achieve indoor flight, the unmanned micro coaxial helicopter required the installation of instruments and sensors on aircraft. In order to install instrumentation on the micro helicopter, it was necessary to understand the helicopter payload capabilities. The weight-lifting experiment will resolve the payload capabilities for the purpose of sizing the instrumentation.

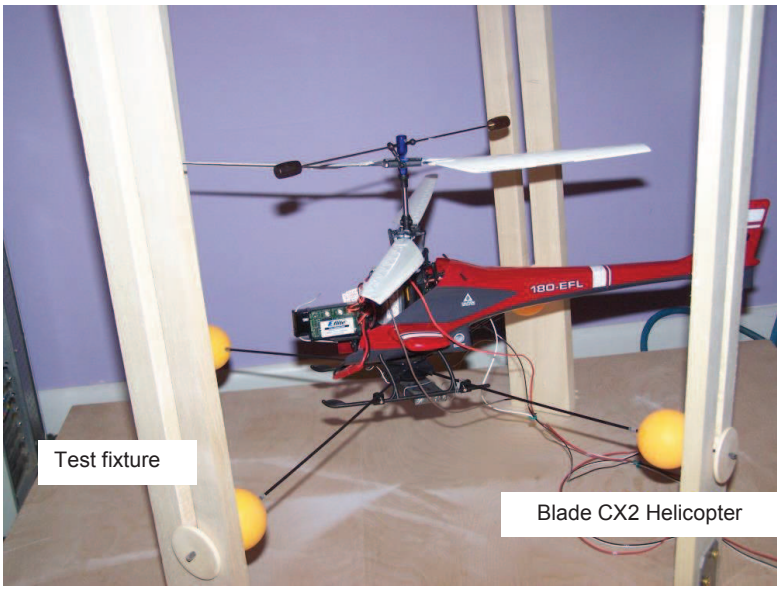

Figure 4.1: Test fixture with coaxial helicopter

While the hover performance of conventional full-scale rotorcraft configurations is known in the literature, the hover performance of micro coaxial helicopter in hover is unknown. Therefore, the baseline configuration micro coaxial helicopter was flown in a laboratory environment. It was tested in a custom-designed hover stand to evaluate its performance. The primary disturbance source is wind gust. Because the helicopter is so small and dense, disturbances are relatively small for indoor flight. Rotor speed was measured by a Portable Stroboscope. Rotor thrust was measured by a digital scale. Input power for the electric motor was recorded by use of a voltmeter attached to the power input cables. Rotor shaft power was estimated using a correction methodology based on electric motor efficiency estimates. Hobbyist radio-controlled (RC) helicopter model Blade CX2 Helicopter was utilized for these experiments [31].

4.4 Description of Experimental Test

Hobbyist radio-controlled helicopter Blade CX2 model with its original rotor blades was used for experiments. In the hovering flight condition, power is expended in producing thrust, while the axial flow velocity seen by the rotor is zero. The lifting rotor needs some other measure of efficiency to judge lifting capability. This is accomplished by comparing the actual power required to hover with the ideal (total) power required to hover. This leads to the rotor Figure of Merit (FM). The Figure of Merit was a crucial factor of efficiency to evaluate effectiveness of helicopter rotors in producing thrust. The larger the value of FM, the smaller the power required to produce a given thrust, or the larger the thrust per unit power. As described in literature [1], [2] and [6], for moderate values of thrust coefficient typical solidity, a good FM value is around 0.75. However, this estimate is based on the assumption of uniform inflow conditions, zero-prone drag, and no tip losses.

The FM shown in Equation 2.8.1 can be used as the efficiency measure of a rotor generating thrust for a given power. The coaxial rotor FM has the same form as for single rotor. As described in literature [22], the rotor FM for the coaxial rotor is much higher than for the single rotor of equal solidity (σ).

The rotor blade solidity factor σ is defined by relationship between the blade area and disc area as follows:

$$\sigma = \frac{\text{blade area}}{\text{disc area}} = \frac{N_b\ c\ R}{\pi\ R^2} = \frac{N_b\ c}{\pi\ R} \tag{4.4.1}$$

where N_b is number of blades on rotor, c is rotor blade chord, R is rotor radius.

The DC Motor characteristics were measured and calculated using the following formulas:

$$\omega_m = (Q_{stm} - Q_m)\ \omega_n\ /\ Q_{stm} \tag{4.4.2}$$

where ω_m is speed of the DC Motor output shaft, Q_{stm} is stall torque, ω_n is speed without load, Q_m is the DC Motor torque.

4.5 Experimental Study Analysis

The micro coaxial helicopter was installed as shown in Figure 4.1. The tests were performed with test results explained below. During our experiment the speed of the DC Motor shaft (rpm) was adjusted remotely by a transmitter. The test stand provided the ability to perform tests in hover and vertical (axial) flight. This test provided fundamental data for developing a new micro coaxial helicopter configuration including a new micro helicopter parts like rotor blade and motors. We would have the ability to install required sensors and instruments on the new micro coaxial helicopter. The new helicopter configuration with the controller and sensors would be able to perform tasks for an indoor flight mission like inspection, surveillance, and so on.

Extensive testing was performed to establish a relationship between the electric motor characteristics and the rotor characteristics. In order to find the relationship between the shaft speed and the motor shaft torque, we computed the electric motor torque using Equation 4.4.2. Current configuration has the electric motor with speed without load (output speed of the motor is max. without torque applied to the output shaft) is $\omega_n = 16\ 000$ (rpm). Torque is inversely proportional to the speed of the motor shaft. The electric motor speed (rpm) and electric motor torque are shown in Figure 4.2. Relationship between the torque generated by the electric motor and by coaxial rotors is shown in Figure 4.3 and expressed by the following equation:

$$\begin{aligned} Q_r &= G_r\ Q_m \\ G_r &= \tfrac{M_g}{T_p} \end{aligned} \qquad 4.5.1$$

where Q_r is rotor torque, Q_m is motor torque, G_r is gear to pinion ratio, M_g is main gear teeth, T_p is pinion teeth.

The electric motor speed and the rotor torque and speed are shown in Figure 4.4. It's useful to have the relationship between the rotor speed and rotor torque as shown in Figure 4.5. The electric motor power is changed with voltage (motor supply) change. Connection between the both rotors speed (upper and lower rotors speed) and electric motors supply (volts) is shown in Figure 4.6.

The thrust and torque coefficients for upper and lower rotor were computed using the thrust and

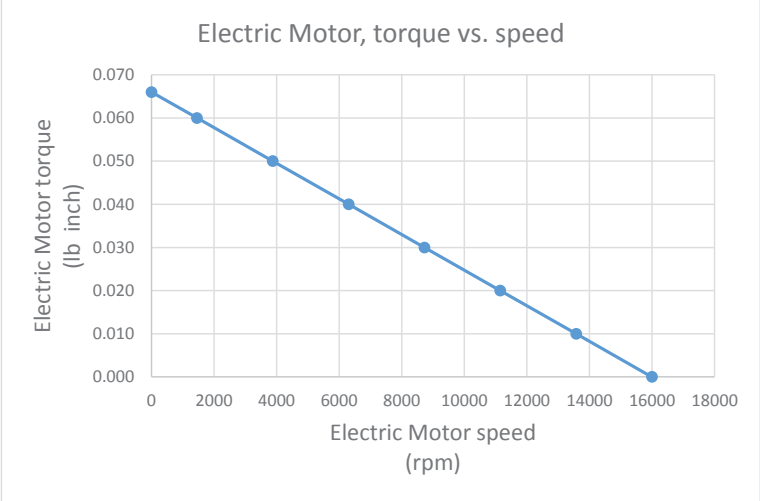

Figure 4.2: The Electric Motor speed and torque

torque coefficients equations described in this work (Equation 2.7.2).

4.5.1 Measurement and test results

The micro coaxial helicopter used during experimental test has the following data:

Gw = 0.4735 lb, A = 1.001 ft^2, R = 6.77 inch, ρ = 0.07647 lb/ft^2

Measurement was performed at the beginning of hover with results as follows: The upper rotor speed (ω_u) was 226 rpm and lower rotor speed (ω_l) was 213 rpm. The helicopter total weight was 0.4735 lb.

The rotor torque are as follows: The upper rotor torque was 0.56 lb-inch, The lower rotor torque was 0.57 lb-inch.

The thrust and torque coefficients are as follows: C_{Tu} = 0.1153, C_{Tl} = 0.1299, C_T = 0.2452, C_{Qu} = 3.45, C_{Ql} = 3.96, C_Q = 7.41.

Figure of Merit (FM) was 0.01158.

.

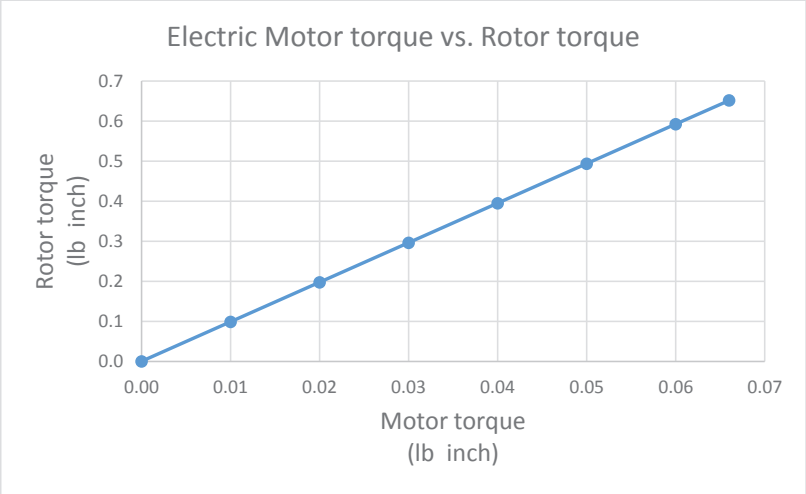

Figure 4.3: The Helicopter's Rotor torque and Electric Motor torque

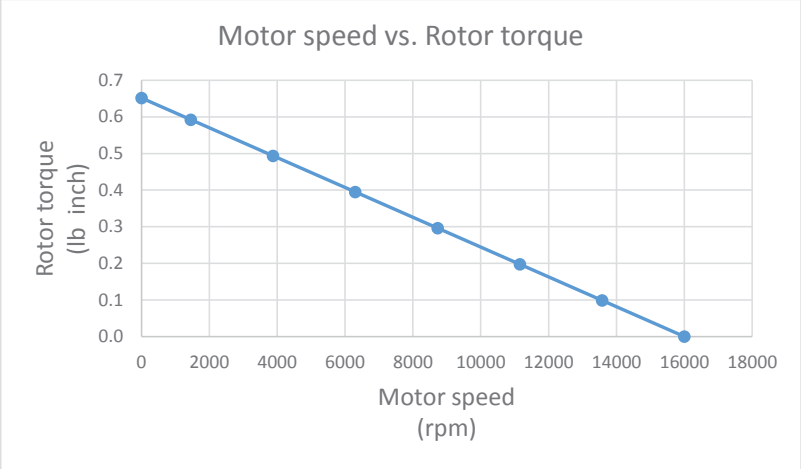

Figure 4.4: The Helicopter's Rotor torque and Electric Motor shaft speed

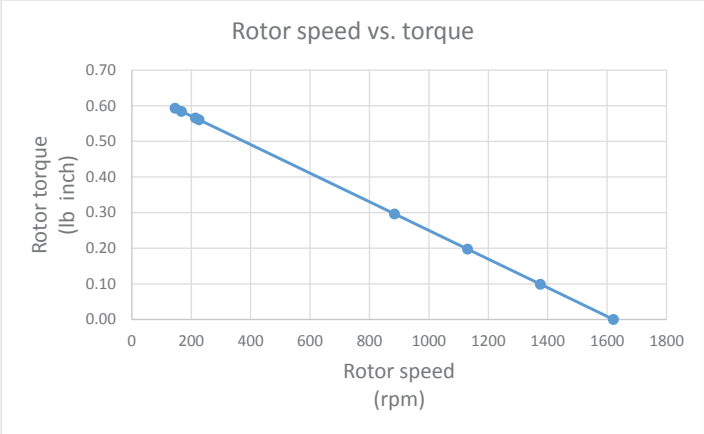

Figure 4.5: The Helicopter's Rotor speed and torque

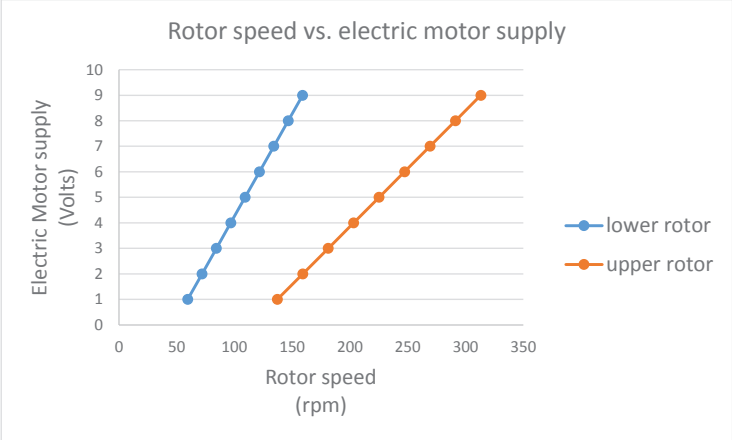

Figure 4.6: The Helicopter's Rotor speed and motor supply (voltage)

4.5.2 Experimental Study Summary

The micro coaxial helicopter analysis offer data (weight, thrust at hover, electric motor supply voltage, the moment of inertia) that we could use during further work on the Controller design and Flight simulation (MatLab, Simulink and FlightGear flight simulator).

The micro coaxial helicopter performance regarding cargo (payload) and efficiency was poor.

It would be necessary to develop a new micro coaxial helicopter with a goal to achieve a helicopter configuration with optimum size and power.

The requirement for indoor flight introduces limits related to the helicopter size. The helicopter power shall be increased to provide lift, optimum speed for indoor flight and payload shall be able

to carry all essential sensors and instruments.

The new micro helicopter configuration should introduce improvement for the rotor blades, electric motor and an electric battery (motor supply). The improved helicopter design would be able to perform flight test and achieve all required tasks.

Chapter 5: Flight Control Design

5.1 Model Analysis

There exists a wide range of studies on the dynamics of full-scale helicopters. The models used in full-scale helicopter simulators are high order and cover a large number of parameters. A few of the full-scale helicopters have the control ability of most active small-scale helicopters. The micro coaxial helicopters are now well within the reach of many hobbyists. However, these helicopters models' are unstable. Even with improved stability amplification devices, a skilled, experienced person is required to control them during flight. The micro helicopter is a highly maneuverable device. In this work we will model the helicopter as a rigid body moving in space. The standard rigid body dynamical equation will be used to model the motion of the helicopter in its environment as it's described in this work and in the literature [1], [2] and [4]. For comprehensive analysis and controller design, it is convenient to work with a closed-form mathematical model of a system. A good mathematical model is one that will approximate the system responses to given inputs in its region of validity with acceptable accuracy. The helicopter is a nonlinear, unstable and highly coupled system and it exhibits considerably different responses to inputs in every flight regime (such as hover, cruise, turning flight, etc.). Hence, it is not always reasonable to develop a single linear model that is valid throughout the flight envelope; the outline must be applied to approximate the model dynamics mathematically using closed-form equations. It is common practice to linearize a complex system about a nominal set point for the purpose of design and analysis. For these linearized models to be valid, the nonlinear system must behave linearly within a defined region about the specified nominal point. Additionally, the system must operate within the defined linear region for the duration of concern. This approach is valid for many nonlinear systems operating at stable steady-state or quasi-steady-state conditions, but is questionable when extremely nonlinear behavior is leading. A sequence of linear models is used to truly approximate the nonlinear system, which allows for linear system analysis and controller design methods to be engaged.

A modeling in state space approach was chosen due to the follow-on computational capabilities. The linear model is also found to be well suited for simulation purposes. The model that takes in a linearized 6-DoF MIMO state-space realization of the aircraft dynamics about a user-defined trim point. The basic structure of the model can be defined in the well-known linear state space form. The control problem schematic representation in its simplest generalized form is shown in Figure 5.1. The G generalized plant is the system to be controlled by the controller, K. Together G and K form the closed-loop system. The problem is categorized by the aspiration for the plant to follow, or track, some reference command θ_r. This is done by creating an appropriate control input to the generalized plant, $u_{(t)}$, the exogenous input to the system w_1, based on the measured output of the plant, $y_{(t)}$, while simultaneously trying to minimize the influence of disturbances on the plant, $v_{(t)}$. The effectiveness of K is evaluated by its ability to minimize the norm of the controlled output vector, $z_{(t)}$. This vector is typically separated into two parts: the output-tracking error, $z_{1(t)}$, and the control input constraints, $z_{2(t)}$.

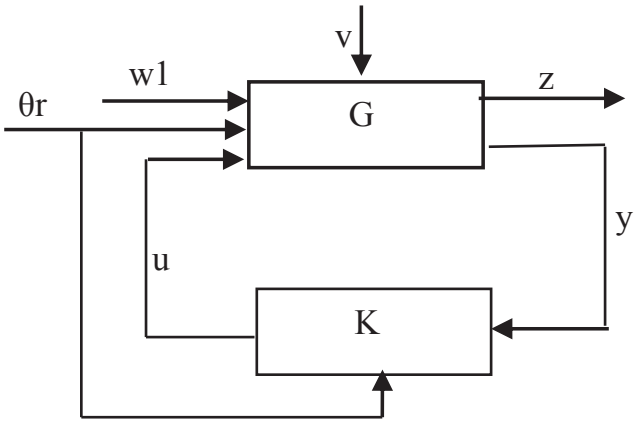

,

Figure 5.1: The tracking closed-loop system

For the work discussed within this dissertation, the controller, K, is designed to stabilize the closed-loop system, to fly the flying aircraft under some itemized condition(s), and to minimize the brief and steady-state tracking errors subject to control input restrictions.

To meet these goals, the servomechanism formulation can be carried out using output-tracking regulation theory with conjunction with H_2 optimization schemes.

The generalized plant G can be described by the equation 5.1.1 ,

$$\begin{aligned} \dot{x}_{(t)} &= A\ \ x_{(t)} + B_1\ \ w_{1(t)} + B_2\ \ u_{(t)} \\ y_{(t)} &= C_2\ \ x_{(t)} + v_{(t)} \end{aligned} \tag{5.1.1}$$

,

$$z(t) = \begin{bmatrix} C_{1u} \\ 0 \end{bmatrix} x(t) + \begin{bmatrix} D_{11u} \\ 0 \end{bmatrix} \theta_{r(t)} + \begin{bmatrix} 0 \\ D_{12d} \end{bmatrix} u(t) \tag{5.1.2}$$

$$B_2 = B \tag{5.1.3}$$

where A is plant state-space internal dynamics matrix, B_1 is state-space input disturbance matrix, B_2 is state-space input control matrix, C_2 is state-space observation matrix, x is the state vector, y is the measured output vector, C_{1u} is control output gain matrix, D_{1lu} is identity matrix, θ_r is reference command, D_{12d} is controlled output gain matrix, u is the control input vector, v is the measurement noise, z is the controlled output vector, w_1 is the input vector to the system developed from external factors (exogenous input or disturbance to the system).

5.2 Controller Design

5.2.1 General

Controller development throughout this dissertation is originated on a very specific control scheme, based on closed-loop multi-variable output-tracking regulation and H_2 optimized feedback control. This structure acts as the basis of each system presented herein. As such, this structure is worth reviewing for the general case before going into specific examples, allowances, and applications. The basic concept of output-tracking control is very direct. An output-tracking controller is a closed-loop system that measures the output of a system plant and adjusts the input to the plant such that the output tracks a desired reference signal. The servomechanism design is engaged to develop a closed-loop output-tracking regulator that uses input gain matrices together with an H_2 feedback controller to regulate the output of the aircraft parameters. The gains are used in combination with

the input signal from external factors to extend the state feedback into the generalized plant. In more advanced cases, the structure of the controller could be extended to include outer-loop compensator and reference input preprocessing subsystems. The basic structure of the model can be defined in the linear state space form. The initial effort is focused on identification of parameters of the model in hover. Since the identified parameters will be valid only around the point of linearization, different models must be identified for other types of flight.

For complex and nonlinear systems, the simulation can be carried out using the in-sequence linearized models. It is similar in nature to a approximation of the nonlinear system, where an approximately equivalent system is created from a set of linear models. The convenience of this approach is that linear analysis and design techniques can later be engaged for working with related dynamics. After simulation, the recorded states can be analyzed and transitional points in the dynamic performance can be distinguished. Linear analysis techniques can therefore be used to govern characteristics of parts of the trajectory as represented by the multi-linear model by using the localized mathematical solutions defined within the multi-linear model. The model is based on a perturbed-state assumptions; hence the trim values around the point of linearization must be accounted for in the model. We account for the known trim values by modeling them as fixed preferences. Input preferences are implemented to account for the initial conditions of the inputs. The initial conditions of other states are also modeled through variable preferences. This structure is derived for a linear system model. When systems act linearly and match the linear model, about which such regulation gains are defined, zero steady-state tracking error is indeed reachable using this control method. However, for poorly modeled systems, or nonlinear systems whose behavior deviates from the region about which dynamics were linearized, this approach must be extended to be effective in practice. The Matlab-Simulink model has four inputs and the 6DoF Block. The 6 (six) control inputs to plant or 6DoF Block (Matlab-Simulink Aerospace Block) are forces and moments (X, Y, Z, L, M, N), shown in Equation 2.4.1. The micro coaxial helicopter forces and moments with 4 control inputs are shown in Equation 3.4.

5.2.2 Controller

To achieve target tracking and subsystem alignment, an optimal controller is constructed based on the H_2 control theory and regulator theory described in this work and in the literature [8], [24], [25] and [26]. This thesis will consider the feedback control system described in the literature for the Tracking controller with full-state feedback. Consider the feedback control system shown in Figure 5.1 in which $G_{(s)}$ is the nominal plant and $K_{(s)}$ is the nominal controller that gives an optimal H_2 closed-loop performance.

The controlled output vector can be defined as

$$z(t) = \begin{bmatrix} z_1(t) \\ z_2(t) \end{bmatrix} = \begin{bmatrix} C_{1u} \\ 0 \end{bmatrix} x(t) + \begin{bmatrix} D_{11u} \\ 0 \end{bmatrix} \theta_{r(t)} + \begin{bmatrix} 0 \\ D_{12d} \end{bmatrix} u(t) \qquad 5.2.1a$$

The tracking command $\theta_{r(t)}$ is described by following

$$\dot{\theta}_{r(t)} = \mathrm{Z}\ \theta_{r(t)} + w_{r(t)} \qquad 5.2.1b$$

Where Z is zero (0) if $\theta_{r(t)}$ is a step function with arbitrary amplitude, $w_{r(t)}$ is an impulse function with arbitrary intensity, $z_{1(t)}$ is the output-tracking error, $z_{2(t)}$ is the control input constraints.

The problem now is to find a controller K as illustrated in Figure 5.2 so that,

i) the closed-loop system is internally stable,

ii) both tracking error and alignment error are zero at steady state,

iii) the performance index is minimized.

This can be achieved using the structure of the controller shown in Figure 5.2. The final step in assembling the tracking controller K is to combine the exogenous input estimator, the regulator parameters W and U, and the state feedback gain F. As long as the closed-loop system is internally stable and matches the plant model well, steady-state regulation will take place if **W** and **U** are chosen to satisfy the equations, as explained in next section of this work.

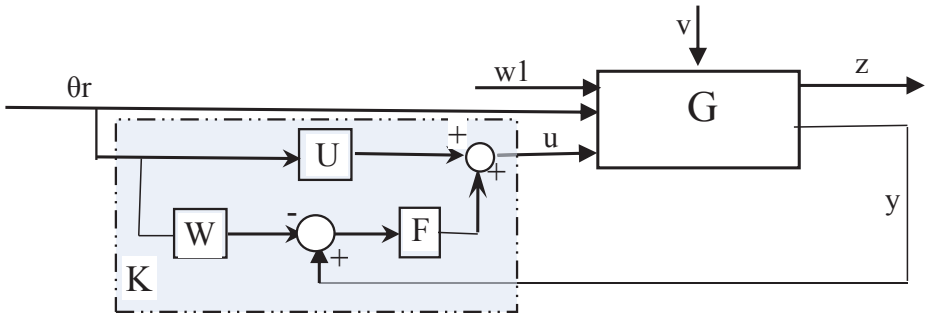

Figure 5.2: Generalized structure of a servomechanism output-tracking control regulator

5.2.3 Controller and Steady-State Regulation

The generalized structure of the controller is illustrated in Figure 5.2. The condition for the stabilizing controller is that the A, B_2 , C_2 are stabilizable and detectable [8], [24] and [25].

For the stabilizable and detectable system defined by A, B_2 , C_2, let ,

$$\bar{x} = x - W \;\; \theta_R \qquad 5.2.2$$

$$\bar{u} = u - U \;\; \theta_R$$

By substitution, the system, defined in Eq. 5.2.1, can now be expressed as,

$$\dot{\bar{x}}_{(t)} = A\,\bar{x}(t) + B_1\,w(t) + B_2\,\bar{u}_{(t)} + (A\,W + B_2\,U) \;\; \theta_{R(t)} \qquad 5.2.3$$

$$z_{1(t)} = C_{1u} \;\; \bar{x}(t) + (C_{1u} \;\; W + D_{11u}) \;\; \theta_{R(t)}$$

Setting coefficients of $\theta_{R(t)}$ to zero ($\theta_{R(t)} \neq 0$), it becomes as shown below,

$$A\,W + B_2\,U = 0 \qquad 5.2.4$$

$$C_{1u}\,W + D_{11u} = 0$$

According to the regulator theory, as described in the literature [7], [8], [24] and [25] zero steady-state tracking error is achievable by designing the controller parameters **W** and **U** to satisfy these equations. Note that, in our case, output regulation gains U and W are calculated in Mathematica [29]. If the closed-loop system is internally stable, the steady-state regulation will take place.

The system can be expressed as,

$$\dot{\bar{x}}_{(t)} = A\,\bar{x}(t) + B_1\,w(t) + B_2\,\bar{u}_{(t)} \qquad 5.2.5$$

$$z(t) = \begin{bmatrix} C_{1u} \\ 0 \end{bmatrix} \bar{x}(t) + \begin{bmatrix} 0 \\ D_{12d} \end{bmatrix} \bar{u}(t) \qquad 5.2.6$$

Where C_{1u} is control output gain matrix (matrix [4x12]) and D_{1lu} is identity matrix ([4x4]).

5.2.4 State Feedback Gain F

The final element necessary for executing this control structure is perhaps the most critical. The state feedback gain **F** is created on chosen weighting matrices that balance the cost of transient performance and input power. For nonlinear systems, this gain may also control overall system stability. Design of the state feedback gain begins with the selection of the above-mentioned weighting matrices. The general form of the servomechanism based output regulating tracking controller using H_2 optimization is thus well-defined. It is now suitable to begin exploring this control scheme. In the state feedback, we assume that the whole state **x** can be measured and as a result it is available for control. In this work, we will implement full-state feedback gain **F** and omit the estimator construction as shown in Figure 5.2.

We will design state feedback using nominal values of parameters and we will try to choose controlled output gains matrices. State feedback Gain F is achieved from the solution of the algebraic Riccati equation. The Gain **F** is computed as follows

$$F = -R^{-1}\ B^T\ X \qquad 5.2.7$$

where **X** is the positive semi-definite stabilizing solution of the following continuous time algebraic Riccati equation

$$A^T\ X + X\ A - X\ B\ R^{-1}\ B^T\ X + Q = 0 \qquad 5.2.8$$

The algebraic Riccati equation determines the solution of the Linear Quadratic Regulator problem (Matlab command lqr).

$$[F1] = lqr\ (A,\ B,\ Q,\ R) \qquad 5.2.9$$

It needs to be noticed that $F = -F_1$. Some methods assume that for state feedback $u = Fx$, though some assume that $u = -Fx$. The Matlab has the state feedback law u = - F x minimize the cost function, so in this work we need to change F to -F for our simulation.

In order to design state feedback, we need to define matrices Q and R. The state feedback is designed by using parameters and matrices Q and R in such a way that the state response is stable. The Q and R matrix choice is an important part of the state feedback gain design.

The most common choice of weighting matrices Q and R is diagonal matrices. The good values of R for micro coaxial helicopter nonlinear simulation were found out by trial and error.

$$R = {D_{12d}}^T \, D_{12d} \tag{5.2.10}$$

$$Q = {C_{1u}}^T \, C_{1u} \tag{5.2.11}$$

where D_{12d} is controlled output gains, $C1u$ is control output gain matrix.

The linear quadratic regulation method is used for determining our state-feedback control gain matrix **F**. The term "linear-quadratic" refers to the linear system dynamics and the quadratic cost function and we seek to find the gain vector F to minimize the "cost function". The MATLAB function **lqr** allows you to choose two parameters, **R** and **Q**, which will balance the relative importance of the control effort (u) and error (deviation from 0), respectively, in the cost function that we are trying to optimize. The cost function corresponding to this **R** and **Q** places equal importance on the control and the state variables which are outputs. Both matrices Q and R are symmetric real, Q is assumed to be at least positive-semi-definite ($Q = Q \geq 0$), R must be positive-definite ($R = R > 0$). If we set Q relatively large compared to R, the optimization procedure will result in the design in which x(t) is relatively "small" compared to $u_{(t)}$. If, in contrast, Q is rather small, that will tend to make $x_{(t)}$ larger and $u_{(t)}$ smaller. Increasing the magnitude of **Q** more would make the tracking error smaller, but would require greater control u. More control effort generally corresponds to greater cost (more energy, larger components and actuator, etc.). The micro helicopter has a fast time domain response due to its small size, and it's sensitive to small changes of parameters and matrices.

Chapter 6: Vertical Flight

6.1 Model Analysis

The micro helicopter is a highly maneuverable device. We will model the helicopter as a rigid body moving in space. The standard rigid body dynamical equation will be used to model the motion of the helicopter in its environment as it's described in this work and in the literature [1], [2] and [4]. For comprehensive analysis and controller design, it is convenient to work with a closed-form mathematical model of a system. The helicopter is a nonlinear, unstable and highly coupled system and it exhibits considerably different responses to inputs in every flight regime (such as hover, cruise, turning during flight etc.). It is common practice to linearize a complex system about a nominal set point for the purpose of design and analysis. A sequence of linear models is used to truly approximate the nonlinear system, which allows for linear system analysis and controller design methods to be engaged. The model incorporate initial conditions of the inputs and initial conditions of other states. They are presented through variable preferences at hover because in this work the initial effort is focused on identification of parameters of the model in hover. Modeling in state space approach was chosen due to the follow-on computational capabilities. The control problem schematic representation in its simplest generalized form is shown in Figure 5.1. The G generalized plant is the system to be controlled by the controller, K. Together, G and K form the closed-loop system.

The problem is categorized by a aspiration for the plant to follow, or track, some reference command θ_r. This is done by creating an appropriate control input to the generalized plant, $u_{(t)}$, the exogenous input to the system w_1, based on the measured output of the plant, $y_{(t)}$, while simultaneously trying to minimize the influence of disturbances on the plant, $v_{(t)}$.

The effectiveness of K is evaluated by its ability to minimize the norm of the controlled output vector, $z_{(t)}$. This vector is typically separated into two parts: the output-tracking error, $z_{1(t)}$, and the control input constraints, $z_{2(t)}$.

For the work discussed within this dissertation, the controller, K, is designed to stabilize the closed-

loop system, to fly the flying aircraft under some itemized condition(s), and to minimize the brief and steady-state tracking errors subject to control input restrictions. To meet these goals, the servomechanism formulation can be carried out using output-tracking regulation theory with conjunction with H_2 optimization schemes. The generalized plant G can be described by the equations 5.1.1. The linear state-space model was compute using the MatLab/Simulink command *linmod*. The linmod command extracts a continuous-time linear state-space model around an operating point.

$$[\text{ A, B, C, D}] = linmod(\text{'OpenLoop'}) \tag{6.1.1}$$

The system **A**, **B**, **C** and **D** matrices are as follows:

$$A = \begin{bmatrix}
0 & 0 & 0 & 0.995 & 0 & 0.0998 & 0.0099 & 0.0895 & -0.1 & 0 & 0 & 0 \\
0 & 0 & 0 & 0 & 1 & 0 & -0.1 & 0 & 0.1095 & 0 & 0 & 0 \\
0 & 0 & 0 & -0.0998 & 0 & 0.995 & 0.0995 & -0.1095 & 0 & 0 & 0 & 0 \\
0 & 0 & 0 & 0 & 0.1 & -0.1 & 0 & 0 & 0 & 0 & -0.1 & 0.1 \\
0 & 0 & 0 & -0.1 & 0 & 0.1 & 0 & 0 & 0 & 0.1 & 0 & -0.1 \\
0 & 0 & 0 & 0.1 & -0.1 & 0 & 0 & 0 & 0 & -0.1 & 0.1 & 0 \\
0 & 0 & 0 & 0 & 0 & 0 & 0.01 & 0.1 & 0 & 1 & 0 & 0.1003 \\
0 & 0 & 0 & 0 & 0 & 0 & -0.1 & 0 & 0 & 0 & 1 & 0 \\
0 & 0 & 0 & 0 & 0 & 0 & 0.1005 & 0.0101 & 0 & 0 & 0 & 1.005 \\
0 & 0 & 0 & 0 & 0 & 0 & 0 & 0 & 0 & 0 & -2×10^{-14} & 2×10^{-14} \\
0 & 0 & 0 & 0 & 0 & 0 & 0 & 0 & 0 & 2×10^{-14} & 0 & -2×10^{-14} \\
0 & 0 & 0 & 0 & 0 & 0 & 0 & 0 & 0 & -2×10^{-14} & 2×10^{-14} & 0
\end{bmatrix} \tag{6.1.2}$$

$$B = \begin{bmatrix}
0 & 0 & 0 & 0 \\
0 & 0 & 0 & 0 \\
0 & 0 & 0 & 0 \\
0 & 0 & 0 & 0 \\
0 & 0 & 0 & 0 \\
0 & 5 & 0 & 0 \\
0 & 0 & 0 & 0 \\
0 & 0 & 0 & 0 \\
0 & 0 & 0 & 0 \\
0 & 0 & 0.0002 & 0 \\
0.0002 & 0 & 0 & 0 \\
0 & 0 & 0 & 0.3
\end{bmatrix} \tag{6.1.3}$$

$$C = \begin{bmatrix} 1 & 0 & 0 & 0 & 0 & 0 & 0 & 0 & 0 & 0 & 0 & 0 \\ 0 & 1 & 0 & 0 & 0 & 0 & 0 & 0 & 0 & 0 & 0 & 0 \\ 0 & 0 & 1 & 0 & 0 & 0 & 0 & 0 & 0 & 0 & 0 & 0 \\ 0 & 0 & 0 & 1 & 0 & 0 & 0 & 0 & 0 & 0 & 0 & 0 \\ 0 & 0 & 0 & 0 & 1 & 0 & 0 & 0 & 0 & 0 & 0 & 0 \\ 0 & 0 & 0 & 0 & 0 & 1 & 0 & 0 & 0 & 0 & 0 & 0 \\ 0 & 0 & 0 & 0 & 0 & 0 & 1 & 0 & 0 & 0 & 0 & 0 \\ 0 & 0 & 0 & 0 & 0 & 0 & 0 & 1 & 0 & 0 & 0 & 0 \\ 0 & 0 & 0 & 0 & 0 & 0 & 0 & 0 & 1 & 0 & 0 & 0 \\ 0 & 0 & 0 & 0 & 0 & 0 & 0 & 0 & 0 & 1 & 0 & 0 \\ 0 & 0 & 0 & 0 & 0 & 0 & 0 & 0 & 0 & 0 & 1 & 0 \\ 0 & 0 & 0 & 0 & 0 & 0 & 0 & 0 & 0 & 0 & 0 & 1 \end{bmatrix} \tag{6.1.4}$$

$$D = \begin{bmatrix} 0 & 0 & 0 & 0 \\ 0 & 0 & 0 & 0 \\ 0 & 0 & 0 & 0 \\ 0 & 0 & 0 & 0 \\ 0 & 0 & 0 & 0 \\ 0 & 0 & 0 & 0 \\ 0 & 0 & 0 & 0 \\ 0 & 0 & 0 & 0 \\ 0 & 0 & 0 & 0 \\ 0 & 0 & 0 & 0 \\ 0 & 0 & 0 & 0 \\ 0 & 0 & 0 & 0 \end{bmatrix} \tag{6.1.5}$$

6.2 Controller Design

6.2.1 General

For the applications discussed in this work, a servomechanism design is engaged to develop a closed-loop output-tracking regulator that uses input gain matrices together with an H_2 feedback controller to regulate the output of the aircraft parameters. The basic structure of the model can be defined in the linear state space form. The initial effort is focused on identification of parameters of the linear model in hover. Since the identified parameters will be valid only around the point of linearization, different models must be identified for other types of flight.

Input preferences are implemented to account for the initial conditions of the inputs. The initial conditions of other states are modeled through variable preferences.

This structure is derived for a linear system model. When systems act linearly and match the linear model, about which such regulation gains are defined, zero steady-state tracking error is indeed reachable using this control method.

The 6 (six) control inputs to plant or 6DOF Block (Matlab-Simulink Aerospace Block) are forces and moments (X, Y, Z, L, M, N), shown in Equation 2.4.1. The micro coaxial helicopter forces and moments with 4 control inputs are shown in Equation 3.4.

We use the MatLab-Simulink [28] 6DoF Aerospace Block-set to implement Euler angle representation of six-degrees-of-freedom equations of motion. The 6DoF (Euler Angles) block considers the rotation of a body-fixed coordinate frame about an Earth-fixed reference frame. The origin of the body-fixed coordinate frame is the center of gravity of the body, and the body is assumed to be rigid, an assumption that eliminates the need to consider the forces acting between individual elements of mass.

6.2.2 Controller

To achieve target tracking and subsystem alignment, an optimal controller is constructed based on the H_2 control theory and regulator theory described in this work and in the literature [8], [24], [25] and [26]. This thesis will consider the feedback control system described in literature for the Tracking controller with full-state feedback. Consider the feedback control system shown in Figure 5.1 in which $G_{(s)}$ is the nominal plant and $K_{(s)}$ is the nominal controller that gives an optimal H_2 closed-loop performance. The controlled output vector can be defined as shown in Equation 5.2.1. The problem now is to find a controller **K** as illustrated in Figure 5.2. The final step in assembling the tracking controller **K** is to combine the exogenous input estimator, the regulator parameters **W** and **U**, and the state feedback gain **F**. As long as the closed-loop system is internally stable and matches the plant model well, steady-state regulation will take place if **W** and **U** are chosen to satisfy Equations, as explained in next section of this work.

6.2.3 Control Inputs

In general control inputs are defined in this work. This section provides additional details specific for the micro coaxial helicopter.

The first control input is for the forward flight. As it's described in this work, the rear servomotor pushes the swash-plate upward or downward. The input to electrical servo motor will control movement upward or downward. When the rear servo motor pushes the swash-plate upward, it will provide input for the forward flight.

The second control input is for the thrust (altitude) control. It is accomplished by varying the rotational speed of the both rotors simultaneously for the same value. The same input is applied to both motors. The lower and upper rotors rotational speed change is identical. The micro coaxial helicopter will climb when the rotors' speed increase.

The third control input is for the rotation about to the x-axes. The control input for the forward servo motor will control the movement of the swash-plate upward or downward. This will control the tilts of the rotors and the angle of rotors left or right. When the upward position is achieved, the micro helicopter will roll to the left.

The fourth control input is for the rotation about to the z-axes. The difference in rotational speed between the lower and upper rotors will turn the helicopter to the right or left. This is accomplished by varying the rotational speed of the lower rotor. The micro coaxial helicopter will turn to the left when the lower rotor increases speed. When the lower rotor decreases rotational speed, the micro coaxial helicopter will turn to the right.

6.2.4 Controller and Steady-State Regulation

The generalized structure of the controller is illustrated in Figure 5.2. The condition for the stabilizing controller is that the A, B_2 , C_2 are stabilizable and detectable. For the stabilizable and detectable system defined by A, B_2 , C_2, see Equations 5.1.1, 5.2.2, 5.2.1 and 5.2.4. According to the regulator theory, as described in the literature [7], and [24], zero steady-state tracking error is achievable by designing the controller parameters **W** and **U** to satisfy these equations. Note that in our case output regulation gains U and W are calculated in Mathematica [29]. If the closed-loop

system is internally stable, the steady-state regulation will take place.

Control output gain matrix has 4 inputs to track and 12 states in state vector.

$$C_{1u} = \begin{bmatrix} cm1 & 0 & 0 & 0 & cm5 & 0 & 0 & cm8 & 0 & cm10 & 0 & 0 \\ 0 & 0 & cz3 & 0 & 0 & 0 & 0 & 0 & 0 & 0 & 0 & cz12 \\ 0 & cl2 & 0 & cl4 & 0 & 0 & cl7 & 0 & 0 & 0 & cl11 & 0 \\ 0 & 0 & 0 & 0 & 0 & cn6 & 0 & 0 & cn9 & 0 & 0 & 0 \end{bmatrix} \tag{6.2.1}$$

where matrix elements "cm", "cz", "cl" and "cn" characterize state vector factors to track for each input.

In addition to the tracking for the pitching moment in horizontal flight, we would like to adjust other inputs for the rolling moment, the altitude and yawing moment.

To accomplish the tracking and adjustment, the regulated variable ($z_{1(t)}$ is defined as follows

$$z_{1(t)} = \begin{bmatrix} 0.05x - 0.01\theta \\ -1z \\ 0.1y \quad 0.2\phi \\ 0.1\psi \end{bmatrix} \tag{6.2.2}$$

As we discuss it earlier in this work, the input vector "u" represents the changes in control inputs, the controlled output vector "z" and state vector "x" are defined as shown in equations 3.3.7, 3.3.7, 5.2.6 and 5.2.1.

$$x = \begin{bmatrix} x & y & z & u & v & w & \phi & \theta & \psi & p & q & r \end{bmatrix}^T \tag{6.2.3}$$

$$u = \begin{bmatrix} u_1 & u_2 & u_3 & u_4 \end{bmatrix} = \begin{bmatrix} \delta_{\mathrm{m}} & \delta_{\mathrm{z}} & \delta_{\mathrm{l}} & \delta_{\mathrm{n}} \end{bmatrix} \tag{6.2.4}$$

$$z(t) = \begin{bmatrix} C_{1u} \\ 0 \end{bmatrix} \bar{x}(t) + \begin{bmatrix} 0 \\ D_{12d} \end{bmatrix} \bar{u}(t)$$

Where C_{1u} is control output gain matrix.

As long as the closed-loop system is internally stable and matches the plant model well, steady-state

regulation will take place if **W** and **U** are chosen to satisfy Equations as explained in this work. The controlled output vector $z_{(t)}$ is described in this work. The first entry is a weighted position for pitching angle theta and distance along x-axis, the second is tracking error along z-axes and the thrust, the third is weighted position for rolling angle and distance along y-axis, and fourth is weighted rotation about the z-axes. During vertical flight, the priority is tracking error for the thrust or position along z-axis. The change of position along z-axis is accomplished by the second control input and varying the rotational speed of both rotors simultaneously. The same input is applied to both motors. The micro coaxial helicopter will climb when the rotors' speed increases. When the helicopter reaches its desired position, it will hover at its picked position. The micro coaxial helicopter will maintains a constant position at a selected point, with the rotors providing lift equal to the total weight of the helicopter. In the hovering case, the downward airflow adjusts the relative wind and changes the angle of attack so less aerodynamic force is produced. This condition requires increase of aerodynamic force to sustain a hover.

Also it is necessary introduce weighting for other entries as described in this work. The damping and input control derivative values are determined experimentally. Tracking error weighting is 1 compared with 0.05 for position along x-axis, 0.01 for pitching angle (θ), 0.1 for position along y-axes, 0.2 for the rolling angle (ϕ) and 0.1 for the yawing angle (ψ).

We got matrices as follows:

$$C_{1u} = \begin{bmatrix} 0.05 & 0 & 0 & 0 & 0 & 0 & 0 & -0.01 & 0 & 0 & 0 & 0 \\ 0 & 0 & -1 & 0 & 0 & 0 & 0 & 0 & 0 & 0 & 0 & 0 \\ 0 & 0.1 & 0 & 0 & 0 & 0 & 0.2 & 0 & 0 & 0 & 0 & 0 \\ 0 & 0 & 0 & 0 & 0 & 0 & 0 & 0 & 0.1 & 0 & 0 & 0 \end{bmatrix} \tag{6.2.6}$$

$$B_2 = \begin{bmatrix} 0 & 0 & 0 & 0 \\ 0 & 0 & 0 & 0 \\ 0 & 0 & 0 & 0 \\ 0 & 0 & 0 & 0 \\ 0 & 0 & 0 & 0 \\ 0 & 5 & 0 & 0 \\ 0 & 0 & 0 & 0 \\ 0 & 0 & 0 & 0 \\ 0 & 0 & 0 & 0 \\ 0 & 0 & 0.0002 & 0 \\ 0.0002 & 0 & 0 & 0 \\ 0 & 0 & 0 & 0.3 \end{bmatrix} \tag{6.2.7}$$

$$D_{11u} = \begin{bmatrix} 0.1 & 0 & 0 & 0 \\ 0 & 0.1 & 0 & 0 \\ 0 & 0 & 0.1 & 0 \\ 0 & 0 & 0 & 0.1 \end{bmatrix} \tag{6.2.8}$$

$$D_{12d} = \begin{bmatrix} 12500 & 0 & 0 & 0 \\ 0 & 10 & 0 & 0 \\ 0 & 0 & 10 & 0 \\ 0 & 0 & 0 & 10 \end{bmatrix} \tag{6.2.9}$$

The output regulation gains **U** and **W** compute was done in Mathematica [29] and matrices are as follows:

$$W = \begin{bmatrix} -2 & 0 & 8\times10^{-21} & 0.2 \\ 0 & 0 & -1 & 8416 \\ 0 & 0.1 & 0 & 0 \\ 0 & 0 & 0 & -0.116 \\ 0 & 0 & -7\times10^{-18} & -420.7 \\ 0 & 0 & 0 & 420.9 \\ 0 & 0 & 0 & -4208.4 \\ 0 & 0 & 0 & 1.009 \\ 0 & 0 & 0 & -1 \\ 0 & 0 & -7\times10^{-21} & -0.226 \\ 0 & 0 & 0 & -420.8 \\ 0 & 0 & 7\times10^{-18} & 420.8 \end{bmatrix} \tag{6.2.10}$$

$$U = \begin{bmatrix} 0 & 0 & 9\times10^{-28} & 5\times10^{-8} \\ 0 & 0 & -8\times10^{-23} & 3\times10^{-15} \\ 0 & 0 & 0 & -1\times10^{-7} \\ 0 & 0 & 6\times10^{-31} & 3\times10^{-11} \end{bmatrix} \tag{6.2.11}$$

6.2.5 State Feedback Gain F

The state feedback gain **F** is created on chosen weighting matrices that balance the cost of transient performance and input power. For nonlinear systems, this gain may also control overall system stability. Design of the state feedback gain begins with the selection of the above-mentioned weighting matrices. In the state feedback we assume that the whole state **x** can be measured and, as a result, it is available for control. In this work we will implement full-state feedback gain **F** and omit the estimator construction as shown in Figure 5.2. We will design state feedback using nominal values of parameters and we will try to choose controlled output gains matrices. State feedback Gain F is achieved from the solution of the algebraic Riccati equation. In order to design state feedback, we need to define matrices Q and R. The state feedback is designed by using parameters and matrices Q and R in such a way that the state response is stable. The Q and R matrix choice is an important part of the state feedback gain design.

The Gain **F** is computed as as shown in Equations 5.2.7, 5.2.8, 5.2.9, 5.2.10 and 5.2.11.

The micro helicopter has a fast time domain response due to its small size and it's sensitive to small changes of parameters and matrices.

The linear quadratic regulation method determines the solution of the state-feedback control gain matrix **F**. The MATLAB function **lqr** allows you to choose two parameters, **R** and **Q**, which will balance the relative importance of the control effort (u) and error (deviation from 0), respectively, in the cost function that we are trying to optimize. The cost function corresponding to this **R** and **Q** places equal importance on the control and the state variables which are outputs. Both matrices Q and R are symmetric real, Q is assumed to be at least positive-semi-definite ($Q = Q \geq 0$) and R must be positive-definite ($R = R > 0$).

If we set Q relatively large compared to R, the optimization procedure will result in the design in which x(t) is relatively "small" compared to $u_{(t)}$.

If in contrast, Q is rather small, that will tend to make $x_{(t)}$ larger and $u_{(t)}$ smaller.

Increasing the magnitude of Q more would make the tracking error smaller, but would require greater control u. More control effort generally corresponds to greater cost (more energy, larger components and actuator, etc.).

$$Q = \begin{bmatrix} 0.0025 & 0 & 0 & 0 & 0 & 0 & 0 & -0.0005 & 0 & 0 & 0 & 0 \\ 0 & 0.01 & 0 & 0 & 0 & 0 & 0.02 & 0 & 0 & 0 & 0 & 0 \\ 0 & 0 & 1 & 0 & 0 & 0 & 0 & 0 & 0 & 0 & 0 & 0 \\ 0 & 0 & 0 & 0 & 0 & 0 & 0 & 0 & 0 & 0 & 0 & 0 \\ 0 & 0 & 0 & 0 & 0 & 0 & 0 & 0 & 0 & 0 & 0 & 0 \\ 0 & 0 & 0 & 0 & 0 & 0 & 0 & 0 & 0 & 0 & 0 & 0 \\ 0 & 0.02 & 0 & 0 & 0 & 0 & 0.04 & 0 & 0 & 0 & 0 & 0 \\ -0.0005 & 0 & 0 & 0 & 0 & 0 & 0 & 0.0001 & 0 & 0 & 0 & 0 \\ 0 & 0 & 0 & 0 & 0 & 0 & 0 & 0 & 0.01 & 0 & 0 & 0 \\ 0 & 0 & 0 & 0 & 0 & 0 & 0 & 0 & 0 & 0 & 0 & 0 \\ 0 & 0 & 0 & 0 & 0 & 0 & 0 & 0 & 0 & 0 & 0 & 0 \\ 0 & 0 & 0 & 0 & 0 & 0 & 0 & 0 & 0 & 0 & 0 & 0 \end{bmatrix} \tag{6.2.12}$$

$$R = \begin{bmatrix} 156250000 & 0 & 0 & 0 \\ 0 & 100 & 0 & 0 \\ 0 & 0 & 100 & 0 \\ 0 & 0 & 0 & 100 \end{bmatrix} \tag{6.2.13}$$

The Gain **F** was computed and matrix is as follows:

$$F = \begin{bmatrix} -1e-10 & -1e-10 & 3e-10 & 1e-09 & -1e-9 & 6e-12 & 1e-09 & 1e-10 & -4e-10 & 1e-07 & -1e-08 & 1e-11 \\ -2e-04 & 1e-04 & -0.099 & -0.026 & -0.023 & -0.198 & -0.0415 & 0.0128 & 0.006 & -0.18 & 0.249 & 0.017 \\ 0.004 & 0.004 & -0.01 & -0.04 & 0.05 & -7e-06 & -0.016 & -0.005 & 0.011 & -10.3 & 0.19 & 0.00073 \\ 0.002 & -0.009 & -0.0002 & 0.07 & 0.08 & 0.001 & -0.09 & 0.04 & -0.058 & 1.09 & 0.027 & -0.67 \end{bmatrix} \tag{6.2.14}$$

Chapter 7: Level Flight

7.1 Model Analysis

The micro helicopter is a highly maneuverable device. We will model the helicopter as a rigid body moving in space. The standard rigid body dynamical equation will be used to model the motion of the helicopter in its environment as it's described in this work and in the literature [1], [2] and [4]. For comprehensive analysis and controller design, it is convenient to work with a closed-form mathematical model of a system. The helicopter is a nonlinear, unstable and highly coupled system and it exhibits considerably different responses to inputs in every flight regime (such as hover, cruise, turning flight etc.). It is common practice to linearize a complex system about a nominal set point for the purpose of design and analysis. A sequence of linear models is used to truly approximate the nonlinear system, which allows for linear system analysis and controller design methods to be engaged. The model incorporates initial conditions of the inputs and initial conditions of other states. They are presented through variable preferences at hover. The modeling in state space approach was chosen due to the follow-on computational capabilities. The control problem schematic representation in its simplest generalized form is shown in Figure 5.1. The G generalized plant, is the system to be controlled by the controller, K. Together, G and K form the closed-loop system.

The explanation provided in the chapter on vertical flight applies to the level flight, as well. The problem is categorized by an objective for the plant to follow, reference command θ_r. This is done by control input to the generalized plant, $u_{(t)}$, the exogenous input to the system w_1, based on the measured output of the plant, $y_{(t)}$, while simultaneously trying to minimize the influence of disturbances on the plant, $v_{(t)}$. The effectiveness of K is evaluated by its ability to minimize the norm of the controlled output vector, $z_{(t)}$. This vector is typically separated into two parts: the output-tracking error, $z_{1(t)}$, and the control input constraints, $z_{2(t)}$.

For the work discussed within this dissertation, the controller, K, is designed to stabilize the closed-

loop system, to fly the flying aircraft under some itemized condition(s), and to minimize the brief and steady-state tracking errors subject to control input restrictions. The generalized plant G can be described by the Equation 5.1.1. The linear state-space model was computed using the MatLab/Simulink command *linmod*. The linmod command extracts continuous-time linear state-space model around an operating point. The system **A** and **B** matrices are shown in this work (reference the equations 6.1.2 and 6.1.3).

7.2 Controller Design

7.2.1 General

For the applications discussed in this work, a servomechanism design is engaged to develop a closed-loop output-tracking regulator that uses input gain matrices together with an H_2 feedback controller to regulate the output of the aircraft parameters. The basic structure of the model can be defined in the linear state space form. The initial effort is focused on identification of parameters of the linear model in hover. Since the identified parameters will be valid only around the point of linearization, different models must be identified for other types of flight.

Input preferences are implemented to account for the initial conditions of the inputs. The initial conditions of other states are modeled through variable preferences.

This structure is derived for a linear system model. When systems act linearly and match the linear model, about which such regulation gains are defined, zero steady-state tracking error is indeed reachable using this control method.

The 6 (six) control inputs to plant or 6DOF Block (Matlab-Simulink Aerospace Block) are forces and moments (X, Y, Z, L, M, N), shown in Equation 2.4.1. The micro coaxial helicopter forces and moments with 4 control inputs are shown in Equation 3.4.

7.2.2 Controller

To achieve target tracking and subsystem alignment, an optimal controller is constructed based on the H_2 control theory and regulator theory described in this work and in the literature [8], [24],

[25] and [26]. This thesis will consider the feedback control system described in literature for the Tracking controller with full-state feedback. Consider the feedback control system shown in Figure 5.1 in which $G_{(s)}$ is the nominal plant and $K_{(s)}$ is the nominal controller that gives an optimal H_2 closed-loop performance. The controlled output vector can be defined as shown in Equation 5.2.1. The problem now is to find a controller **K** as illustrated in Figure 5.2.

7.2.3 Control Inputs

In general control inputs are defined in this work. This section provides additional details specific for the micro coaxial helicopter.

The first control input is for the forward flight. As it's described in this work, the rear servomotor pushes the swash-plate upward or downward. The input to electrical servo motor will control movement upward or downward. When the rear servo motor pushes the swash-plate upward, it will provide input for the forward flight.

The second control input is for the thrust (altitude) control. It is accomplished by varying the rotational speed of the both rotors simultaneously for the same value. The same input is applied to both motors. The lower and upper rotors rotational speed change is identical. The micro coaxial helicopter will climb when the rotors' speed increase.

The third control input is for the rotation about to the x-axes. The control input for the forward servo motor will control the movement of the swash-plate upward or downward. This will control the tilts of the rotors and the angle of rotors left or right. When the upward position is achieved, the micro helicopter will roll to the left.

The fourth control input is for the rotation about to the z-axes. The difference in rotational speed between the lower and upper rotors will turn the helicopter to the right or left. This is accomplished by varying the rotational speed of the lower rotor. The micro coaxial helicopter will turn to the left when the lower rotor increases speed. When the lower rotor decreases rotational speed, the micro coaxial helicopter will turn to the right.

7.2.4 Controller and Steady-State Regulation

The generalized structure of the controller is illustrated in Figure 5.2. The condition for the stabilizing controller is that the A, B_2 , C_2 are stabilizable and detectable. For the stabilizable and detectable system defined by A, B_2 , C_2, see Equations 5.1.1, 5.2.2, 5.2.1 and 5.2.4. According to the regulator theory, as described in the literature [7], and [24], zero steady-state tracking error is achievable by designing the controller parameters **W** and **U** to satisfy these equations. Note that in our case output regulation gains U and W are calculated in Mathematica [29]. If the closed-loop system is internally stable, the steady-state regulation will take place.

Control output gain matrix has 4 inputs to track and 12 states in state vector.

In addition to the tracking for the pitching moment in horizontal flight, we would like to adjust other inputs for the rolling moment, the altitude and yawing moment. To accomplish the tracking and adjustment, the regulated variable ($z_{1(t)}$ is defined as follows

$$z_{1(t)} = \begin{bmatrix} -x - \theta \\ 0.1z \\ 0.2y - 0.01\phi \\ 0.1\psi \end{bmatrix} \tag{7.2.1}$$

As we discuss it earlier in this work, the input vector "u" represents the changes in control inputs, the controlled output vector "z" and state vector "x" are defined as shown in equations 3.3.7, 3.3.7, 5.2.6 and 5.2.1.

$$x = \begin{bmatrix} x & y & z & u & v & w & \phi & \theta & \psi & p & q & r \end{bmatrix}^T \tag{7.2.2}$$

$$u = \begin{bmatrix} u_1 & u_2 & u_3 & u_4 \end{bmatrix} = \begin{bmatrix} \delta_{\mathrm{m}} & \delta_{\mathrm{z}} & \delta_{\mathrm{l}} & \delta_{\mathrm{n}} \end{bmatrix} \tag{7.2.3}$$

$$z(t) = \begin{bmatrix} C_{1u} \\ 0 \end{bmatrix} \bar{x}(t) + \begin{bmatrix} 0 \\ D_{12d} \end{bmatrix} \bar{u}(t)$$

Where C_{1u} is control output gain matrix.

As long as the closed-loop system is internally stable and matches the plant model well, steady state regulation will take place if **W** and **U** are chosen to satisfy Equations explained in this work.

The controlled output vector $z_{(t)}$ is described in this work. The first entry is tracking error for forward flight, the second is weighted position along z-axes, the third is weighted rotation about x-axes and the fourth is weighted rotation about the z-axes.

During forward level flight, the priority is tracking error for the pitch angle theta and position along x-axes. The change of position along x-axis and forward flight is accomplished by the first and second control input.

The first control input for the rear servomotor will control movement of the swash-plate upward or downward. When the rear servo motor push the swash-plate upward it will provide input for the forward flight. The second control input is for the thrust (altitude) control. This control input will change the rotational speed of the both rotors simultaneously. The same input is applied to both electrical motors.

The control inputs will provide the pitch angle and thrust required for the forward level flight. Due to restriction for indoor flight we have priority for tracking error for the pitch angle theta and position along x-axes. The damping and input control derivative values are determined experimentally. Tracking error weighting is 1 compared with 0.1 for thrust and position along z-axis, 0.01 for rolling angle (ϕ), 0.2 for position along y-axes and 0.1 for the yawing angle (ψ).

Matrices B_2, D_{11} and D_{11} in the chapter on vertical flight applies to the level flight, as well. We got matrix C_{1u} as follows:

$$C_{1u} = \begin{bmatrix} -1 & 0 & 0 & 0 & 0 & 0 & 0 & -1 & 0 & 0 & 0 & 0 \\ 0 & 0 & 0.1 & 0 & 0 & 0 & 0 & 0 & 0 & 0 & 0 & 0 \\ 0 & 0.2 & 0 & 0 & 0 & 0 & 0.01 & 0 & 0 & 0 & 0 & 0 \\ 0 & 0 & 0 & 0 & 0 & 0 & 0 & 0 & 0.1 & 0 & 0 & 0 \end{bmatrix} \tag{7.2.5}$$

The output regulation gains **U** and **W** compute was done in Mathematica [29] and matrices are as follows:

$$W = \begin{bmatrix} 0.1 & 0 & 0 & -1.009 \\ 0 & 0 & -0.5 & 210.42 \\ 0 & -1 & 0 & 0 \\ -8 \times 10^{-19} & 0 & 0 & -0.116 \\ 0 & 0 & 0 & -420.731 \\ -3 \times 10^{-15} & 0 & 0 & 420.94 \\ 0 & 0 & -1 \times 10^{-15} & -4208.4 \\ -1 \times 10^{-17} & 0 & 0 & 1.009 \\ 3 \times 10^{-18} & 0 & 0 & -1 \\ 3 \times 10^{-18} & 0 & 0 & -0.226 \\ 7 \times 10^{-15} & 0 & -1 \times 10^{-16} & -420.84 \\ -3 \times 10^{-15} & 0 & 0 & 420.83 \end{bmatrix} \tag{7.2.6}$$

$$U = \begin{bmatrix} 0 & 0 & 1 \times 10^{-26} & 5 \times 10^{-08} \\ 4 \times 10^{-20} & 0 & 0 & 1 \times 10^{-15} \\ 1 \times 10^{-24} & 0 & 0 & -1 \times 10^{-07} \\ -3 \times 10^{-28} & 0 & 0 & 3 \times 10^{-11} \end{bmatrix} \tag{7.2.7}$$

7.2.5 State Feedback Gain F

The state feedback gain **F** is created on chosen weighting matrices that balance the cost of transient performance and input power. For nonlinear systems, this gain may also control overall system stability. Design of the state feedback gain begins with the selection of the above-mentioned weighting matrices. In the state feedback we assume that the whole state **x** can be measured and, as a result, it is available for control. In this work we will implement full-state feedback gain **F** and omit the estimator construction as shown in Figure 5.2. We will design state feedback using nominal values of parameters and we will try to choose controlled output gains matrices. State feedback Gain F is achieved from the solution of the algebraic Riccati equation. In order to design state feedback, we need to define matrices Q and R. The state feedback is designed by using parameters and matrices Q and R in such a way that the state response is stable. The Q and R matrix choice is an important part of the state feedback gain design.

The Gain **F** is computed as as shown in Equations 5.2.7, 5.2.8, 5.2.9, 5.2.10 and 5.2.11. The micro helicopter has a fast time domain response due to its small size and it's sensitive to small changes

of parameters and matrices. The linear quadratic regulation method determines the solution of the state-feedback control gain matrix **F**. The MATLAB function **lqr** allows you to choose two parameters, **R** and **Q**, which will balance the relative importance of the control effort (u) and error (deviation from 0), respectively, in the cost function that we are trying to optimize. The cost function corresponding to this **R** and **Q** places equal importance on the control and the state variables which are outputs. Both matrices Q and R are symmetric real, Q is assumed to be at least positive-semi-definite ($Q = Q \geq 0$) and R must be positive-definite ($R = R > 0$). If we set Q relatively large compared to R, the optimization procedure will result in the design in which x(t) is relatively "small" compared to $u_{(t)}$. If in contrast, Q is rather small, that will tend to make $x_{(t)}$ larger and $u_{(t)}$ smaller. Increasing the magnitude of Q more would make the tracking error smaller, but would require greater control u. More control effort generally corresponds to greater cost (more energy, larger components and actuator, etc.). Matrix R in the chapter on vertical flight applies to the level flight, as well. We got matrix Q as follows:

$$Q = \begin{bmatrix} 1 & 0 & 0 & 0 & 0 & 0 & 0 & 1 & 0 & 0 & 0 & 0 \\ 0 & 0.04 & 0 & 0 & 0 & 0 & 0.002 & 0 & 0 & 0 & 0 & 0 \\ 0 & 0 & 0.01 & 0 & 0 & 0 & 0 & 0 & 0 & 0 & 0 & 0 \\ 0 & 0 & 0 & 0 & 0 & 0 & 0 & 0 & 0 & 0 & 0 & 0 \\ 0 & 0 & 0 & 0 & 0 & 0 & 0 & 0 & 0 & 0 & 0 & 0 \\ 0 & 0 & 0 & 0 & 0 & 0 & 0 & 0 & 0 & 0 & 0 & 0 \\ 0 & 0.002 & 0 & 0 & 0 & 0 & 0.0001 & 0 & 0 & 0 & 0 & 0 \\ 1 & 0 & 0 & 0 & 0 & 0 & 0 & 1 & 0 & 0 & 0 & 0 \\ 0 & 0 & 0 & 0 & 0 & 0 & 0 & 0 & 0.01 & 0 & 0 & 0 \\ 0 & 0 & 0 & 0 & 0 & 0 & 0 & 0 & 0 & 0 & 0 & 0 \\ 0 & 0 & 0 & 0 & 0 & 0 & 0 & 0 & 0 & 0 & 0 & 0 \\ 0 & 0 & 0 & 0 & 0 & 0 & 0 & 0 & 0 & 0 & 0 & 0 \end{bmatrix} \tag{7.2.8}$$

The Gain **F** was computed and matrix is as follows:

$$F = \begin{bmatrix} -1 \times 10^{-10} & -6 \times 10^{-11} & 1 \times 10^{-10} & -8 \times 10^{-11} & -1 \times 10^{-9} & -5 \times 10^{-13} & 7 \times 10^{-10} & -2 \times 10^{-11} & -1 \times 10^{-10} & 6 \times 10^{-8} & -8 \times 10^{-9} & 2 \times 10^{-10} \\ -0.017 & -0.02 & -0.002 & -0.23 & -0.7 & -0.14 & 0.09 & 0.03 & 0.03 & 0.68 & -0.02 & 0.32 \\ 0.004 & 0.004 & -0.009 & -0.04 & 0.05 & 2 \times 10^{-5} & -0.01 & -0.004 & 0.01 & -10 & 0.1 & -0.0005 \\ 0.09 & -0.003 & 8 \times 10^{-5} & 0.75 & 0.8 & 0.02 & -0.24 & 0.06 & -0.14 & -0.8 & 0.7 & -1 \end{bmatrix} \tag{7.2.9}$$

Chapter 8: Simulation

8.1 Vertical Flight Simulation

This chapter details the development of highly reliable six degree-of-freedom mathematical and simulation models, and the design of a stability augmentation system for the micro helicopter. We use the MatLab-Simulink 6DOF Aerospace Block set to implement Euler angle representation of six-degrees-of-freedom equations of motion. The 6 (six) control inputs to plant or 6DOF Block (Matlab-Simulink Aerospace Block) are forces and moments (X, Y, Z, L, M, N), shown in Equation 2.4.1. The micro coaxial helicopter forces and moments with 4 control inputs are shown in Equation 3.4. The 6DoF (Euler Angles) block considers the rotation of a body-fixed coordinate frame about an Earth-fixed reference frame. The origin of the body-fixed coordinate frame is the center of gravity of the body, and the body is assumed to be rigid, an assumption that eliminates the need to consider the forces acting between individual elements of mass. The Earth-fixed reference frame is considered inertial, an excellent approximation that allows the forces due to the Earth's motion relative to the "fixed stars" to be neglected. The translational motion of the body-fixed coordinate frame is given below, where the applied forces are in the body-fixed frame, and the mass of the body is assumed constant. The relationship between the body-fixed angular velocity vector, and the rate of change of the Euler angles, can be determined by resolving the Euler rates into the body-fixed coordinate frame. The six degree-of-freedom nonlinear model provides the perfect frame-work to see the coupling between the longitudinal and the lateral dynamics, to design and evaluate the various recovery designs, and to carry out the bifurcation analysis. A linear controller is designed, using Eigen structure assignment, following guidelines outlined in the literature. Though the observed response appears to be nonlinear and complex, it is arguably possible that a single linear model could capture these dynamics and repeat them in simulation.

The Matlab-Simulink 6 DoF Model is shown in Figure 8.1. To test this possibility, a single linearized model was created about the nominal trim condition defined in Table 8.1.

Table 8.1: Trim conditions for 6-DoF simulation

Trimmed States			
velocity in body axis	$u = 0.1 \ \ ft/s$	$v = 0.1 \ \ ft/s$	$w = 0.1 \ \ ft/s$
rotation rates	$p = 0.1 \ \ ft/s^2$	$q = 0.1 \ \ ft/s^2$	$r = 0.1 \ \ ft/s^2$
Euler orientation, radians	$roll = 0$	$pitch = 0.1$	$yaw = 0$

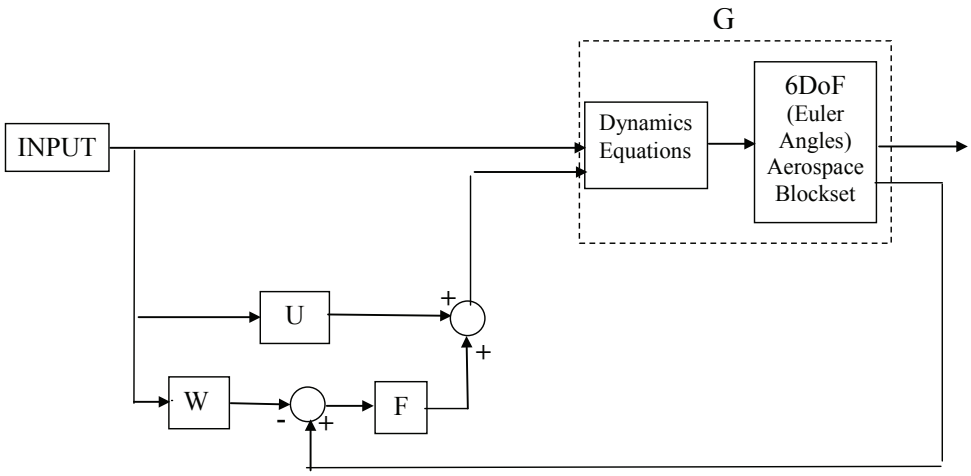

Figure 8.1: 6 DOF Matlab - Simulink Model

A linear controller is designed, using Eigen structure assignment, following guidelines outlined in the literature. Weighting matrices Q and R are used to define the cost function. The matrix Q is state-weighting matrix (n x n) and the matrix R is input-weighting matrix (m x m). This section will provide general guidelines on how to choose Q and R.

The design procedure for finding the feedback is:

- Select design parameter matrices **Q** and **R**.

- Solve the algebraic Riccati equation

- Find the state feedback gain **F**

Note that output regulation gains **U** and **W** are solved in Mathematica [29].

The Matlab routine that performs numerical procedure for solving the algebraic Riccati equation is "lqr (A,B,Q,R)". The most common choice of weighting matrices Q and R are diagonal matrices.

In general one has to find a good ratio between the values of R and Q. For the micro coaxial helicopter simulation, we found out by trial and error good values of R and Q. The general form of the servomechanism-based output regulating tracking controller using H_2 optimization is thus well-defined. It is now suitable to begin exploring this control scheme. In the state feedback we assume that the whole state $\mathbf{x}$ can be measured and as a result it is available for control. In this work we will implement full-state feedback gain $\mathbf{F}$ and omit the estimator construction as shown in Figure 5.2.

We will design state feedback using nominal values of parameters and we will try to choose controlled output gains matrices. State feedback Gain F is achieved from the solution of the algebraic Riccati equation. The Gain $\mathbf{F}$ is computed as shown in Equation 5.2.7. The matrices $\mathbf{R}$ and $\mathbf{Q}$ are computed with the help of output gains D_{12d} and C_{1u} as as shown in Equations 5.2.10 and 5.2.11. We use the MatLab-Simulink [28] 6DoF Aerospace Block set to implement Euler angle representation of six-degrees-of-freedom equations of motion. The closed-loop system in Figure 5.2 was simulated to test the controller's performance. The input to the closed-loop system is the desired step input, and the output is the actual helicopter movement. The tracking signal simulated was a step input to the micro helicopter thrust, only. Other inputs to the pitch, roll and yaw were zero. This correspond to the helicopter's vertical flight. The change of position along the z-axis is accomplished by the second control input and varying the rotational speed of both rotors simultaneously. The same input is applied to both motors. The micro coaxial helicopter will climb when the rotors' speed increases. The helicopter will maintain a constant position at a selected point, with the rotors providing lift equal to the total weight of the helicopter. The input is shown in Figure 8.2.

Realistically, most electromechanical structures can only be run within an obviously defined range. With the theory that the actuator modeled here can only run between $-12\ VDC$ and $+12\ VDC$, the simulation can be arranged to saturate the control voltage within this range, e.g. $-12\ VDC \leq$ u $\leq +12\ VDC$.

Simulation results are shown in this chapter for the system run with the step inputs such that would achieve the chosen position and speed. The simulation was performed using the individual models.

The results of the micro coaxial helicopter simulation of vertical and hover flight are shown in this section.

Simulation of vertical flight was performed as follows.

The first tracking signal simulated was a step input to the micro helicopter thrust, only. Other inputs to the pitch, roll and yaw were zero. These inputs correspond to the helicopter's vertical flight. The change of position along the z-axis is accomplished by the step control input and varying the rotational speed of the both rotors simultaneously. The same input is applied to both electrical motors. The micro coaxial helicopter will climb when the rotors' speed increase. When the helicopter reaches the required position, it will maintain a constant position at a selected point, with the rotors providing lift equal to the total weight of the helicopter. The micro coaxial helicopter would reach position in z-axes of 1.0 ft with w maximum speed along z-axis of 0.3 ft/s, as shown in Figure 8.6 and 8.5. The micro helicopter initially chatters with insignificant amplitude that could be ignored. The system is quick to respond and errors are dispensed quickly. The required position of 1 ft was achieved in 5 seconds with a small overshoot. The output signal exceeded the final steady-state value (overshoot) for approx. 0.04 ft. The stability was achieved quickly in 5 seconds without hunting (unwanted oscillation of signal). All other output signals are zero and could be ignored for this simulation.

Results for the first simulation are shown in Figures 8.2 to 8.17.

The results of the micro coaxial helicopter simulation of vertical flight are as follows:

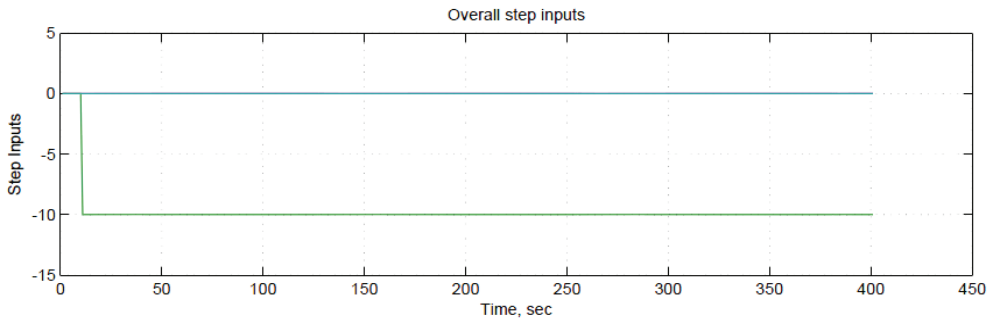

Figure 8.2: Inputs for first simulation of vertical flight

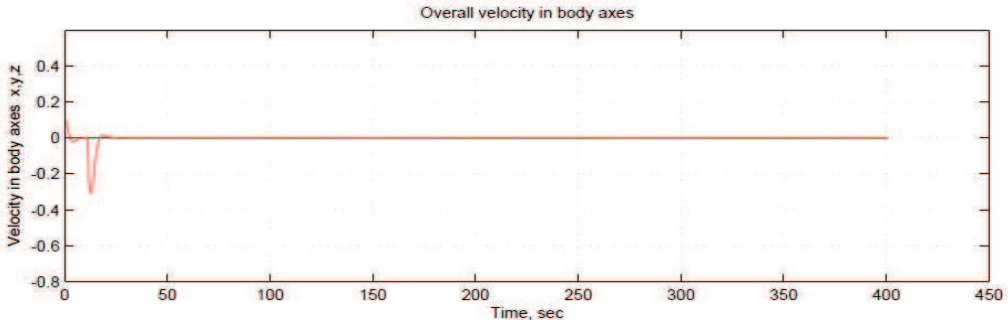

Figure 8.3: Velocity during first simulation of vertical flight

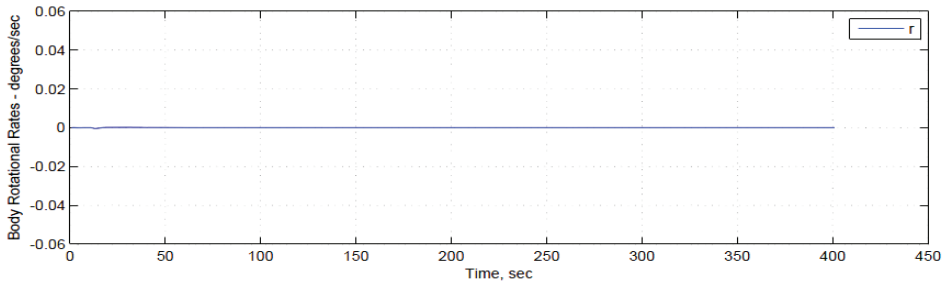

Figure 8.4: Angular velocity "r" during first simulation of vertical flight

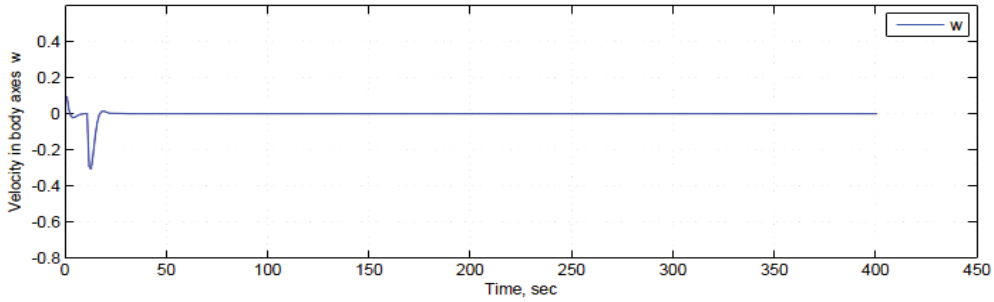

Figure 8.5: Velocity "w" during first simulation of vertical flight

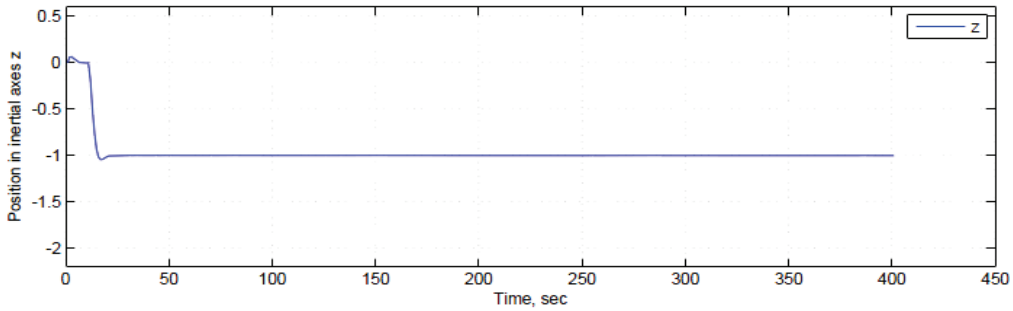

Figure 8.6: Position "z" during first simulation of vertical flight

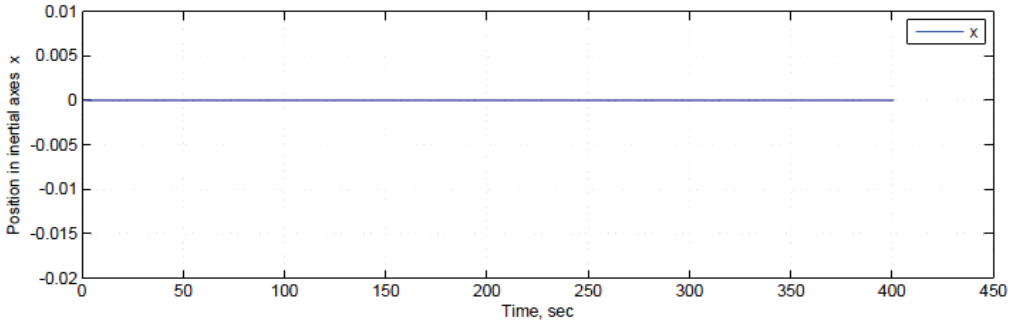

Figure 8.7: Position "x" during first simulation of vertical flight

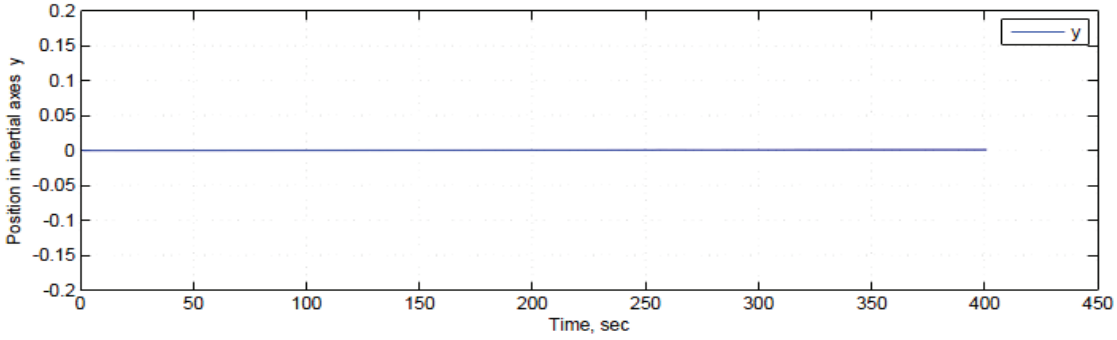

Figure 8.8: Position "y" during first simulation of vertical flight

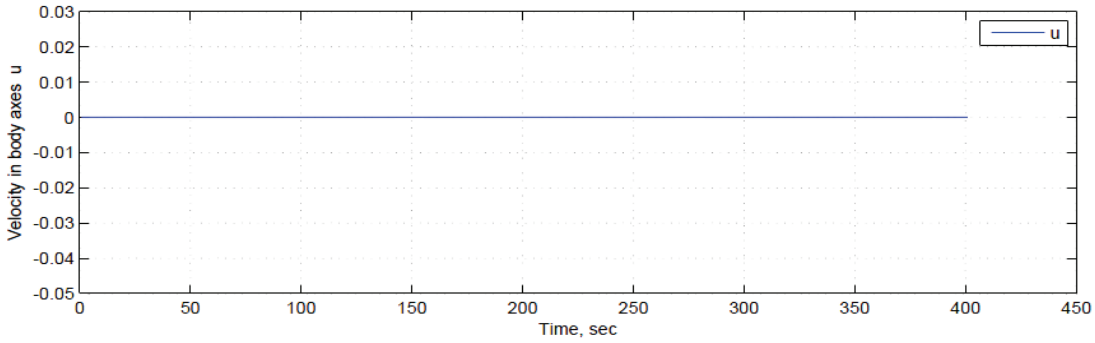

Figure 8.9: Velocity "u" during first simulation of vertical flight

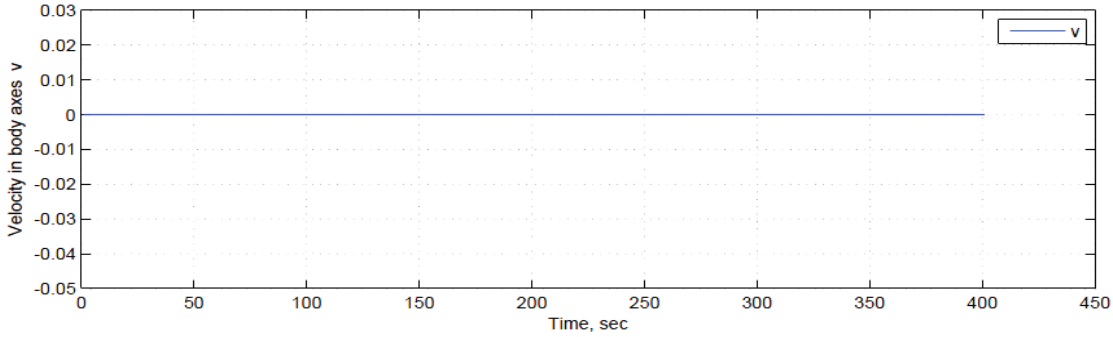

Figure 8.10: Velocity "v" during first simulation of vertical flight

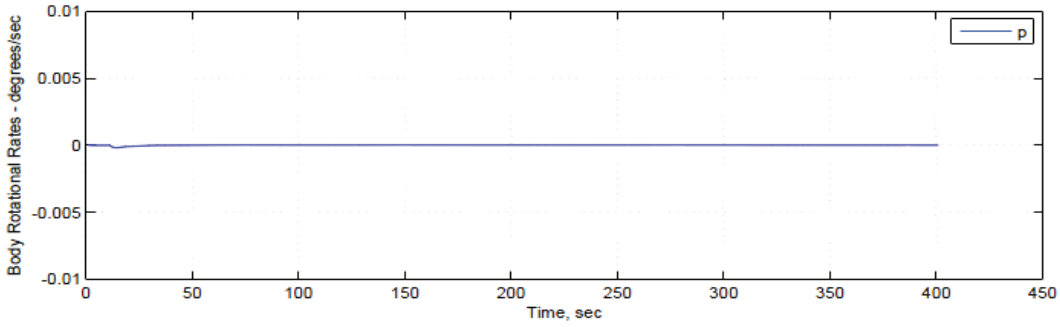

Figure 8.11: Angular velocity "p" during first simulation of vertical flight

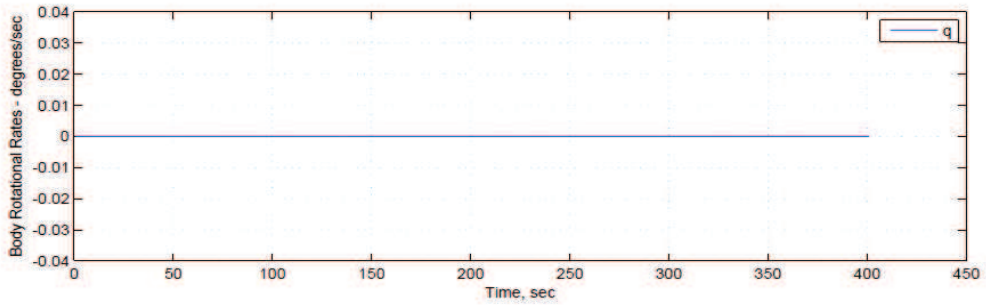

Figure 8.12: Angular velocity "q" during first simulation of vertical flight

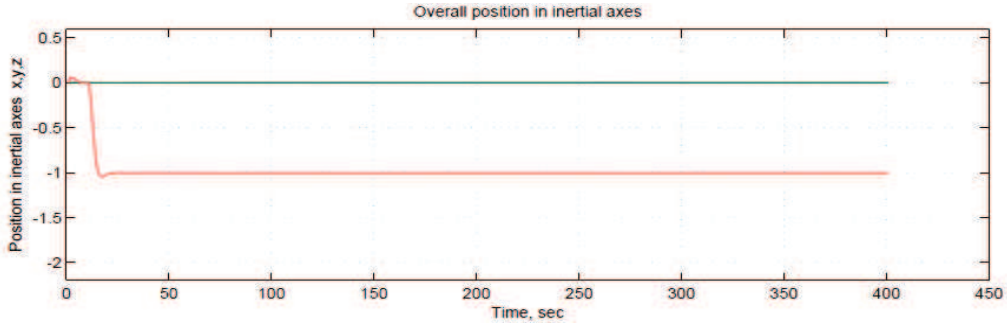

Figure 8.13: Position during first simulation of vertical flight

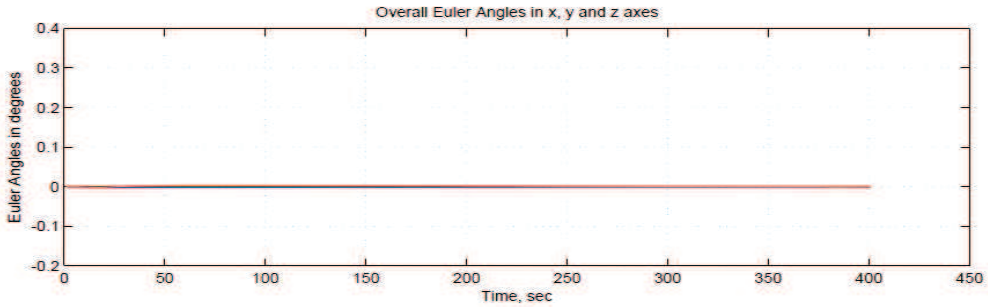

Figure 8.14: Euler angles during first simulation of vertical flight

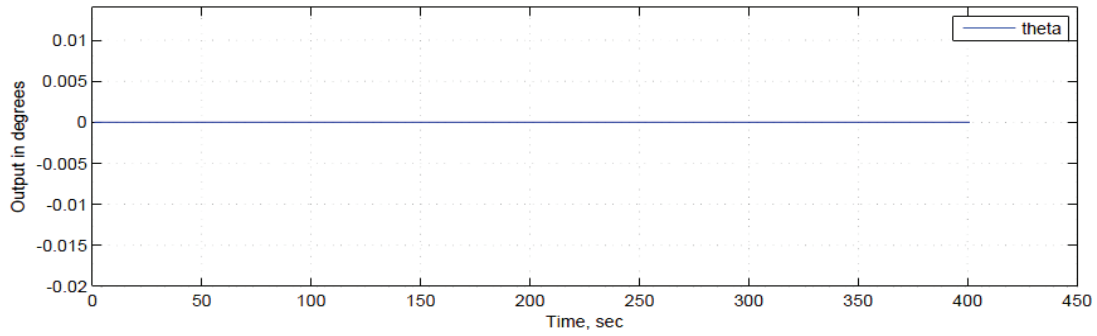

Figure 8.15: Euler angle θ during first simulation of vertical flight

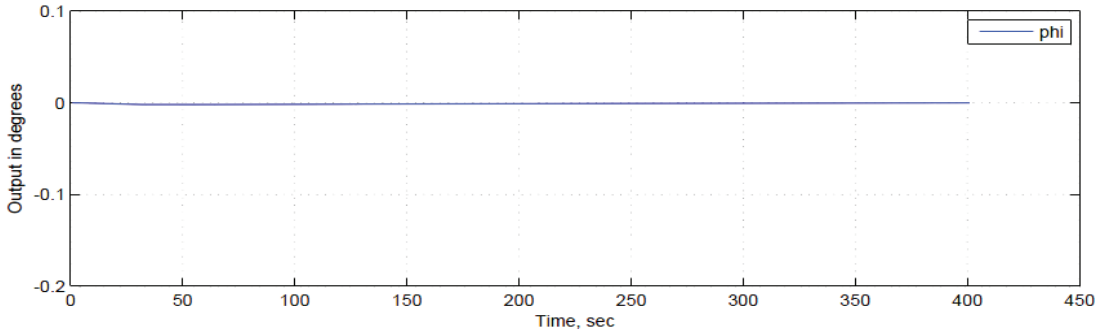

Figure 8.16: Euler angle ϕ during first simulation of vertical flight

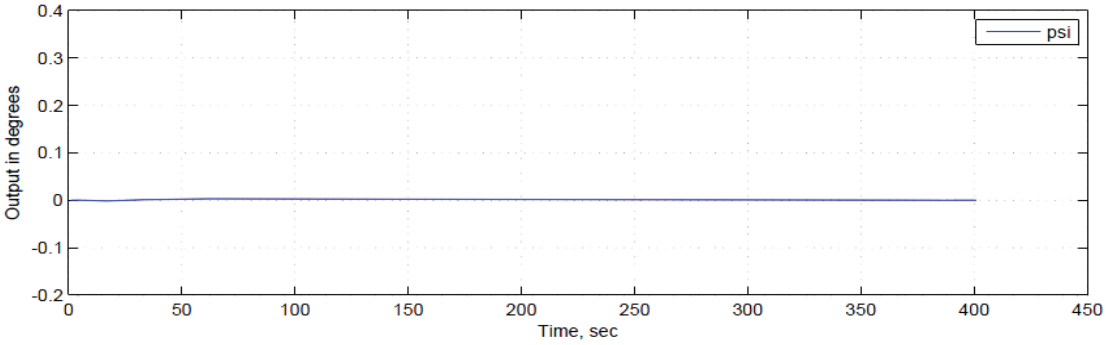

Figure 8.17: Euler angle ψ during first simulation of vertical flight

The second vertical flight simulation was with the step input increase 2x (two times) compared to the first simulation, to the micro helicopter thrust, only. Other inputs to the pitch, roll and yaw were zero. This corresponds to the helicopter's vertical flight.

The change of position along z-axis is accomplished by the step control input and varying the rotational speed of the both rotors simultaneously. The same input is applied to both electrical motors. The micro coaxial helicopter will climb when the rotors' speed increase. When the helicopter reaches the required position, it will maintain a constant position at a selected point, with the rotors providing lift equal to the total weight of the helicopter. The input is shown in Figure 8.23.

This simulation results would reach position in z-axes of 2.0 ft with a maximum speed of 0.6 ft/s, as shown in Figures 8.18 and 8.19. The micro helicopter initially chatters with insignificant amplitude that could be ignored. The system is quick to respond and errors are dispensed quickly. The required position of 2 ft was achieved in 5 seconds with a small overshoot. The output signal exceeded the final steady-state value (overshoot) for approx. 0.09 ft. The stability was achieved quickly in 5 seconds without hunting (unwanted oscillation of signal). All other output signals are zero and could be ignored for this simulation.

Results for the simulation are shown in Figures 8.18 to 8.23.

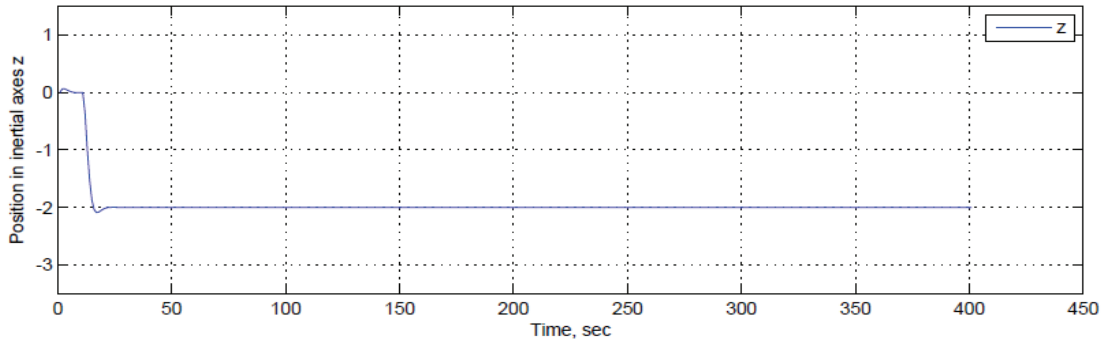

Figure 8.18: Position "z" during second simulation of vertical flight

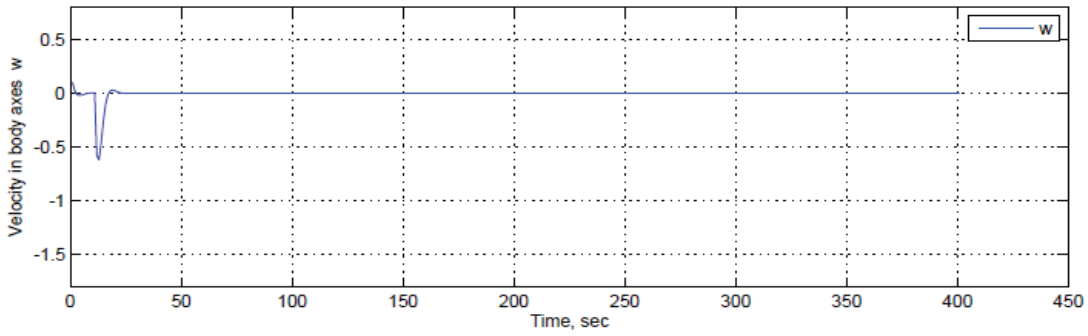

Figure 8.19: Velocity "w" during second simulation of vertical flight

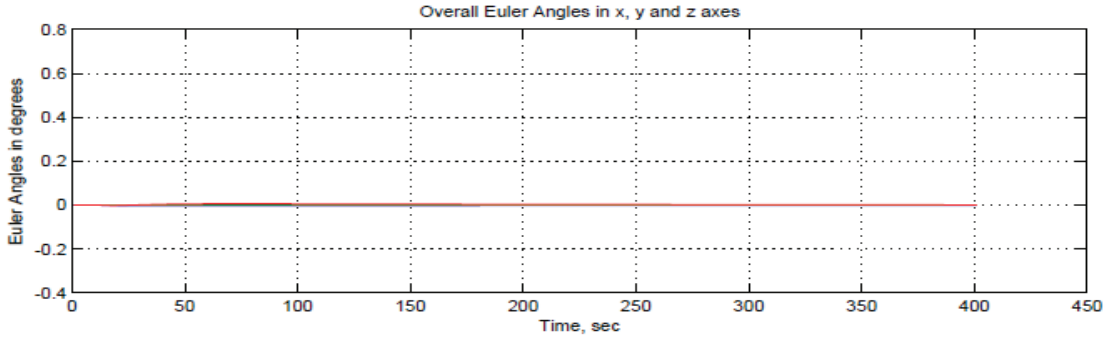

Figure 8.20: Euler angles during second simulation of vertical flight

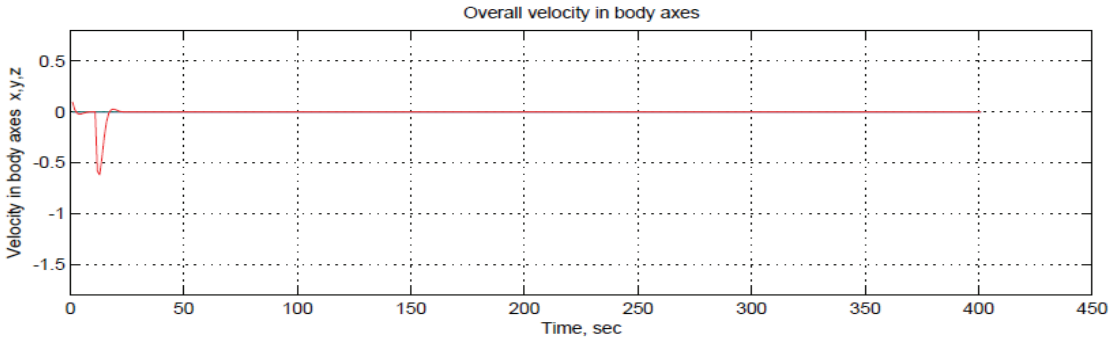

Figure 8.21: Velocity during second simulation of vertical flight

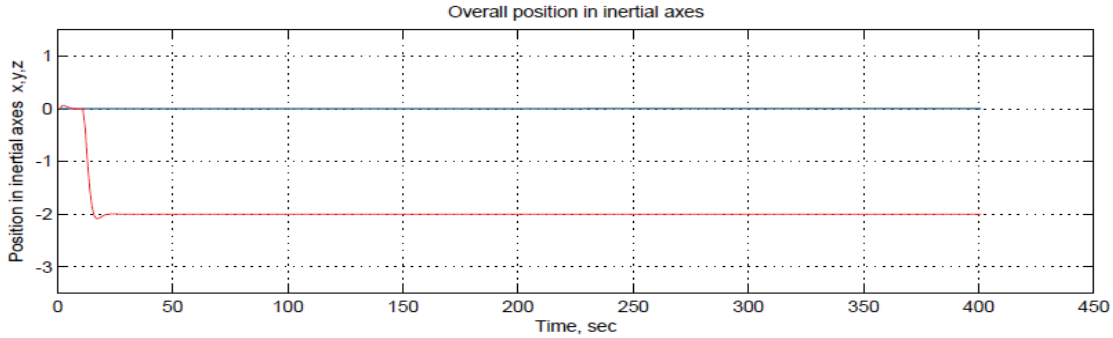

Figure 8.22: Position during second simulation of vertical flight

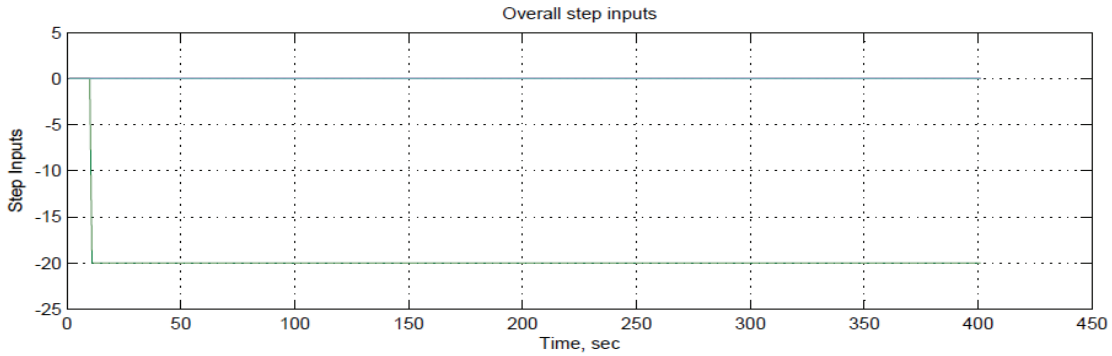

Figure 8.23: Inputs for second simulation of vertical flight

The third vertical flight simulation was with the step input increase 3x (three times) compared to the first simulation, to the micro helicopter thrust, only. Other inputs to the pitch, roll and yaw were zero. This corresponds to the helicopter's vertical flight.

The change of position along z-axis is accomplished by the step control input and varying the rotational speed of the both rotors simultaneously. The same input is applied to both electrical motors. The micro coaxial helicopter will climb when the rotors' speed increase. When the helicopter reach the required position it will maintains a constant position at a selected point, with the rotors providing lift equal to the total weight of the helicopter. The input is shown in Figure 8.29.

This simulation results would reach position in z-axes of 3.0 ft with a maximum speed of 0.9 ft/s, as shown in Figure 8.24 and 8.25. The micro helicopter initially chatters with insignificant amplitude that could be ignored. The system is quick to respond and errors are dispensed quickly. The required position of 3 ft was achieved in 5 seconds with a small overshoot. The output signal exceeded the final steady-state value (overshoot) for approx. 0.14 ft. The stability was achieved quickly in 5 seconds without hunting (unwanted oscillation of signal). All other output signals are zero and could be ignored for this simulation.

Results for the simulation are shown in Figures 8.24 to 8.29.

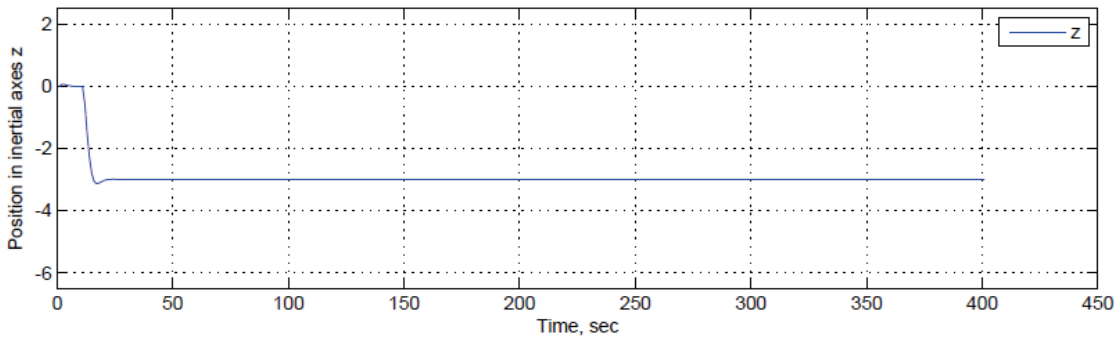

Figure 8.24: Position "z" during third simulation of vertical flight

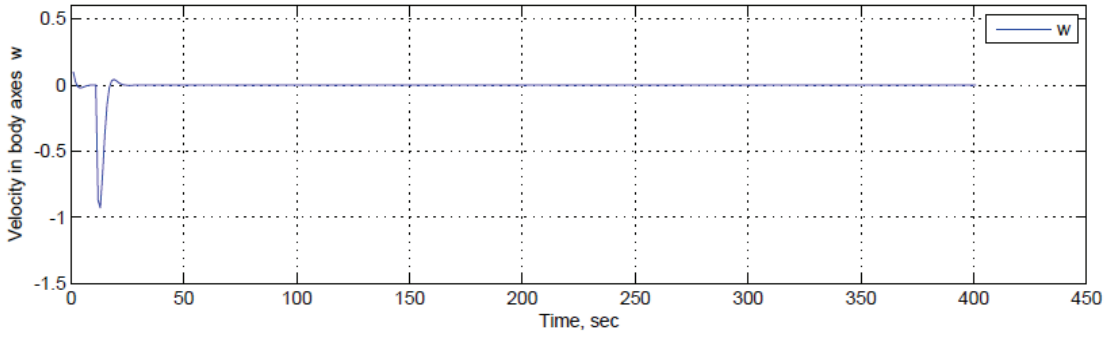

Figure 8.25: Velocity "w" during third simulation of vertical flight

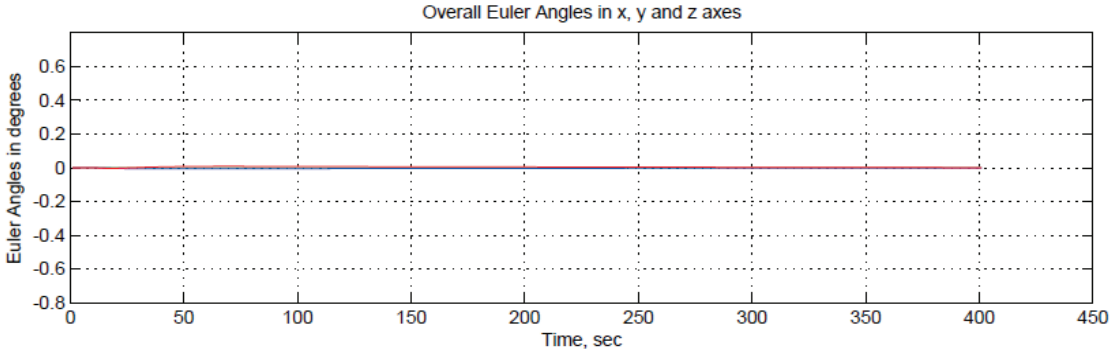

Figure 8.26: Euler angles during third simulation of vertical flight

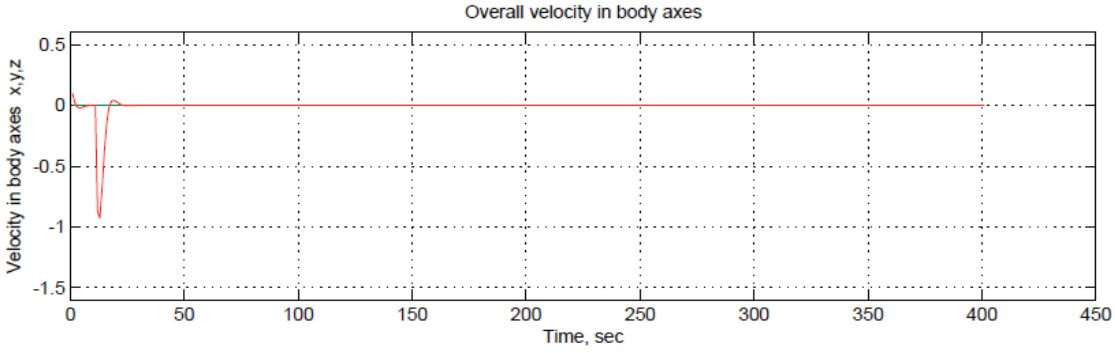

Figure 8.27: Velocity during third simulation of vertical flight

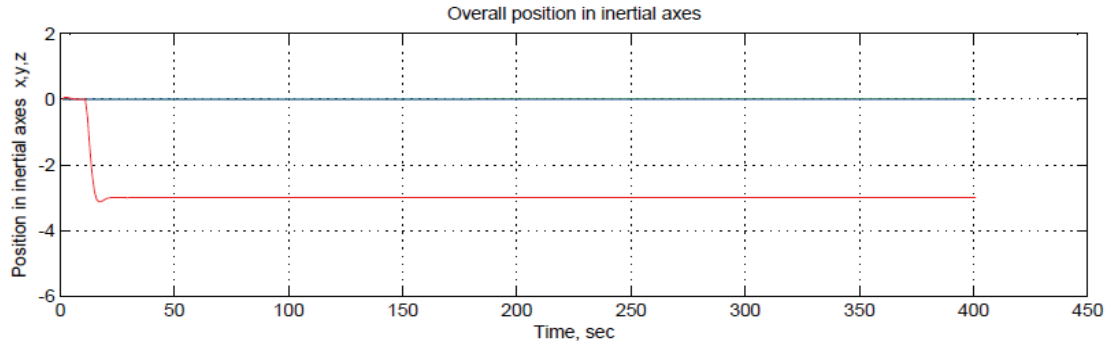

Figure 8.28: Position during third simulation of vertical flight

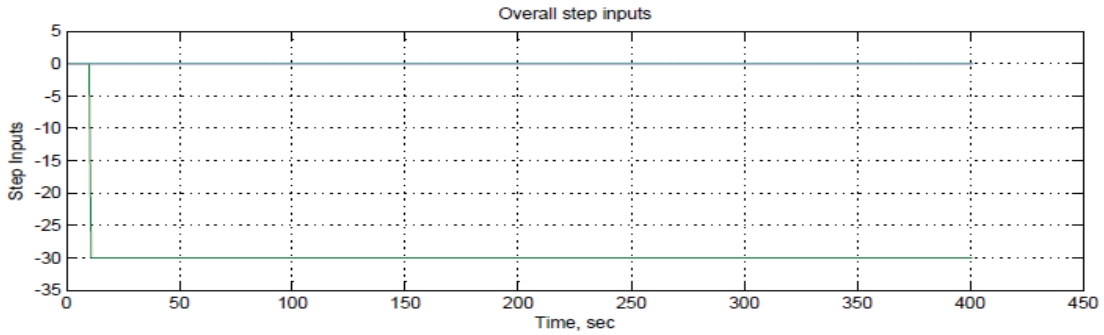

Figure 8.29: Inputs for third simulation of vertical flight

The fourth vertical flight simulation was with the step input increase 10x (ten times) compared to the first simulation, to the micro helicopter thrust, only. Other inputs to the pitch, roll and yaw were zero. This corresponds to the helicopter's vertical flight. The change of position along the z-axis is accomplished by the step control input and varying the rotational speed of the both rotors simultaneously. The same input is applied to both electrical motors. The micro coaxial helicopter will climb when the rotors' speed increase. When the helicopter reaches the required position, it will maintains a constant position at a selected point, with the rotors providing lift equal to the total weight of the helicopter. The input is shown in Figure 8.35.

This simulation results would reach position in z-axes of 10.0 ft with a maximum speed of 3.0 ft/s, as shown in Figures 8.30 and 8.31. The micro helicopter initially chatters with insignificant amplitude that could be ignored. The system is quick to respond and errors are dispensed quickly. The required position of 10 ft was achieved in 5 seconds with a small overshoot. The output signal exceeded the final steady-state value (overshoot) for approx. 0.4 ft. The stability was achieved quickly in 5 seconds without hunting (unwanted oscillation of signal). All other output signals are zero and could be ignored for this simulation.

Results for the simulation are shown in Figures 8.30 to 8.35.

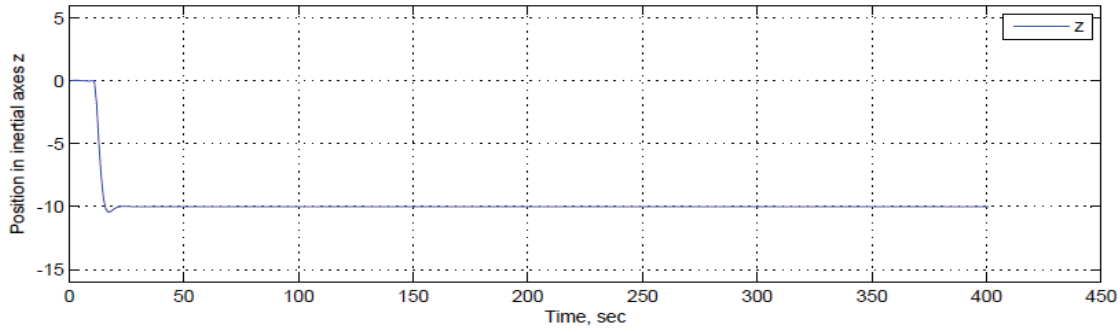

Figure 8.30: Position "z" during fourth simulation of vertical flight

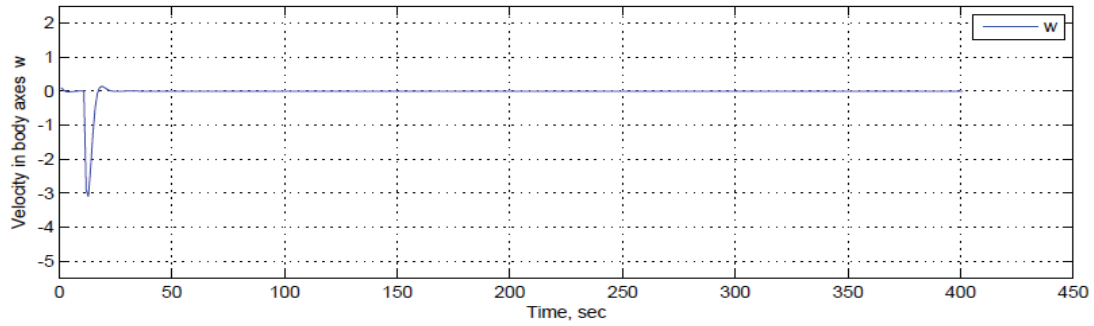

Figure 8.31: Velocity "w" during fourth simulation of vertical flight

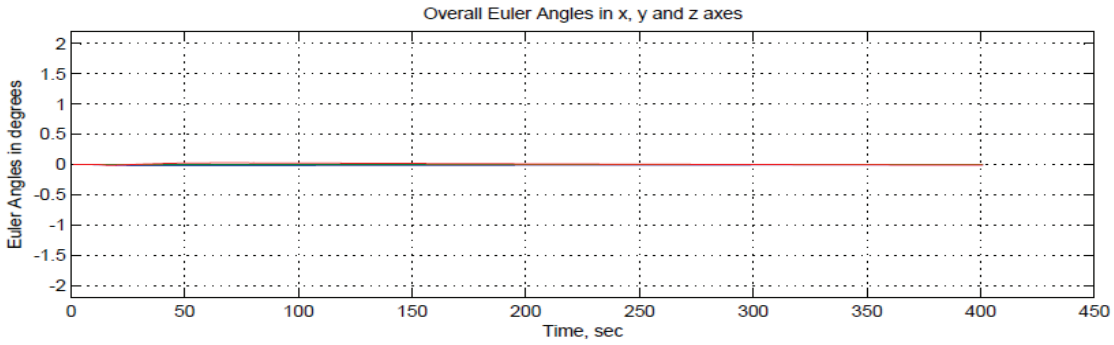

Figure 8.32: Euler angles during fourth simulation of vertical flight

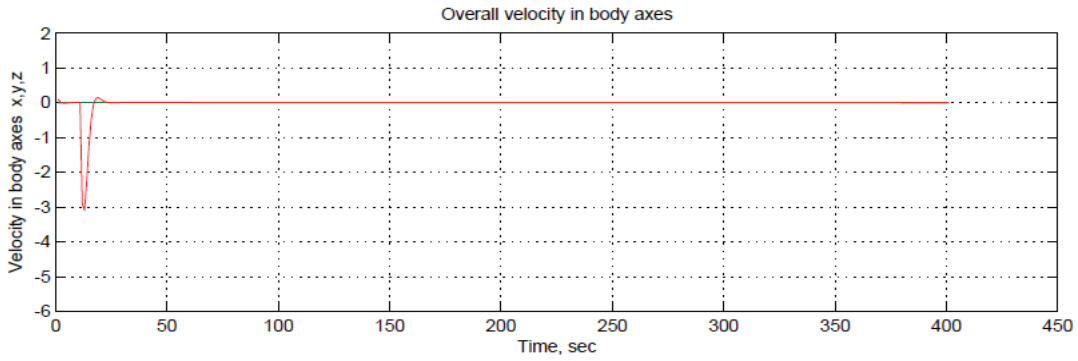

Figure 8.33: Velocity during fourth simulation of vertical flight

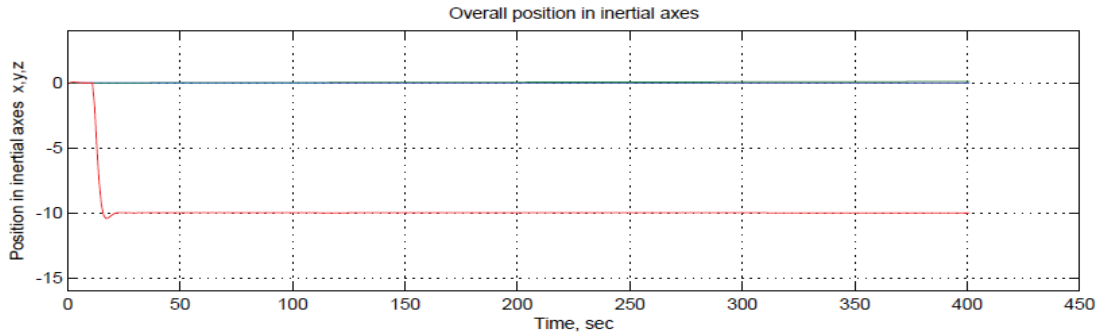

Figure 8.34: Position during fourth simulation of vertical flight

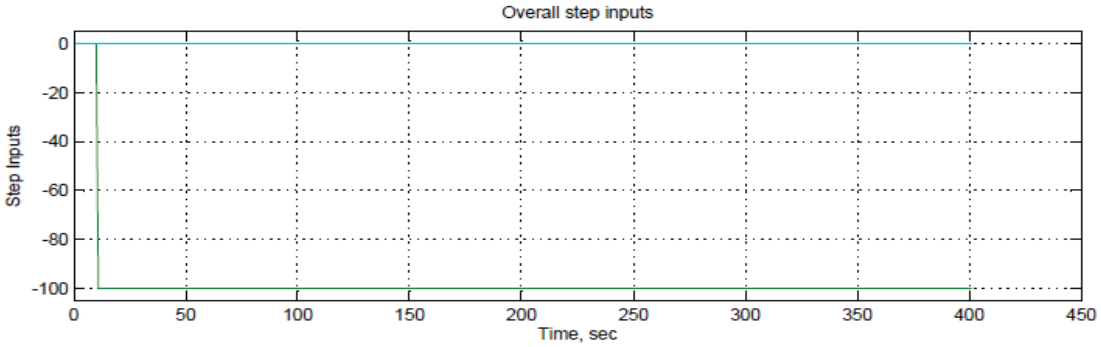

Figure 8.35: Inputs for fourth simulation of vertical flight

8.2 Level Flight Simulation

This chapter details the development of high reliability six degree-of-freedom mathematical and simulation models, and the design of a stability augmentation system for the micro helicopter. Explanations in this work provided as part of the chapter for the level flight apply to the vertical flight too.

We use the MatLab-Simulink 6DoF Aerospace Block set to implement Euler angle representation of six-degrees-of-freedom equations of motion. The 6 (six) control inputs to plant or 6DoF Block (Matlab-Simulink Aerospace Block) are forces and moments (X, Y, Z, L, M, N), shown in Equation 2.4.1. The micro coaxial helicopter forces and moments with 4 control inputs are shown in Equation 3.4. The 6DoF (Euler Angles) block considers the rotation of a body-fixed coordinate frame about an Earth-fixed reference frame. Though the observed response appears to be nonlinear and complex, it is possible that a single linear model could capture these dynamics and repeat them in simulation. The Matlab-Simulink 6 DoF Model is shown in Figure 8.1. To test this possibility, a single linearized model was created about the nominal trim condition defined in Table 8.1. A linear controller is designed, using Eigen structure assignment, following guidelines outlined in the literature. Weighting matrices Q and R are used to define the cost function. The matrix Q is state-weighting matrix and the matrix R is input-weighting matrix. This section will provide general guidelines on how to choose Q and R. Note that output regulation gains U and W are solved in Mathematica. The Matlab routine that performs numerical procedure for solving the algebraic Riccati equation is "lqr (A,B,Q,R)". For the micro coaxial helicopter simulation we found by trial and error a good values of R and Q.

The general form of the servomechanism-based output regulating tracking controller using H_2 optimization is thus well-defined. In the state feedback, we assume that the whole state $\mathbf{x}$ can be measured and, as a result, it is available for control. In this work we will implement full-state feedback gain $\mathbf{F}$ and omit the estimator construction as shown in Figure 5.2. We will design state feedback using nominal values of parameters and we will try to choose controlled output gains matrices. State feedback Gain F is achieved from the solution of the algebraic Riccati equation. The

Gain **F** is computed as shown in Equation 5.2.7. The matrices **R** and **Q** are computed with help of output gains D_{12d} and C_{1u} as as shown in Equations 5.2.10 and 5.2.11. The linear quadratic regulation method for determining our state-feedback control gain matrix **F**. The MATLAB function **lqr** allows you to choose two parameters, **R** and **Q**, which will balance the relative importance of the control effort (u) and error (deviation from 0), respectively, in the cost function that we are trying to optimize. The cost function corresponding to this **R** and **Q** places equal importance on the control and the state variables which are outputs. Both matrices Q and R are symmetric real, Q is assumed to be at least positive-semi-definite ($Q = Q \geq 0$), R must be positive-definite ($R = R > 0$). If, we set Q relatively large compared to R, the optimization procedure will result in a design in which x(t) is relatively "small" compared to $u_{(t)}$. If in contrast, Q is rather small, that will tend to make $x_{(t)}$ larger and $u_{(t)}$ smaller. Increasing the magnitude of **Q** more would make the tracking error smaller, but would require greater control u. More control effort generally corresponds to greater cost (more energy, larger components and actuator, etc.). The closed-loop system in Figure 5.2 was simulated to test the controller's performance. The input to the closed-loop system is the desired step input, and the output is the actual helicopter movement. The tracking signal simulated was a step input to the micro helicopter pitch and thrust. Other inputs to the roll and yaw were zero. This correspond to the helicopter level flight. The change of position along the x-axis and forward flight is accomplished by the first and second control input. The control inputs will provide the pitch angle and thrust required for the forward level flight. The first control input for the rear servomotor will control movement of the swash-plate upward or downward. When the rear servo motor pushes the swash-plate upward it will provide input for the forward flight. The second control input is for the thrust (altitude) control. This control input will change the rotational speed of the both rotors simultaneously. The same input is applied to both electrical motors. The change of position along the x-axis is accomplished by the step control input to the rear servo motor to push the swash-plate upward and input to electrical motors for both rotors. It will provide inputs for the forward flight by change of pitch angle and varying the rotational speed of the both rotors simultaneously. The rotors speed shall provide a total force such to have a lift equal to the total weight of the helicopter

and forward flight thrust.

In case of the micro coaxial helicopter indoor flight, the assumption is that drag coefficient is so small that it could be ignored in this work and simulation. Due to flight restriction for indoor flight we have priority for tracking error for the pitch angle theta, thrust and position along x-axes.

In this work, it's shown that we accomplished the stable change of pitch angle. The steady pitch angle is a fundamental requirement for forward flight, together with both rotors' speed. Forward flight is along the x-axis, so we introduced the tracking for x-axis position. This method provides change from forward flight to stop, with change of one of inputs required for flight. It was accomplished by controlling the rotors' speed, while a pitch angle would stay at the same, stable position. With this approach, the micro coaxial helicopter is able fly in a forward direction, stop and immediately switch to forward flight or to vertical flight or hover. When the helicopter reaches the required speed and position it maintains a constant pitch angle, with the rotors' speed change such that the helicopter will stop. It will require more control effort to minimize the transient error if the initial values are reasonably very high for the micro coaxial helicopter.

Realistically, most electromechanical structures can only be run within an obviously defined range. With the theory that the actuator modeled here can only run between $-12\ VDC$ and $+12\ VDC$, the simulation can be arranged to saturate the control voltage within this range, e.g. $-12\ VDC \leq$ u $\leq +12\ VDC$.

Simulation results are shown in this chapter for the system run with the step inputs such that would achieve the chosen position and speed.

First simulation of level flight was performed as described below.

The micro coaxial helicopter would reach a u speed of maximum 0.05 ft/s, pitch angle $\theta = 0.4$ deg, with position in x-axis of 0.9 ft, as shown in Figures 8.38, 8.37 and 8.42. Results for the simulation are shown in Figures 8.36 to 8.48. The micro helicopter initially changed speed within an insignificant time period that could be ignored. After initially approx. 1.5 seconds, the speed along x-axis was slowly changing without hunting or any unwanted oscillation. The system is quick to respond. The required pitch angle of 0.4 deg. was achieved in 20 seconds without an overshoot or oscillation.

The stop was accomplished after 50 seconds. The speed was decreasing slowly between 20 and 50 seconds, until the helicopter completely stopped. Also, it was noticed that the micro helicopter initially had an insignificant change of angular velocity "r" around z-axis, with a maximum value of 0.04 degrees/s. It is without an impact to flight and it's ignored in this work. All other output signals are zero and could be ignored for this simulation.

The results of the micro coaxial helicopter simulation of level flight are as follows:

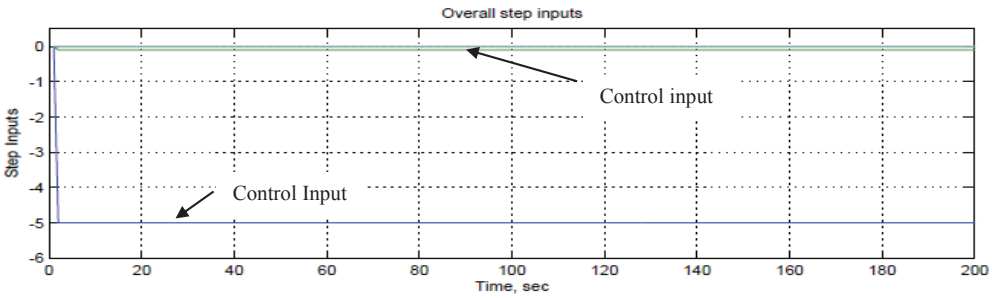

Figure 8.36: Inputs for first simulation of level flight

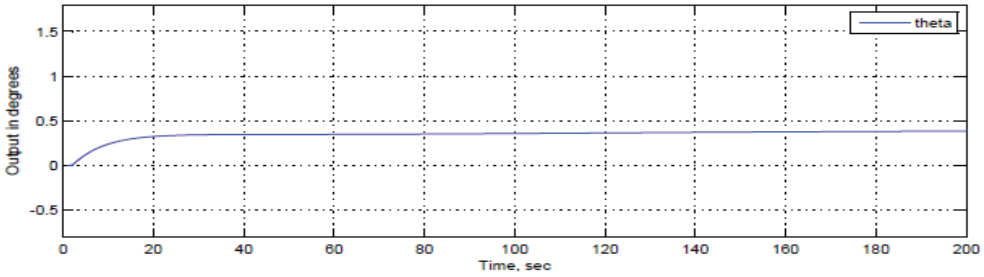

Figure 8.37: Euler angle θ during first simulation of level flight

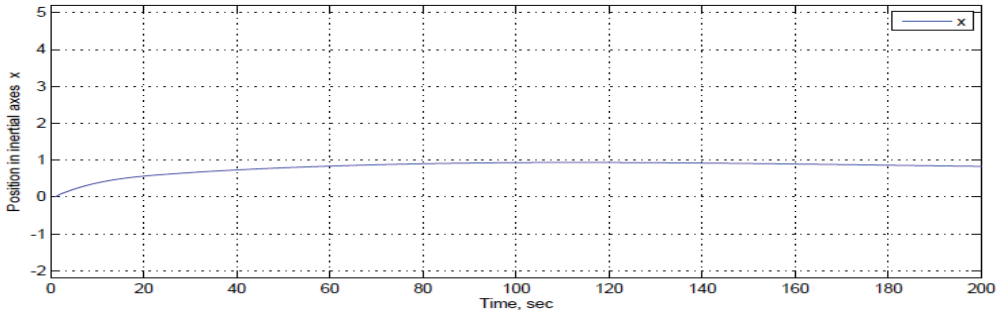

Figure 8.38: Position "x" during first simulation of level flight

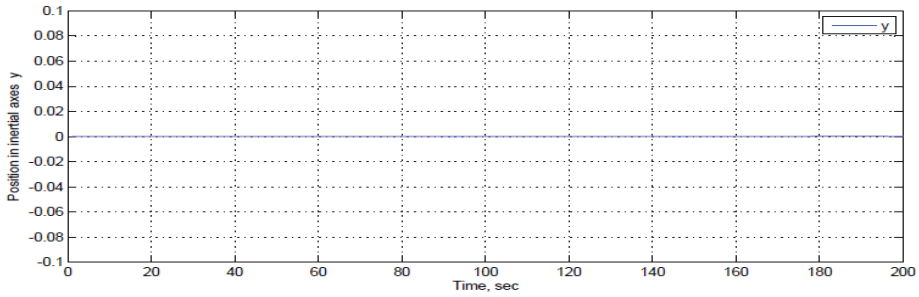

Figure 8.39: Position "y" during first simulation of level flight

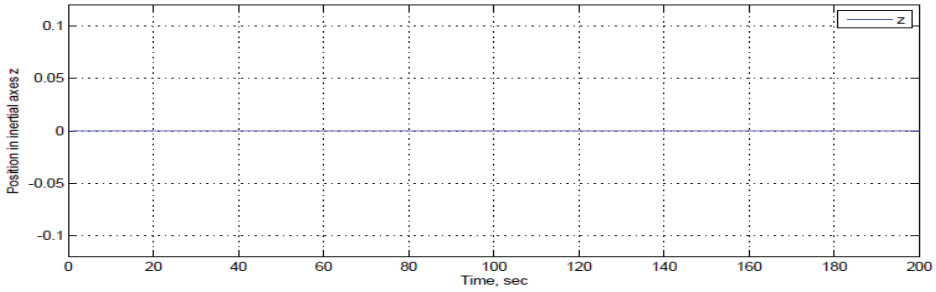

Figure 8.40: Position "z" during first simulation of level flight

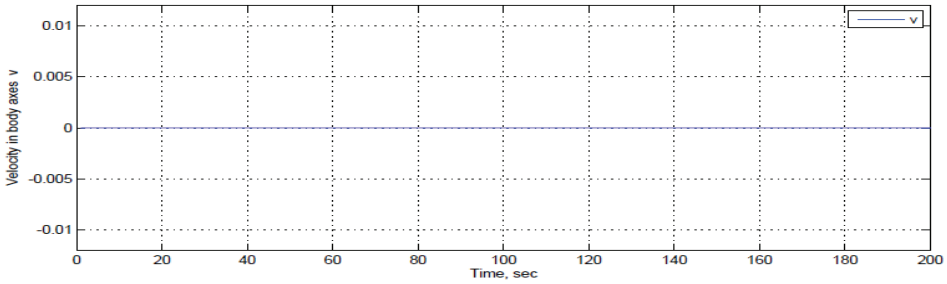

Figure 8.41: Velocity "v" during first simulation of level flight

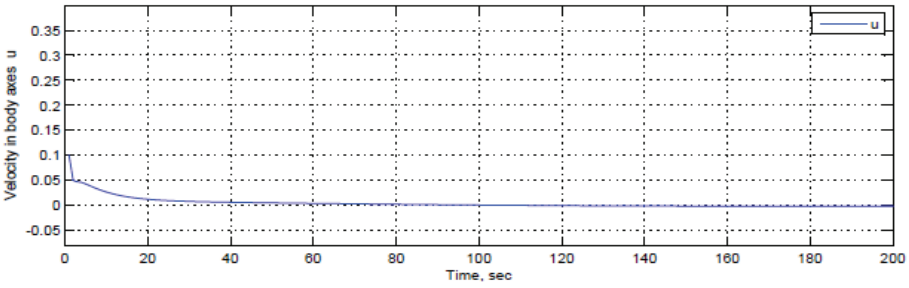

Figure 8.42: Velocity "u" during first simulation of level flight

.

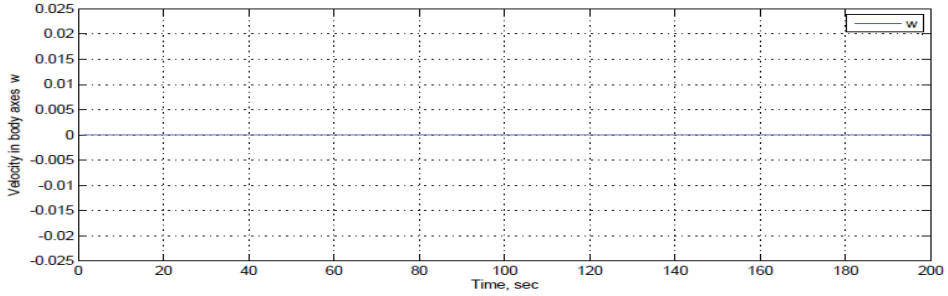

Figure 8.43: Velocity "w" during first simulation of level flight

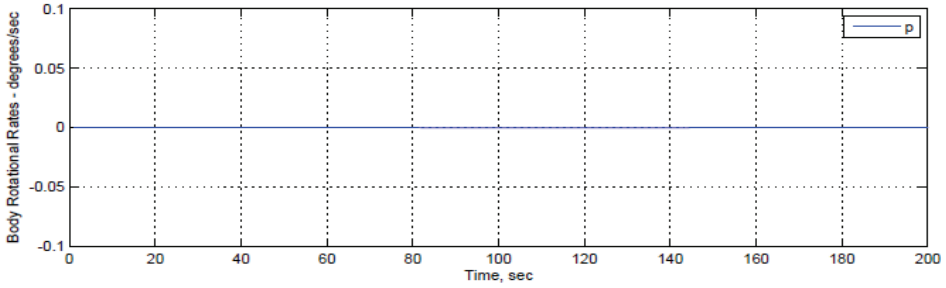

Figure 8.44: Angular velocity "p" during first simulation of level flight

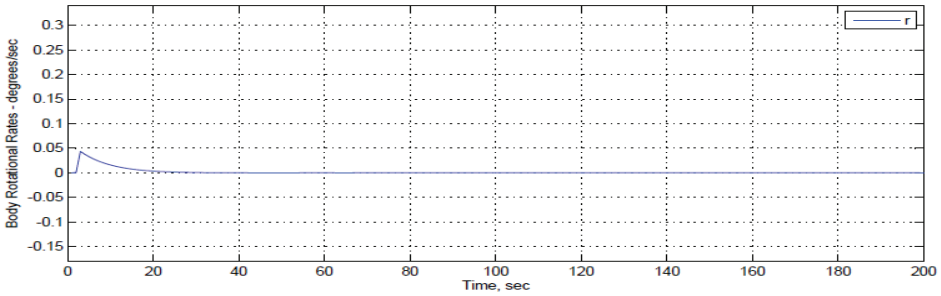

Figure 8.45: Angular velocity "r" during first simulation of level flight

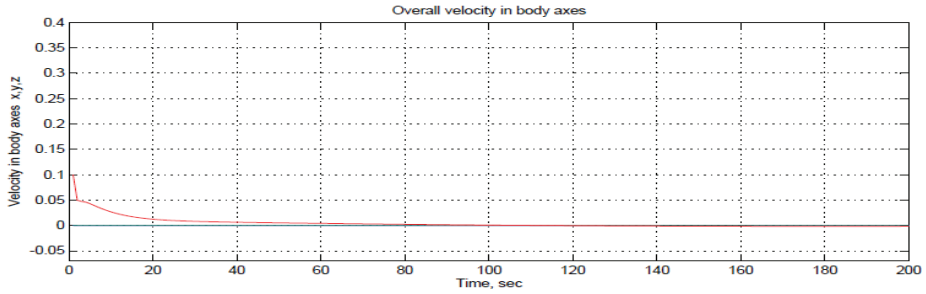

Figure 8.46: Velocity during first simulation of level flight

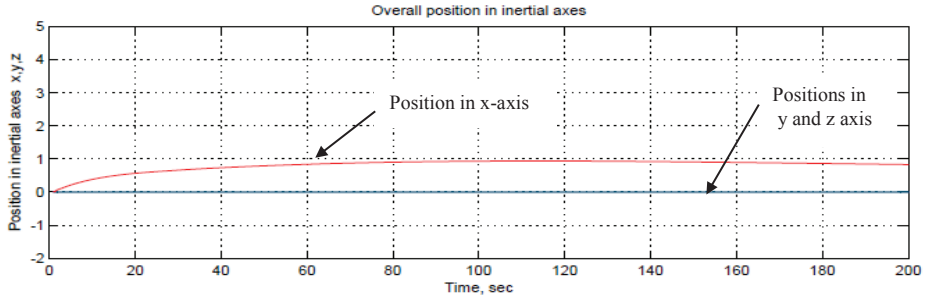

Figure 8.47: Position during first simulation of level flight

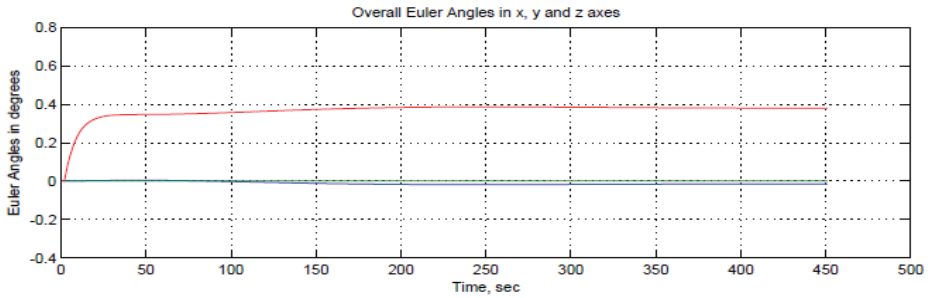

Figure 8.48: Euler angles during first simulation of level flight

The second simulation of level flight was with the step input increase of 2x (two times) compared to the first simulation. The tracking signal simulated was a step input to the micro helicopter pitch and thrust. Other inputs to the roll and yaw were zero. This corresponds to the helicopter's level flight. The change of position along the x-axis is accomplished by the step control input to the rear servo motor to push the swash-plate upward and input to electrical motors for both rotors. It will provide inputs for the forward flight by change of pitch angle and varying the rotational speed of the both rotors simultaneously. The rotors' speed shall provide a total force such to have a lift equal to the total weight of the helicopter and forward flight thrust.

In case of the micro coaxial helicopter indoor flight, the assumption is that drag coefficient is so small that this coefficient could be ignored in this work and simulation. Due to flight restrictions for indoor flight, we have priority for tracking error for the pitch angle theta, thrust and position along x-axes. It is important to have the ability to have a stable flight and stop. In this work, it's shown that we accomplished the stable change of pitch angle. Its fundamental requirement for forward flight, together with both rotors' speed. Forward flight is along the x-axis, so we introduced the tracking for the x-axis position. This method provides a change from forward flight to stop, with change of one of the inputs required for flight. It was accomplished by controlling the rotors' speed, while a pitch angle would stay at the same, stable position. With this approach, the micro coaxial helicopter is able fly in a forward direction, stop and immediately switch to forward flight or to vertical flight or hover. When the helicopter reaches the required speed and position, it will maintain a constant pitch angle, with the rotors' speed change such that the helicopter will stop. The micro helicopter initially changed speed within an insignificant time period that could be ignored. After initially approx. 1.5 seconds, the speed along the x-axis was slowly changing without hunting or any unwanted oscillation. The system is quick to respond. The required pitch angle of 0.8 deg. was achieved in 20 seconds without an overshoot or oscillation. The stop was accomplished after 80 seconds. The speed was decreasing slowly between 20 and 80 seconds, until the helicopter completely stopped. It was noticed that, with increase of the forward speed, there is an overshoot and sluggish response for position along the x-axis, but without any unwanted oscillation. It is

without an impact to flight simulation and its ignored in this work. All other output signals are zero and could be ignored for this simulation. The micro coaxial helicopter would reach a u speed of maximum 0.08 ft/s, pitch angle $\theta = 0.8$ deg, with position on the x-axis of 1.5 ft, as shown in Figures 8.52, 8.50 and 8.54. Results for the simulation are shown in Figures 8.49 to 8.54.

The simulation was performed using the individual models. The results of the micro coaxial helicopter simulation of level flight are as follows:

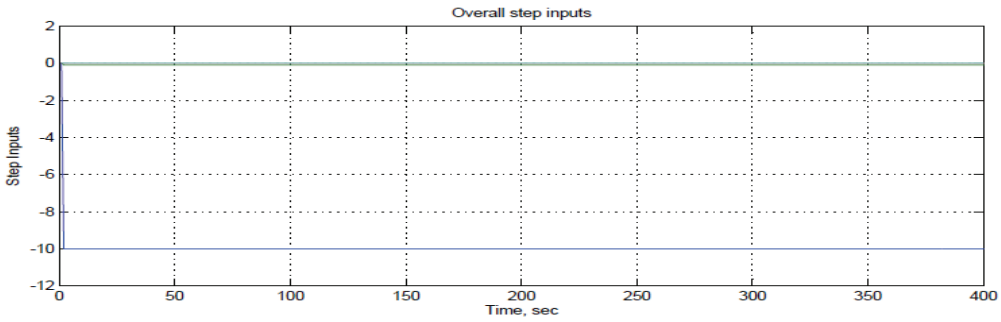

Figure 8.49: Inputs for second simulation of level flight

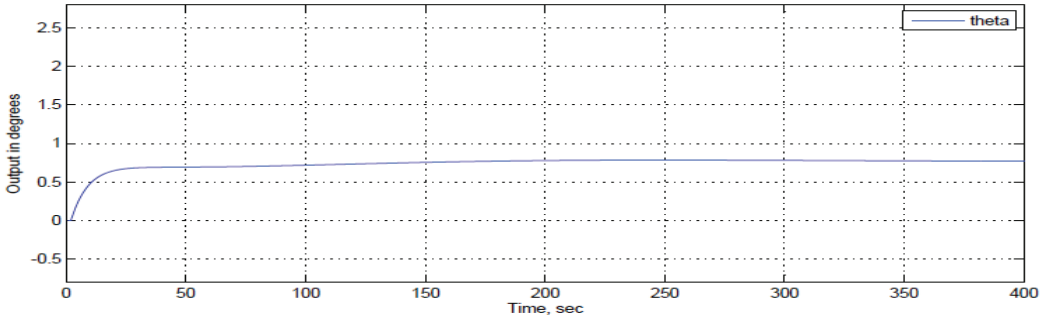

Figure 8.50: Euler angle θ during second simulation of level flight

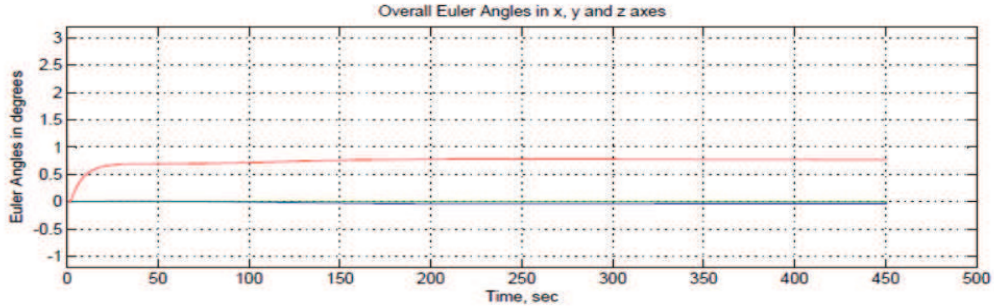

Figure 8.51: Euler angles during second simulation of level flight

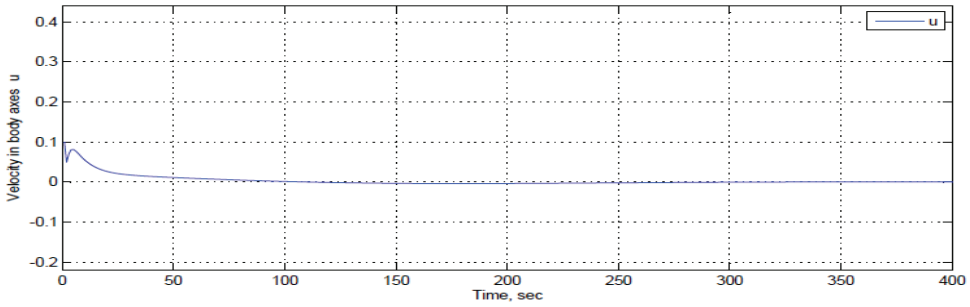

Figure 8.52: Velocity "u" during second simulation of level flight

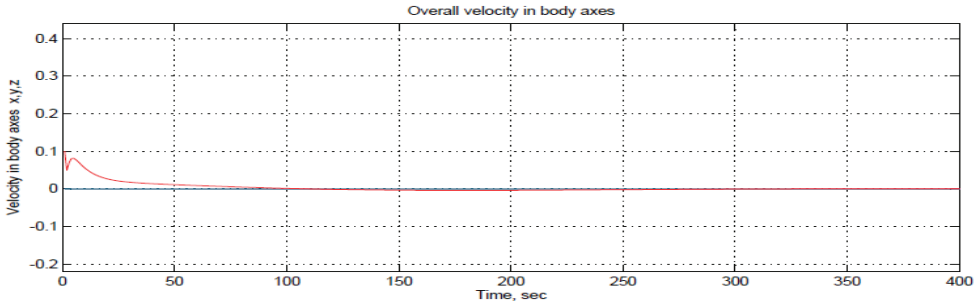

Figure 8.53: Velocity during second simulation of level flight

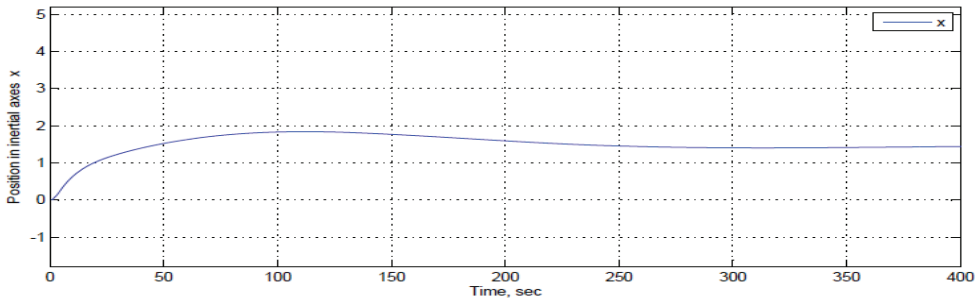

Figure 8.54: Position "x" during second simulation of level flight

The third simulation of level flight was with the step input increase of 5x (five times) compared to the first simulation. The tracking signal simulated was a step input to the micro helicopter pitch and thrust. Other inputs to the roll and yaw were zero. This corresponds to the helicopter's level flight. The change of position along the x-axis is accomplished by the step control input to the rear servo motor to push the swash-plate upward and input to electrical motors for both rotors. It will provide inputs for the forward flight by change of pitch angle and varying the rotational speed of both rotors simultaneously. The rotors' speed shall provide a total force such to have a lift equal to the total weight of the helicopter and forward flight thrust.

In case of the micro coaxial helicopter indoor flight, the assumption is that drag coefficient is so small that it could be ignored in this work and simulation. Due to flight restrictions for indoor flight we have priority for tracking error for the pitch angle theta, thrust and position along the x-axes. In this work it's shown that we accomplished the stable change of pitch angle. It's a fundamental requirements for forward flight, together with both rotors' speed. Forward flight is along the x-axis, so we introduced the tracking for the x-axis position. This method provide change from forward flight to stop, with change of one of inputs required for flight. It was accomplished by controlling the rotors' speed, while a pitch angle would stay at the same, stable position. With this approach the micro coaxial helicopter is able fly in a forward direction, stop and immediately switch to forward flight or to vertical flight or hover. When the helicopter reaches the required speed and position, it will maintain a constant pitch angle, with the rotors speed changing such that the helicopter will stop. The micro helicopter initially changed speed within an insignificant time period that could be ignored. After initially approx. 1.5 seconds, the speed along the x-axis was slowly changing without hunting or any unwanted oscillation. The system is quick to respond. The required pitch angle of 2.0 deg. was achieved in 20 seconds without an overshoot or oscillation. The stop was accomplished after 80 seconds. The speed was decreasing slowly between 20 and 80 seconds, until the helicopter completely stopped. It was noticed that, with increase of the forward speed, there is an overshoot and sluggish response for position along the x-axis, but without any unwanted oscillation. It is without an impact to flight simulation and it's ignored in this work. All other output signals are

zero and could be ignored for this simulation. The micro coaxial helicopter would reach a u speed of maximum 0.2 ft/s, pitch angle $\theta = 2.0$ deg, with position in "x" axis of 3.5 ft, as shown in Figures 8.56, 8.58 and 8.60. Results for the simulation are shown in Figures 8.55 to 8.60.

The simulation was performed using the individual models. The results of the micro coaxial helicopter simulation of level flight are as follows:

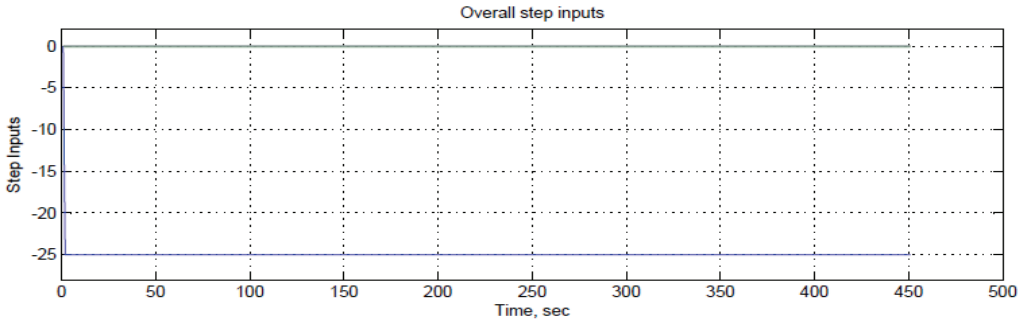

Figure 8.55: Inputs for third simulation of level flight

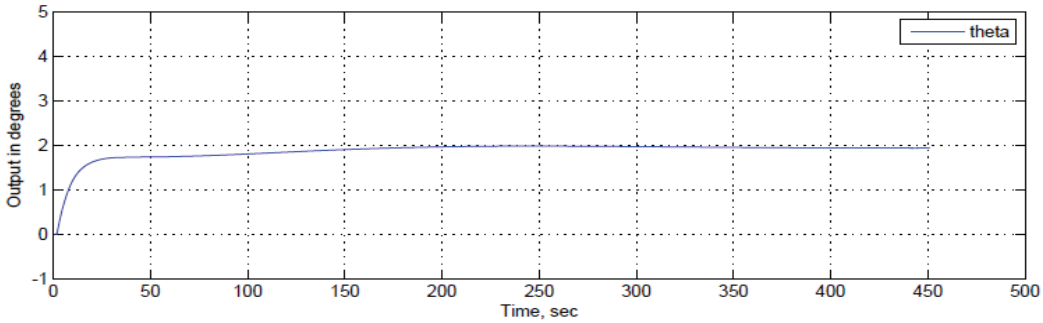

Figure 8.56: Euler angle θ during third simulation of level flight

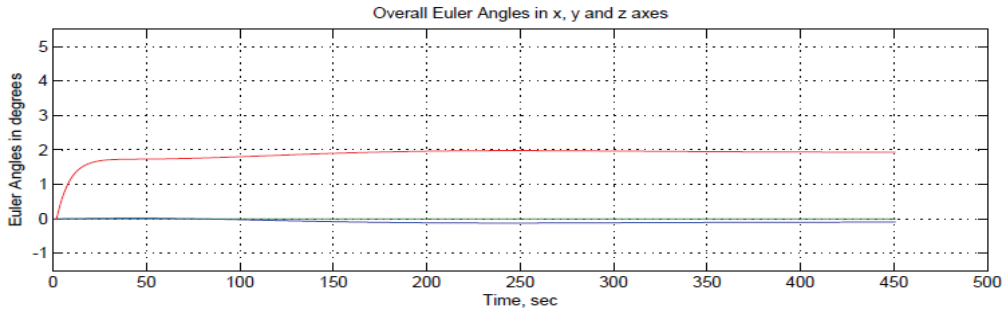

Figure 8.57: Euler angles during third simulation of level flight

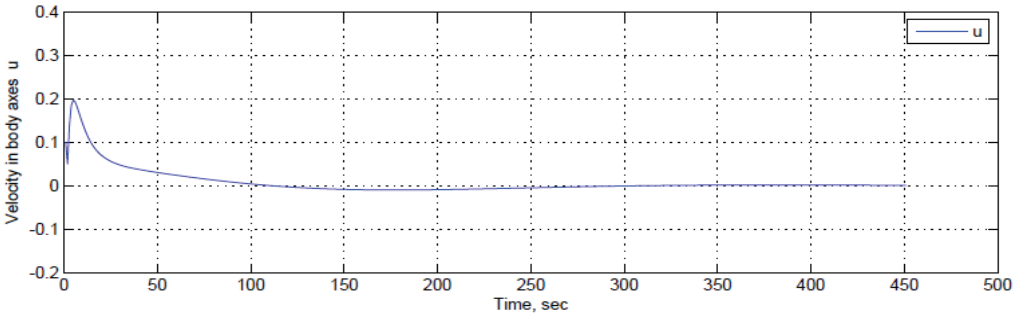

Figure 8.58: Velocity "u" during third simulation of level flight

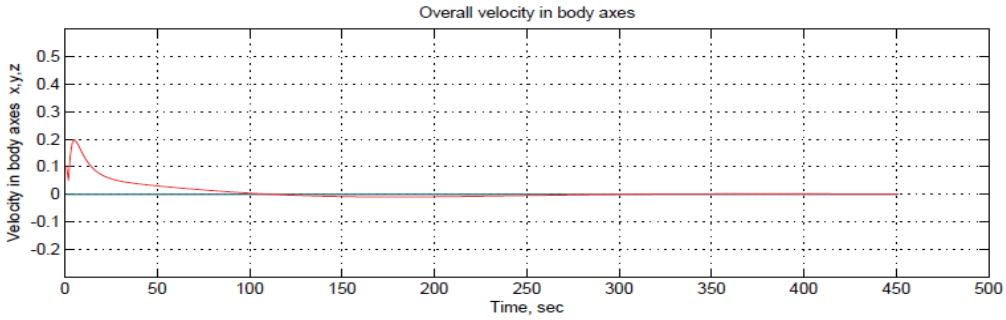

Figure 8.59: Velocity during third simulation of level flight

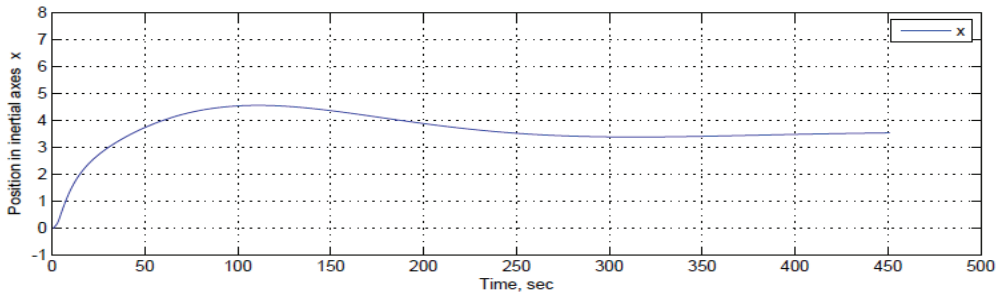

Figure 8.60: Position "x" during third simulation of level flight

The fourth simulation of level flight was with the step input increase of 8x (eight times) compared to the first simulation. The tracking signal simulated was a step input to the micro helicopter pitch and thrust. Other inputs to the roll and yaw were zero. This corresponds to the helicopter's level flight. The change of position along the x-axis is accomplished by the step control input to the rear servo motor to push the swash-plate upward and input to electrical motors for both rotors. It will provide inputs for the forward flight by change of pitch angle and varying the rotational speed of both rotors simultaneously. The rotors' speed shall provide a total force such to have a lift equal to the total weight of the helicopter and forward flight thrust.

In case of the micro coaxial helicopter indoor flight, the assumption is that drag coefficient is so small that it could be ignored in this work and simulation. Due to flight restrictions for indoor flight we have priority for tracking error for the pitch angle theta, thrust and position along the x-axes. In this work it's shown that we accomplished the stable change of pitch angle. It's a fundamental requirements for forward flight, together with both rotors' speed. Forward flight is along the x-axis, so we introduced the tracking for the x-axis position. This method provide change from forward flight to stop, with change of one of inputs required for flight. It was accomplished by controlling the rotors' speed, while a pitch angle would stay at the same, stable position. With this approach the micro coaxial helicopter is able fly in a forward direction, stop and immediately switch to forward flight or to vertical flight or hover. When the helicopter reaches the required speed and position, it will maintain a constant pitch angle, with the rotors speed changing such that the helicopter will stop. The micro helicopter initially changed speed within an insignificant time period that could be ignored. After initially approx. 1.5 seconds, the speed along the x-axis was slowly changing without hunting or any unwanted oscillation. The system is quick to respond. The required pitch angle of 2.9 deg. was achieved in 20 seconds without an overshoot or oscillation. The stop was accomplished after 90 seconds. The speed was decreasing slowly in period between 20 and 90 seconds, until the helicopter completely stopped. It was noticed, that with increase of the forward speed, there is an overshoot and sluggish response for position along x-axis, but without any unwanted oscillation. It is without an impact to flight simulation and it's ignored in this work. All other output signals are

zero and could be ignored for this simulation. The micro coaxial helicopter would reach a u speed of maximum 0.28 ft/s, pitch angle $\theta = 2.9$ deg, with position in the x-axis of 4.5 ft, as shown in Figures 8.62, 8.64 and 8.66. Results for the simulation are shown in Figures 8.61 to 8.66.

The simulation was performed using the individual models. The results of the micro coaxial helicopter simulation of level flight are as follows:

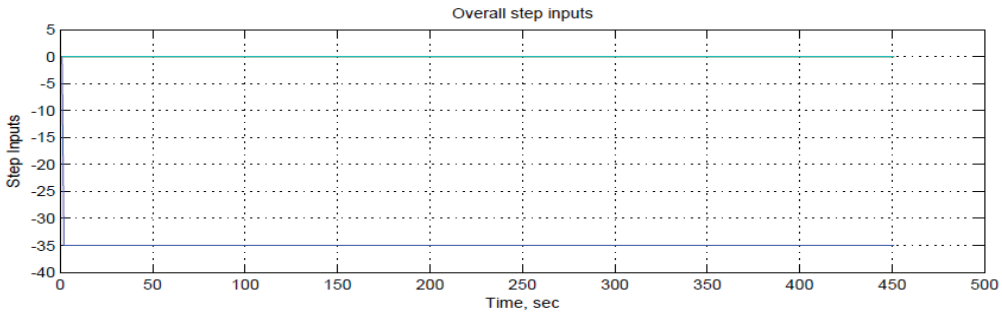

Figure 8.61: Inputs for fourth simulation of level flight

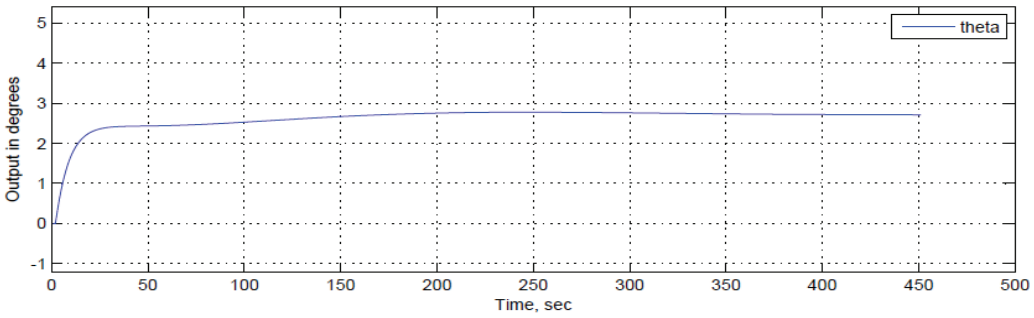

Figure 8.62: Euler angle θ during fourth simulation of level flight

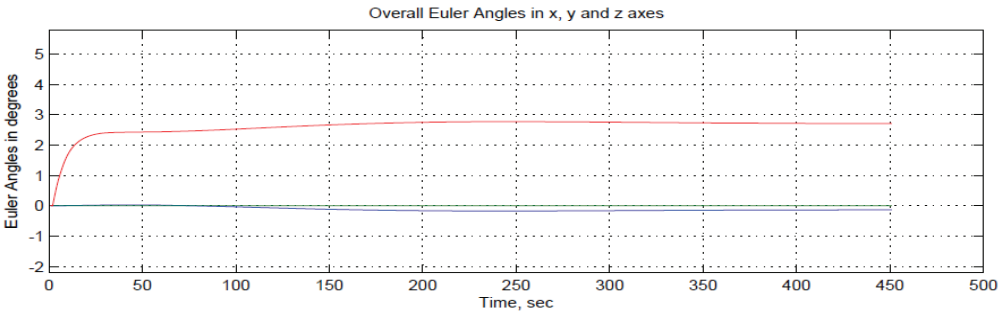

Figure 8.63: Euler angles during fourth simulation of level flight

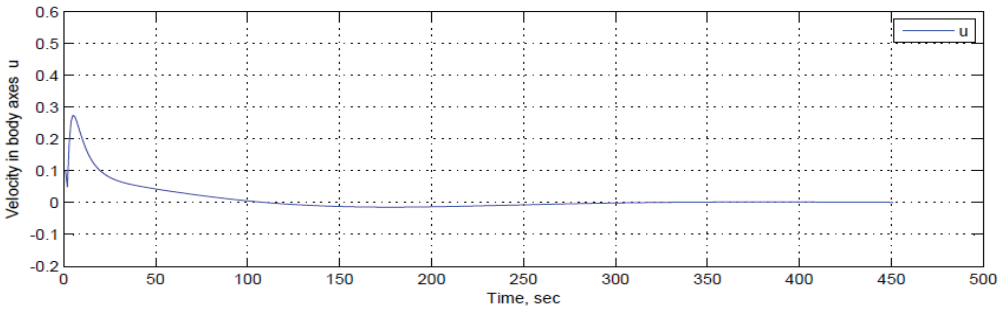

Figure 8.64: Velocity "u" during fourth simulation of level flight

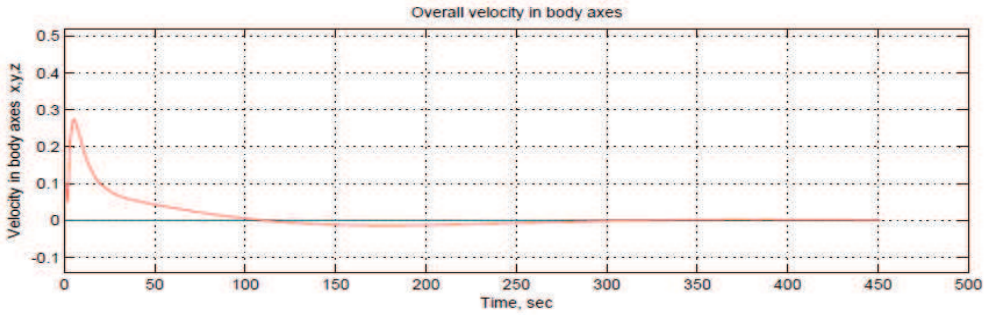

Figure 8.65: Velocity during fourth simulation of level flight

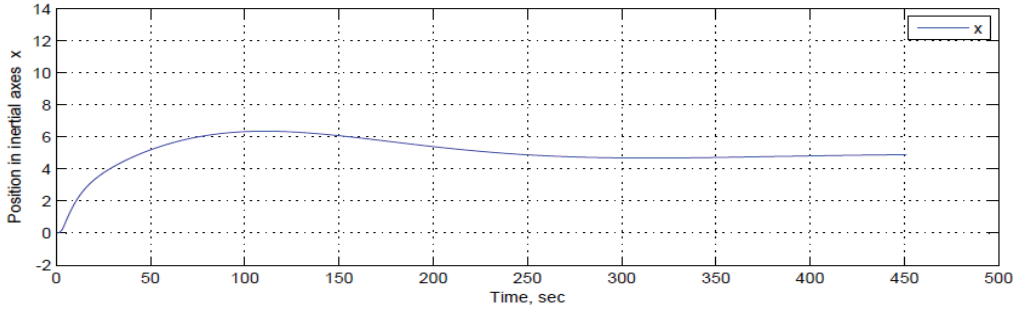

Figure 8.66: Position "x" during fourth simulation of level flight

8.3 Simulation Results

We use the MatLab-Simulink 6DoF Aerospace Blockset to implement Euler angle representation of six-degrees-of-freedom equations of motion. Though the controllers appear to work perfectly for the linearized dynamics models, this performance is not matched with the highly nonlinear system. In an effort to better understand the micro coaxial helicopter we, used the MATLAB and Simulink for advanced simulation and analysis of the helicopter flight dynamics. Via these tools, a nominal condition can be found for the safe flight envelope, and simulations can be run where the helicopter is disturbed from this condition by from external forces or control command inputs.

External forces and moments are neglected in our simulation of the indoor flight of the micro coaxial helicopter. In future work, they could be added to the system to simulate wind and other disturbances. Even with the ability to record simulation parameters and states, the complex behavior of an helicopter is difficult to completely understand solely by reviewing simulation data. For this cause, we have attached the Matlab/Simulink model with the open-source FlightGear flight simulator software [27].

Combining these tools allows the examiner to observe animations of aircraft flight simulations in real-time. Observing the trajectories of the helicopter flight has proven to be very useful for interpreting recorded simulation data and for more realistic sense of the micro coaxial helicopter behavior. Applying the FlightGear, MatLab [28], and Simulink [28] allows us to better discover flight, as will be shown in the chapters of this work. The flight path was recorded and observed through FlightGear animations, and the recorded state data were used to create a multi-linear model as discussed. The trim condition is provided in Table 8.1. The helicopter maintains the specified level of flight using these trim and predisposition parameters.

The simulation was performed using the individual models. Results with the Flight Gear animation screen snapshots for the 6 DoF simulation of level flight are shown in Figure 8.67, illustrating the behavior of the micro coaxial helicopter during the level flight.

The system performed simulation of the level flight as follows:

The simulation of level flight was with the step inputs to the micro helicopter pitch and thrust. This

(a) Snapshot at beginning of level flight

(b) Snapshot after a few seconds of level flight

(c) Snapshot during level flight

(d) Snapshot at end of level flight

Figure 8.67: FlightGear animation screen snapshots for the 6 DoF simulation of level flight

corresponds to the helicopter's level flight. The change of position along the x-axis is accomplished by the step control input to the rear servo motor to push the swash-plate upward and an input to electrical motors for both rotors. It will provide inputs for the forward flight by change of pitch angle and varying the rotational speed of both rotors simultaneously. The rotors' speed shall provide a total force such to have a lift equal to the total weight of the helicopter and forward flight thrust.

In case of the micro coaxial helicopter indoor flight, assumption is that drag coefficient is so small that it could be ignored in this work and simulation. Due to flight restrictions for indoor flight, we have priority for tracking error for the pitch angle theta, thrust and position along the x-axes. It is important to have the ability to have a stable flight and stop.

In this work, it's shown that we accomplished the stable change of pitch angle. It is a fundamental requirement for forward flight, together with both rotors' speed. Forward flight is along the x-axis, so we introduced the tracking for x-axis position. This method provides change from forward flight to stop, with change of one of inputs required for flight. It was accomplished by controlling the rotors' speed, while a pitch angle would stay at the same, stable position. With this approach the

micro coaxial helicopter is able fly in a forward direction, stop and immediately switch to forward flight or to vertical flight or hover. When the helicopter reaches the required speed and position it will maintain a constant pitch angle, with the rotors' speed changing such that the helicopter will stop. The micro helicopter initially changed speed within an insignificant time period that could be ignored. After initially approx. 1.5 seconds the speed along the x-axis was slowly changing without hunting or any unwanted oscillation. The system is quick to respond. The required pitch angle of 2.0 deg. was achieved in 20 seconds without an overshoot or oscillation. The stop was accomplished after 80 seconds. The speed was decreasing slowly between 20 and 80 seconds, until the helicopter completely stopped. It was noticed, that with increase of the forward speed, there is an overshoot and sluggish response for position along the x-axis, but without any unwanted oscillation. It is without an impact to flight simulation and it's ignored in this work. All other output signals are zero and could be ignored for this simulation.

The system performed simulation of the vertical flight as follows.

The vertical flight simulation was with the step input to the micro helicopter thrust, only. Other inputs to the pitch, roll and yaw were zero. This corresponds to the helicopter's vertical flight. The change of position along the z-axis is accomplished by the step control input and varying the rotational speed of the both rotors simultaneously. The same input is applied to both electrical motors. The micro coaxial helicopter will climb when the rotors' speed increases. When the helicopter reaches the required position, it will maintain a constant position at a selected point, with the rotors providing lift equal to the total weight of the helicopter.

The simulation was performed using the individual models. Results with the Flight Gear animation screen snapshots for the 6 DoF simulation of vertical flight are shown in Figure 8.68, illustrating the behavior of the micro coaxial helicopter during the vertical flight.

This simulation results would reach position in the z-axes of 10.0 ft with maximum speed of 3.0 ft/s. The micro helicopter initially chatters with insignificant amplitude that could be ignored. The system is quick to respond and errors are dispensed quickly. The required position of 10 ft was achieved in 5 seconds with a small overshoot. The output signal exceeded the final steady-state

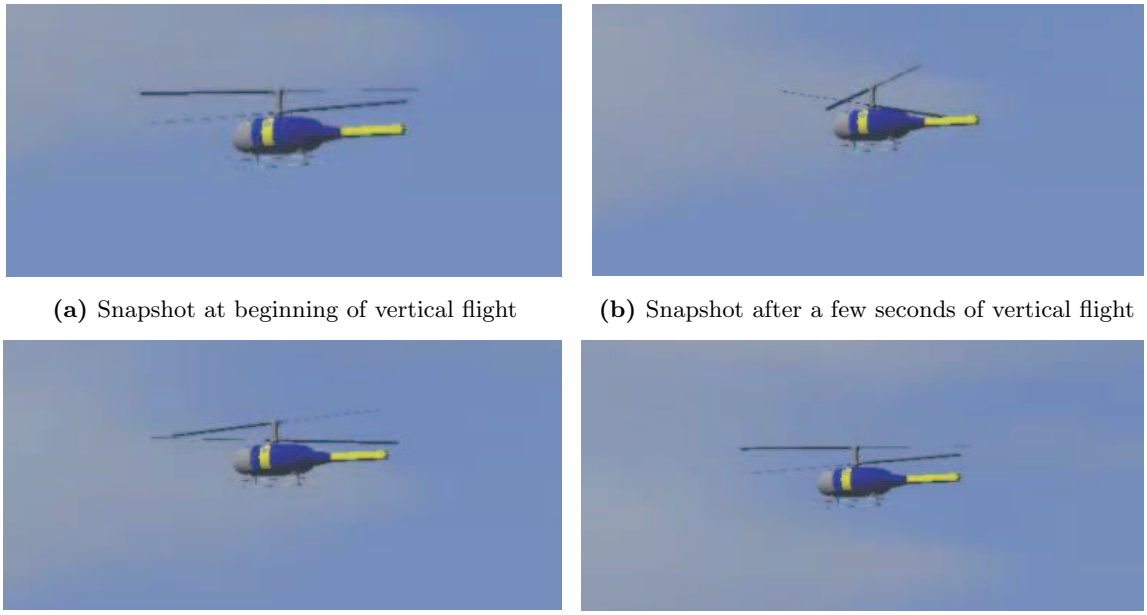

(a) Snapshot at beginning of vertical flight

(b) Snapshot after a few seconds of vertical flight

(c) Snapshot during vertical flight

(d) Snapshot at end of vertical flight

Figure 8.68: FlightGear animation screen snapshots for the 6 DoF simulation of vertical flight

value (overshoot) for approx. 0.4 ft. The stability was achieved quickly in 5 seconds without hunting (unwanted oscillation of signal). All other output signals are zero and could be ignored for this simulation.

It will require more control effort to minimize the transient error if the initial values are reasonably very high for the micro coaxial helicopter.

8.4 Discussion

It was shown in this chapter that the controller for the micro coaxial helicopter can be formulated as an step tracking control problem. The reference input can be modeled as the sum of step signals. The magnitude of the step may be subjectively chosen. Optimal H_2 regulator control theory was engaged to design an output-tracking regulating controller that achieves stability, tracking, minimal transient error, and robustness. Results offered in this work are exciting.

The controller was able to track signals of numerous sizes. Velocity up to 10 $\frac{ft}{s}$ and position in axes up to 100 ft where tracked accurately with the same controller. In addition to the condition when the system may be safe and stable, there are practical limits to the range of the deployed variable. The micro coaxial helicopter reasonable speed range is up to 0.3 $\frac{ft}{s}$ characterizing the indoor flight desired speed. The indoor desired speed is achieved with the ability to control the helicopter flight and position along the body axis.

To implement the proposed control system on the micro coaxial helicopter, several practical issues still need to be considered. The micro coaxial helicopter performance regarding payload and efficiency needs to be improved. Aerodynamic loads also need to be reflected in the design and analysis of the system to evaluate its real-world possibility. Additional work is required on developing a new micro-coaxial helicopter configuration including possibility to use a new rotor blades.

There are four inputs available for the model helicopter, each with two degrees of freedom. The control inputs for the micro coaxial helicopter are applied in a particular way, not appropriate for bigger helicopters. The rotational velocity of the rotors is controlled by two different electro motors. Pitch (longitudinal pitch) is controlled by the rear electro servomotor. Roll is controlled by the forward electro servomotor. Yaw control can be performed by varying the difference in rotational speed between the two rotors. For instance, the helicopter will turn to the left with an increase in the speed of the lower rotor.

The micro coaxial helicopter configuration should introduce improvement for the rotor blade, electric motor and an electric battery (motor supply). The helicopter is driven by two DC motors and two servomotors. Further research will hopefully consider electrical motors with higher rotational speed

and minimum increase of weight. The improved helicopter design would enable flight tests with all sensors and test equipment, and achieve all required tasks.

This work is significant because it allows the micro coaxial helicopter to be controlled more smoothly than existing approaches. It is original because it develops a simple reference model for tracking, and it is significant for determining the range and steady maneuverability of the micro coaxial helicopters for indoor flight.

Chapter 9: Conclusions and Future Work

9.1 Conclusions

System identification techniques for full-scale helicopters have been successfully applied to model-scale micro coaxial unmanned helicopters. The identified model is employed for the flight control design, handling quality evaluation, and simulation applications. The flight dynamics of the helicopter is quite different from the conventional helicopter due to its small size and coaxial rotor configuration. It has better maneuverability and can fly in a narrow space with obstacles. The multi-variable tracking and H_2 control theory were employed to design a flight control system that provided the desired stability and performance.

A six degree-of-freedom (6DoF) flight dynamics model are employed for control system design, analysis, and simulations. These analysis and simulation results show that the closed-loop system is stable at the described condition. These results validates that the nominal controller has been successfully designed and implemented.

This work is noteworthy because it enables a micro helicopter to successfully track multiple desired maneuvers, and it is significant because this system can be used to autonomously fly the micro coaxial helicopter. Using the work developed and contributed in this dissertation, we can now fly a micro coaxial helicopter in a way that has never been done before.

This work is significant because it allows the micro coaxial helicopter to be controlled more smoothly than allowed by existing approaches. Another important achievement is the development of an unmanned helicopter model that includes specific of the micro coaxial helicopter design. This work validates the presented scenarios for the micro coaxial helicopter indoor flight and provides a groundwork for control systems designed to address this type of helicopter and indoor operating conditions. Overall, this body of work presents a brief methodology for designing, analyzing, and implementing new multi-variable output-tracking regulators with high levels of robustness and functionality implemented for micro coaxial helicopters.

9.2 Future Work

Many aspects of this thesis call for additional research. The results obtained from the 6DoF dynamic model are encouraging. The development of the dynamic model is being done on a step-by-step basis, and a model good enough to be used for control system design is achieved.

The performance of the controller with a nonlinear regulator gain remains to be investigated. The regulator design approach adopted in this work is based on the estimates of the disturbance states. Good results of system identification with a high quality instrumentation and an optimal integration of the sensor information would further improve the results.

It is anticipated that there will continue to be rapid progress in the data acquisition and parameter identification processes, as well as in the 6DoF dynamic modeling effort. The reconfigured controllers for flight conditions such as descent, climb, yaw, roll and other special maneuvers must be investigated. The final configuration should be able to take account of as many scenarios as possible. It will be necessary to improve the test rig and test instrumentation for testing in hover, vertical (altitude) flight, yaw movement, roll movement and pitch movement.

Bibliography

[1] G. Padfield *Helicopter flight dynamics* Second edition 2007, Blackwell Publishing

[2] A. R. S. Bramwell, G. Done, D. Balmford *Bramwell's helicopter dynamics* Second Edition, Butterworth-Heinemann, 2001

[3] B.C. Chang *Aircraft flight dynamics and control I* MEM453-601 (Drexel),

[4] E. Petrosyan *Aerodynamics of coaxial configuration helicopters* in Russian, Moskva Poligon Press, 2004

[5] I. Raptis, K. Valavanis *Linear and nonlinear control of small − scale unmanned helicopters*, Springer Science 2011.

[6] J. Seddon, S. Newman *Basic helicopter aerodynamics* Second Edition, Blackwell Science, 2002

[7] S. Wu, Z. Zheng, K.Y. Cai *Indoor autonomous hovering control for a small unmanned coaxial helicopter*, 2010 8th IEEE International Conference on Control and Automation, June 9-11, 2010, Xiamen, China,

[8] B.C. Chang, M. Salman *Active coning compesation for control of spinning flying vehicles* (IEEE Conference, Yokohama, Japan, September, 2010)

[9] A. Bogdanov, D. Kieburtz, R. Merwe, E. Wan, *State dependent riccati equation* (*SDRE*) *controller for a small unmanned helicopter* AIAA 2003-5672, Austin, Texas

[10] B. Mettler, C. Dever, E. Feron *Scaling effects and dynamic characteristics of miniature rotorcraft*, Journal of Guidance, Control, and Dynamics Vol. 27, No. 3, May-June 2004

[11] V. Gavrilets, B. Mettler, E. Feron; *Dynamic model for a miniature aerobatic helicopter*; Massachusetts Institute of Technology. January 24, 2004 , web,

[12] B. Mettler, T. Kanade, M. Tischler *System identification modeling of a model − scale helicopter* CMU-RI-TR-00-03, The Robotics Institute Carnegie Mellon University Pittsburgh, Pennsylvania

[13] C. M. Velez, A. Agudelo, J. Alvarez; *Modeling, simulation and rapid prototyping of an unmanned mini − helicopter* AIAA 2006-6737

[14] Li Chen, P. McKerrow *Modelling the lama coaxial helicopter* University of Wollongong, Australia

[15] E. N. Johnson, P. A. DeBitetto *Modeling and simulation for small autonomous helicopter development*, Copyright 1997 by the AIAA,

[16] Anne Marie Spence, Roberto Celi, *Coupled rotor − fuselage dynamics and aero − elasticity in turning flight*, AIAA-92-2109-CP,

[17] B. Wang, F. Wang, B. M. Chen, T. H. Lee *Robust flight control system design for an indoor miniature coaxial helicopter*, 2012 10th World Congress on Intelligent Control and Automation,

July 6-8, Beijing, China

[18] S. Sunada, K. Tanaka, K. Kawashima *Maximization of thrusttorque ratio of a coaxial rotor*, Journal of Aircraft Vol. 42, No. 2, MarchApril 2005

[19] L.A. Young, E.W. Aiken, J.L. Johnson, R. Demblewski, J. Andrews, J. Klem *New concepts and perspectives on micro − rotorcraft and small autonomous rotary − wing vehicles*, AIAA 2002-2816

[20] T. Valkov *Aerodynamic loads computation on coaxial hingeless helicopter rotors*, AIAA 90-0070

[21] P. Fankhauser, S. Bouabdallah, S. Leutenegger, R. Siegwart *Modeling and decoupling control of the coax micro helicopter*, 2011 IEEE/RSJ International Conference on Intelligent Robots and Systems, September 25-30, 2011. San Francisco, CA, USA

[22] C. P. Coleman *A survey of theoretical and experimental coaxial rotor aerodynamic research* NASA Technical Paper 3675, 1997

[23] S. K. Kirn, D. M. Tilbury; *Mathematical modeling and experimental identification of a model helicopter* AIAA-98-4357

[24] B. C. Chang, C. Hu; *Multivarable control and failure accommodation in eye − head − torso target tracking* Proceedings of the 42nd IEEE; Conference on Decislon and Control; Maui, Hawaii USA, December 2003

[25] B. C. Chang, G. Bajpai, H. G. Kwatny, *A regulator design to address actuator failures* Proceedings of the 40th IEEE Conference on Decision and Control, Volume: 2, pp. 1454 -1459, Dec. 2001

[26] J. Doyle, K. Glover, P. Khargonekar, B. Francis, *State − space solutions to standard H_2 and H_∞ control problems* IEEE Transactions on Automatic control, Vol.34, No. 8, August 1989.

[27] FlightGear Flight Simulator v2.0. GNU General Public License, http://www.flightgear.org/, 2011.

[28] MATLAB. version R2012a., Student Version, The MathWorks Inc., Natick, Massachusetts, 2012.

[29] Wolfram Mathematica 8, Student Version, Wolfram Research Inc. , Champaign, IL (worldwide headquarters)

[30] K. Zhou, J. Doyle, K. Glover *Robust and optimal control* Prentice Hall, Englewood Cliffs, New Jersey, USA

[31] E-Flite Blade CX2 Specifications, Horizon, Champaign, Illinois 61822, USA

[32] M. Harun-Or-Rashid, J.B. Song, S. Chae, Y.S. Byun, B.S. Kang *Unmanned coaxial rotor helicopter dynamics and system parameter estimation*, Journal of Mechanical Science and Technology 28 (9) (2014) 3797-3805,

Appendix A: Nomenclature, Acronyms, and Symbols

u = component along the longitudinal axis or linear velocity in x-axis

v = component along the lateral axis or linear velocity in y-axis

w = component along the vertical axis or linear velocity in z-axis

p = helicopter body rotational rates, angular velocity along x-axis (rate of roll)

q = helicopter body rotational rates, angular velocity along y-axis (rate of pitch)

r = helicopter body rotational rates, angular velocity along z-axis (rate of yaw)

ϕ = Roll Angle (Euler angle for roll (x-axis))

θ = Pitch Angle (Euler angle for pitch (y-axis))

ψ= Yaw Angle (Euler angle for yaw (z-axis))

x = linear position of the helicopter in body coordinates in x body axis

y = linear position of the helicopter in body coordinates in y body axis

z = linear position of the helicopter in body coordinates in z body axis

x = the state vector

y = the measured output vector

u = the input vector,

X,Y,Z = external forces acting at the helicopter center of gravity

X_u = force along the x - axis acting at upper rotor

X_l = force along the x - axis acting at lower rotor

X_{pl} = force along the x - axis acting at fuselage

Y_u = force along the y - axis acting at upper rotor

Y_l = force along the y - axis acting at lower rotor

Y_{pl} = force along the y - axis acting at fuselage

Z_u = force along the z - axis acting at upper rotor

$Z_l =$ force along the z - axis acting at lower rotor

$Z_{pl} =$ force along the z - axis acting at fuselage

L = Aerodynamics and inertial moment along the x - axis,

M = Aerodynamics and inertial along the y - axis

N = Aerodynamics and inertial along the z - axis

L_u = Aerodynamics moment along the x - axis acting at upper rotor

L_l = Aerodynamics moment along the x - axis acting at lower rotor

L_{pl} = Aerodynamics moment along the x - axis acting at fuselage

M_u = Aerodynamics moment along the y - axis acting at upper rotor

$M_l =$ Aerodynamics moment along the y - axis acting at lower rotor

$M_{pl} =$ Aerodynamics moment along the y - axis acting at fuselage

N_u = Aerodynamics moment along the z - axis acting at upper rotor

$N_l =$ Aerodynamics moment along the z - axis acting at lower rotor

N_{pl} = Aerodynamics moment along the z - axis acting at fuselage

N_{up} = Rotational moment along the z - axis acting at upper rotor

N_{lr} = Rotational moment along the z - axis acting at lower rotor

M_{up} = Rotational moment along the y - axis acting at upper rotor

M_{lr} = Rotational moment along the y - axis acting at lower rotor

L_{up} = Rotational moment along the x - axis acting at upper rotor

L_{lr} = Rotational moment along the x - axis acting at lower rotor

I_x = moment of inertia about the body x - axis

I_y = moment of inertia about the respectively body y - axis

I_z = moment of inertia about the respectively body z - axis

I_{xy} = the product of inertia

Gw = weight of helicopter

m = helicopter mass, or mass of shaft, fuselage or blade

d_m = elementary masses of the helicopter

g = gravitational acceleration (gravity)

Q_r = rotor torque

Q_m = motor torque

G_r = gear to pinion ratio

M_g = main gear teeth

T_p = pinion teeth

ω_m = speed of the DC Motor output shaft

Q_m = the DC Motor torque

Q_{stm} = stall torque (torque is max. but the shaft is not rotating)

ω_n = speed without load (output speed of the motor is max. without applied torque)

A = plant state-space internal dynamics matrix

B_1 = state-space input disturbance matrix

B_2 = state-space input control matrix

C_2 = state-space observation matrix,

D_{22} = state-space output disturbance matrix

D = the input feed-through matrix

D_{12d} = controlled output gain matrix,

w_1 = the exogenous input vector to the system (input disturbance)

u = the control input vector

v = is the measurement noise

z = the regulated signal vector

z_1 = is the output-tracking error to be minimized

z_2 = the control-input constraints

Q = state-weighting matrix

R = input-weighting matrix

δ_{th} = altitude (thrust)

δ_{lat} = roll control input;

δ_{lon} = pitch control input

$\delta_{yaw} =$ yaw control input;

$FM =$ figure of merit

$C_T =$ thrust coefficient

$C_Q =$ torque coefficient

$x_T =$ Distance from c.g. to the rotor axis along x - axis

$y_T =$ Distance from c.g. to the rotor axis along y - axis

$z_{up} =$ Distance from c.g. to the upper rotor along z - axis

$z_{lr} =$ Distance from c.g. to the lower rotor along z - axis

$\omega_u =$ Rotational speed of the upper rotor

$\omega_l =$ Rotational speed of the lower rotor

$m_{up} =$ Rotational moment coefficient for upper rotor

$m_{lr} =$ Rotational moment coefficient for lower rotor

$\sigma =$ rotor solidity factor

$\rho =$ density of air at 15 ^0C and sea level

$A =$ the rotor disc area ($A = R^2\ \pi$)

$N_b =$ number of blades on rotor

$c =$ rotor blade chord

$R =$ rotor radius

$\omega_m =$ speed of the DC Motor output shaft

$Q_{stm} =$ stall torque (torque is max. but the shaft is not rotating)

$Q_m =$ the DC Motor torque

$\omega_n =$ speed without load (output speed of the motor is max. without torque applied to the output shaft)

$T =$ thrust

$T_u =$ upper rotor disk thrust

$T_l =$ lower rotor disk thrust

$T_{li} =$ inner area of lower rotor disk thrust

$T_{lo} =$ outer area of lower rotor disk thrust

Q = rotor torque

Q_u = upper rotor disk torque

Q_l = lower rotor disk torque

Q_{lo} = outer area of lower rotor disk torque

Q_{li} = inner area of lower rotor disk torque

Ω = angular velocity

Ω_u = upper rotor angular velocity

Ω_l = lower rotor angular velocity

p_∞ = initial or atmospheric pressure

V_u = upper rotor disk velocity

V_{li} = inner area of lower rotor disk velocity

V_{lo} = outer area of lower rotor disk velocity

V_{uo} = outer area of undisturbed flow velocity

V_c = axial velocity of the rotor

V_2 = inner area of undisturbed flow velocity

V_{l22} = undisturbed flow velocity in outer area of lower rotor

C_{Tu} = upper rotor thrust coefficient

C_{Tl} = lower rotor disk thrust coefficient

C_{Tli} = inner area of lower rotor disk thrust coefficient

C_{Tlo} = outer area of lower rotor disk thrust coefficient

C_{Qu} = upper rotor torque coefficient

C_{Ql} = lower rotor disk torque coefficient

Vita

Education

Doctor of Philosophy, Mechanical Engineering, Drexel University, Philadelphia, PA, 2014
Master of Science, Mechanical Engineering, Drexel University, Philadelphia, PA, 2004
Bachelor of Science, Mechanical Engineering, Mostar, Bosnia and Herzegovina, 1980

Research Interests

Control systems, robotics, embedded control, regulation theory, autonomous systems, aerospace control, UAVs, aircraft hydraulics systems.

Experience

Recognized authority on Hydraulic System for Chinook, H46 and V-22 Osprey, and Lead hydraulic systems and mechanical controls engineer for the Chinook program. Developed and qualified new sources of supply for various hydraulic components. Responsible for development and design of new components, troubleshooting of hydraulics system and design improvements of components. Boeing, 1997 to Present.
Responsible for quality assurance and managed final testing and diagnostic of mechanical systems and military aircraft equipment. Soko-Aircraft Industry, Bosnia and Herzegovina, 1992

Recognition, Quality Pride Awards

2007 - Recognizing exceptional performance - V22 Affordability Trade Studies
2007 - Recognizing exceptional performance - A10 Wing Replacement Program
2005 - Certificate of Accomplishment - the troubleshooting and repair of the Hydraulic System on the ATA (V-22) aircraft
2003 - Certificate of Appreciation - Iraqi 5 Proposals of the H-46 Program
2000 - Certificate of Achievement - Chinook Mechanical Systems IPT
2000 - Certificate of Appreciation - Engineering investigation of the Fort Rucker CH-47D flight controls
1998 - Commendable Performance Award - vibration reduction on ICH EMD aircraft
1997 - Outstanding Performance, Hydraulics - a zero delinquency metric